A STUDY OF THE MECHANISM OF ACTION OF NOVEL INHIBITORS OF TUMOUR CELL INVASION

by

LIANNE M. MCHARDY

B.Sc., University of British Columbia, 2000

A THESIS SUBMITTED IN PARTIAL FULFILLMENT OF
THE REQUIREMENTS FOR THE DEGREE OF

DOCTOR OF PHILOSOHPY

in

THE FACULTY OF GRADUATE STUDIES

(Biochemistry and Molecular Biology)

THE UNIVERSITY OF BRITISH COLUMBIA

December, 2007

Abstract

Metastasis is the leading cause of death in cancer patients. Tumour invasion and migration are critical aspects of metastatic progression. A forward chemical genetics project was initiated in an effort to identify novel compounds that inhibit tumour invasion. After screening a natural extract library, two novel inhibitors were identified: motuporamine C (MotC) and strongylophorine-26 (STP-26). Structure-activity studies identified dihdyromotuporamine C (dhMotC) as a potent and easily synthesized analogue. In this work, the mechanism of activity of dhMotC and STP-26 was investigated. It was found that both dhMotC and STP-26 affect cellular shape. dhMotC induced thick central actin stress fibres and large focal adhesions and caused cells to contract. STP-26 also induced adhesion formation but it reduced stress fibres and caused increased cell spreading. Both inhibitors activated Rho GTPase, a result which was shown to mediate, in large part, the anti-invasion activity of these molecules. Motuporamines also induce the formation of membrane-rich inclusions at the peri-nuclear region in cells. Motuporamines cause an increase in lysosomal pH and inhibit lysosomal function, such that EGFR/EGF complexes internalized in the presence of dhMotC do not get degradad. This inhibition of EGF degradation is not dependent on Rho activity. However, the anti-invasive activity of motuporamine analogues correlates well with their ability to induce the formation of membrane-rich inclusions. Thus, alteration in membrane trafficking or degradation of cellular membranes may be mechanistically related to the anti-invasion effect of motuporamines. A systematic genome-wide yeast haploinsufficiency screen was employed in an effort to identify possible targets of dhMotC. Yeast screening resulted in a list of 21 mutant strains which showed increased drug sensitivity. Sphingolipid biosynthesis was identified as a target in yeast cells. By testing other

genes from the list, ARF1 was identified as a target that partially mediates the anti-invasive activity in human cells. The results of this body of work show that Rho and ARF1 are important molecular players in the mechanism of tumour cell invasion. This knowledge will contribute to the development of future anti-metastasis therapies and to the development of small molecules for use as biological probes to investigate the molecular basis of metastasis.

Table of Contents

List of Tables

List of Figures

List of Abbreviations

DNA	Deoxyribonucleic Acid
EMT	Epithelial to Mesenchymal Transition
ECM	Extracellular Matrix
MotC	Motuporamine C
STP-26	Strongylophorine-26
dhMotC	dihydroMotuporamine C
ARF1	ADP-ribosylation factor 1
DMEM	Dulbecco's Modified Eagle's Medium
HBSS	Hank's Balanced Salts
MTT	3-(4,5- dimethylthiazol-2-yl)-2,5-diphenyltetrazolium bromide
EGF	Epidermal Growth Factor
EGFR	Epidermal Growth Factor Receptor
TfR	Transferrin Receptor
LAMP2	Lysosomal Associated Protein 2
PDI	Protein disulfide isomerase
GM-130	Golgi matrix protein of 130 kDa
FBS	Fetal Bovine Serum
PBS	Phosphate Buffered Saline
BSA	Bovine Serum Albumin
FITC	Fluorescein Isothiocyanate
GTP	Guanosine Triphosphate

DMSO	Dimethyl Sulfoxide
YPD	Yeast extract, Peptone, Dextrose
DMA	Deletion Mutant Array
IGCD	Integrative Growth Curve Difference
ROCK	Rho Kinase
FRET	Fluorescence Resonance Energy Transfer
HUMEC	Human Uterus Microvascular Endothelial Cells
TCA	Tricyclic Antidepressant
MLB	Multi-Lamellar Body
Mot#49	Motuporamine Analogue Number 49
Mot#4	Motuporamine Analogue Number
Mot#5	Motuporamine Analogue Number
Mot#20	Motuporamine Analogue Number
CAD	Cationic Amphiphilic Drug
PHS	Phytosphingosine
DHS	Dihydrosphingosine
LCB	Long Chain Base
ESCRT-III	Endosomal Sorting Complex Required for Transport III

Acknowledgements

Firstly, I would like to express heartfelt gratitude to Dr. Michel Roberge and Dr. Calvin Roskelley for their supervision, guidance, and support throughout the years that I have spent working in their laboratories. I feel fortunate to have had the opportunity to work closely with two individuals whom I sincerely respect and with whom I have enjoyed the process of learning and discovery. I would also like to thank all of the members of the Roberge and Roskelley laboratories that I have worked with in past and present years, for both technical and intellectual contributions to my work, and for friendships that have enriched my experience at UBC. In particular, thank you to Tamsin Tarling, Barbara Lelj, Sonya Cressman and Kaley Wilson for your invaluable friendships that have supported me in completing this endeavor.

I would like to acknowledge and thank those that have contributed to this work through scientific collaborations. Transmission electron microscopy was conducted in collaboration with Dr. Wayne Vogl. Thank you also to Marcia McCoy for technical assistance in preparing samples for electron microscopy, and to Aruna Balgi for performing the experiments with lysotracker red to assess lysosomal pH. Members of the laboratories of Dr. Phil Heiter and Dr. Michel Roberge collaborated in the development of the yeast haploinsufficiency screen and in the investigation of the role of sphingolipids in the mechanism of action of dhMotC in yeast cells. For this work, specific mention is due to Kristen Baetz and Tamsin Tarling. Dr. Jenny Bryan developed the statistical methods for

analyzing and comparing yeast growth. Dr. Teresa Dunn's group collaborated in the effort to assess the affect of dhMotC on ceramide levels in yeast cells.

Thank you to Dr. Masayuki Numata for critical evaluation of this manuscript and for providing technical and intellectual guidance as a member of my project committee.

Lastly, I must acknowledge and thank the Michael Smith Foundation for Health Research and the Canadian Institute for Health Research for the funding granted in support of this work.

Chapter 1: General Introduction

1.1. Carcinogenesis and Strategies for Treatment

Cancer is a disease that results from unregulated cellular proliferation. Tumours form when mutations in a cell's genetic program cause a loss of restriction on division. Surgical removal of the primary tumour is often the first course of action for treatment. However, not all tumours are amenable to surgery because of their location in the body. Metastasis is the process by which cancer cells detach from the primary tumour and spread to distant sites. Once metastasis has occurred, the efficacy of surgical removal is severely reduced. The leading cause of death in cancer patients is the aggressive growth of secondary tumours resulting from metastases (Sporn, 1996).

In 2000, Hanahan and Weinberg (Hanahan & Weinberg, 2000) described six hallmark traits of cancer cells; self-sufficiency in growth signals, insensitivity to anti-growth signals, the ability to evade apoptosis, the ability to sustain angiogenesis, the ability to invade tissues and metastasize, and limitless replicative potential (Fig. 1.1). Through successive genetic or epigenetic mutations, a normal cell can take on one or more of these phenotypes which would confer a selective advantage for clonal outgrowth. Hanahan and Weinberg's proposal of carcinogenesis predicts that a cell must acquire all six traits for a full malignant transformation to occur.

More recently, Axelrod *et al.* (Axelrod *et al.*, 2006) described the concept of tumour cell evolution by cooperation. Partially transformed cells that have acquired some, but not all of the hallmark traits of cancer can support the growth of other partially transformed cells. This occurs by sharing diffusible byproducts such as growth factors or angiogenesis-inducing signals. Non-cancerous cells, such as stromal cells in the tumour microenvironment, can also contribute to tumour growth and transformation through a similar mechanism. The cooperation theory provides an explanation for the commonly observed genetic heterogeneity within tumours. Although it is broadly accepted that the hallmark traits of cancer are required for full transformation, the evolution of multiple tumour subclones likely occurs simultaneously through the cooperation of tumour cells with other cells in the tumour microenvironment.

This modern understanding of carcinogenesis calls into question the use of classical cancer treatments such as chemotherapy or radiation regimes that attempt to induce cancer cell death by apoptosis. Many chemo- and radiation therapies induce DNA damage, and it is thought that rapidly dividing cancer cells are more sensitive to DNA damage because large aberrations in DNA structure can lead to mis-segregation of chromosomes at mitosis, which can result in mitotic catastrophe (Brown & Wilson, 2003). However, the use of chemo- and radiation therapies has had limited success, in part due to the unpredictable apoptotic responses of cancer cells with distinct genetic backgrounds (Johnstone *et al.*, 2002). For example, tumour cells with genetic mutations which confer the ability to evade apoptosis would be resistant to classical treatments. This problem is confounded by toxic side effects that limit the maximum tolerated treatment dose and prevent the administration of doses

which are lethal to tumour cells. Thus a great need exists for new therapeutic strategies which incorporate a modern understanding of tumour progression and transformation. Regardless of initial treatment responses, it is metastasis that kills the majority of cancer patients. Thus, tumour invasion and metastasis are critical targets in the development of novel cancer therapies.

1.2. Tumour Cell Invasion and Migration

In order for metastasis to occur, a cancer cell must have the ability to invade through the basement membrane of a tissue layer, the interstitial stroma, and the walls of blood capillaries (Bogenrieder & Herlyn, 2003; Geho *et al.*, 2005; Gupta & Massague, 2006). If invasive cells access the bloodstream, they can spread quickly throughout the circulatory system. Extravasation through capillary walls and colonization of new tissues is also required for tumours to multiply at secondary sites in the body. (Fig. 1.2)

90% of human cancers originate in tissue epithelium. In epithelial cancers, or carcinomas, invasive transformation often requires that tumour cells undergo an 'epithelial to mesenchymal transition' or EMT (Thiery, 2002) (Thiery & Sleeman, 2006). Firstly, primary tumour cells must lose their cell-cell attachments. Tight junctions, adherens junctions and desmosomes are three important sites of molecular attachment between epithelial cells which are essential for maintenance of tissue architecture and polarity. Of note, loss of function of the junctional protein, E-cadherin, has been well characterized as an EMT indicator and a marker for invasive transformation (Beavon, 2000). Mesenchymal cells are loosely organized

and unpolarized cells which are often characterized by the expression of the cytoskeletal protein, vimentin. Mesenchymal cells have increased migratory capabilities.

Following a loss of attachment, the next critical step towards tumour metastasis is the invasion of the extracellular matrix (ECM), a multi-molecular matrix of proteins that acts as a physical scaffold surrounding the cells (Kalluri, 2003). Cancerous cells with a mesenchymal phenotype must induce degradation of the ECM in order to clear a path for cell movement. This occurs through the secretion of proteases such as matrix metalloproteinases, or protease activators such as the urokinase-type plasminogen activator. Proteases not only causes degradation of the ECM, but the cleavage of matrix proteins also serves to generate binding sites for cell-substrate adhesion molecules called integrins. Integrin binding to the ECM is required to anchor cells during mesenchymal invasion. Furthermore, secreted proteases can also cleave and activate extracellular growth factors or chemokines which induce the forward motion of tumour cells (Koblinski *et al.*, 2000).

The mesenchymal mode of invasion has been characterized classically for its dependence on ECM degradation, the directed extension of the leading edge plasma membrane and cellular anchoring through integrin based adhesions. However, therapeutic attempts to inhibit tumour invasion by inhibiting matrix proteases has revealed a phenotypic plasticity in tumour cells (Turk, 2006). It has been recently discovered that tumour cells have the ability to migrate in a proteinase and integrin independent fashion, a process coined ‘amoeboid’ invasion (Friedl & Brocker, 2000; Friedl & Wolf, 2003) (Wolf *et al.*, 2003). This mechanism is characterized by a dynamic blebbing in cell shape. Inhibition of pericellular

proteolysis also drives the transition from collective/multi-cellular invasion to single cell invasion (Wolf, 2007). In the latter case, cell movement is more random and the cell will conform to the physical constraints of the ECM (Fig. 1.3).

Although the tumour microenvironment plays an important role in regulating cell migration during tumour invasion, classical studies in cell migration have been carried out extensively in two-dimensional tissue culture. These studies have yielded an in depth understanding of cell migration as a coordinated process involving the regulation of many signaling molecules and cellular structures (Carragher & Frame, 2004). In a simplified model of two-dimensional migration, directed cell movement is initiated by the protrusion of a broad leading membrane, termed the lamellipodium. This membrane is anchored to the underlying substratum by small integrin-dependent adhesions called focal complexes. Coordinately, contraction within the cell body leads to detachment of trailing adhesions and retraction of the rear membrane, thus, enabling translocation of the cell body in the forward direction. Cytoskeletal rearrangement is the underlying mechanism for the change in morphology during this migration process. Actin polymerization occurs within a dense meshwork of actin filaments that make up the lamellipodium (Pollard & Borisy, 2003). Growing actin filaments push against the plasma membrane and provide the force for forward protrusions. Within the cell body, actin filament bundles, called stress fibers, terminate at larger adhesion sites called focal adhesions. Acto-myosin contractile forces generated from stress fibers pull against focal adhesions and induce the cell rear retraction required for movement (Mitchison & Cramer, 1996) (Figure 1.4).

RhoGTPases are important regulators of both actin dynamics and cell-substratum adhesions in migratory cells, and thus, are critical proteins involved in tumour invasion (Hoang *et al.*, 2004; Price & Collard, 2001; Schmitz *et al.*, 2000). The effects of Rho and Rac, two sub-groups of the RhoGTPases, on actin and adhesion dynamics have been studied extensively (Burridge & Wennerberg, 2004; Hall, 1998). Rho induces the formation of stress fibers and mature focal adhesions. Rac induces lamellipodial extensions, also referred to as membrane ruffles, and the formation of smaller focal complexes which line the lamellipodium and are transient in nature. Rac1 activity has been correlated with increased migratory and invasive ability (Schmitz *et al.*, 2000). Both Rho and Rac are overexpressed in some invasive cancers (Sahai & Marshall, 2002). However, there is evidence that over-activation of Rho can lead to inhibition of cell migration through the formation of highly stable focal adhesions which impede adhesion turnover and thus the rate of cell movement (Barker *et al.*, 2004; Cetin *et al.*, 2004; Ilic *et al.*, 1995; Ren *et al.*, 2000; Vial *et al.*, 2003). Furthermore, recent studies indicate that Rho signaling is an important determinant of the cellular migration mode in three dimensional culture. In amoeboid movement during invasion, activation of Rho and the Rho effector, Rho kinase is high (Sahai & Marshall, 2003; Wilkinson *et al.*, 2005) (Gadea *et al.*, 2007). Interestingly, subcellular activation of Rho has been shown to be a critical determinant of the amoeboid transition. The E3 ubiquitin ligase Smurf1 is recruited to lamellipodial protrusions and functions to degrade RhoA at this region of the cell (Bose & Wrana, 2006; Wang *et al.*, 2003). Sahai *et al*. (Sahai *et al.*, 2007) show that loss of Smurf1 results in increased RhoA activity and loss of leading edge protrusions. Loss of Smurf1 also causes tumour cells to migrate with in an amoeboid manner.

Microtubules also play a role in the dynamic changes at the leading and trailing edges of motile cells through their involvement in vesicular trafficking. Molecular motors such as dynamin link microtubules to cargo vesicles and facilitate vesicle mediated transport of membrane proteins along microtubule tracks (Caviston & Holzbaur, 2006). For example, membrane receptors or integrins are recycled back to the leading edge of motile cells after endocytosis, sorting and targeting of endocytic vesicles (Caswell & Norman, 2006) (Jones *et al.*, 2006). In addition, vesicle transport is important for the distribution of regulatory proteins to the sites of actin reorganization at the leading and trailing edges of motile cells (Basu & Chang, 2007; Rodriguez *et al.*, 2003; Small & Kaverina, 2003). The Rab and Arf families of GTPases are key regulators of vesicular trafficking in the endocytic and secretory pathways.

1.3. Cancer Drug Discovery and Forward Chemical Genetics

Classical approaches in cancer drug discovery have utilized the target-guided method to identify potential lead chemicals for new therapies. Using this method, the selection of a potential therapeutic target is made based on the current understanding of a given biological process. Thus target-guided drug discovery is hypothesis driven, and requires an assay system that is capable of detecting the activity of the target molecule. For instance, high throughput *in vitro* enzyme assays have been commonly used for drug screening in the pharmaceutical industry (Kawasumi & Nghiem, 2007). Molecular modeling and combinatorial chemistry are fueling a rapid escalation in the *de novo* generation of synthetic compound libraries that can be used in such drug discovery endeavors. However, natural

product libraries continue to be an important reservoir of chemically diverse bioactive molecules that can be screened in the form of crude extracts (Koehn & Carter, 2005; Mann, 2002). Because target-guided drug discovery reduces the need for lengthy studies on drug mechanism of action, this approach has had some success in the discovery of novel anti-tumour drugs. However, caveats in the target-guided approach exist. Importantly, and particularly for cancer, selection of the therapeutic target is based on an incomplete understanding of the disease mechanism. Furthermore, the biologically simplified context of the *in vitro* assay is a limitation. These assays may identify inhibitors that lack therapeutic potential in the molecularly complex *in vivo* environment. Drug specificity is a major issue because additional off-target drug interactions may lead to toxic side effects. These factors often negate the development of a lead chemical for clinical use (Stockwell, 2000). Because i*n vivo* efficacy is of ultimate importance, the use of high throughput cell-based assays and a 'forward chemical genetics' approach has become a popular alternative to *in vitr*o, target driven methods for cancer drug discovery.

'Forward chemical genetics' is a term used to describe the use of chemicals as tools or probes to facilitate the investigation of a biological process (Lokey, 2003) (Fig. 1.5). Rather than specifically testing the activity against a pre-selected protein, in forward chemical genetics, cell based assays are used to screen compound libraries for activity against a disease phenotype. By investigating the mechanism of action and pursuing drug target identification of lead chemicals, researchers are guided to better understand the molecular biology that governs a specific disease event. In particular, this approach can lead to the identification of a new function or involvement of the drug target in the phenomenon

of interest. Understanding the mechanism of action of a lead compound will also support the development of the lead compound for therapeutic use.

1.4. High-throughput Assessment of Tumour Cell Invasion

The quantitative assessment of *in vitro* cell migration or tumour invasion is not a trivial task. A handful of techniques are available to assess cell migration in two or three dimensions (depending on the presence of extracellular matrix components in the assay context) (Decaestecker *et al.*, 2007), however, few exist that satisfy all the requirements of high-throughput quantitation while maintaining biological relevance. Cell migration in two-dimensions can be assessed by observing the time required for closure of a wounded monolayer on tissue culture plastic. However, wound closure assays lack the presence of ECM, which provides the conditions that are relevant to the tumour microenvironment. Therefore, these two-dimensional assays are used because of their simplicity, and can be complemented with parallel observations of the cells' capacity to invade ECM. Matrigel is a commercially available ECM (originating from an *in vitro* cultured mouse sarcoma (Kleinman & Martin, 2005)) that is often used in tissue culture to provide the biologically relevant microenvironment for invasion studies.

Quantitation of tumour invasion through ECM is often achieved by employing the classical Boyden Chamber assays (Waller *et al.*, 1986) These assays are carried out in two-chambered tissue culture dishes in which the top and bottom chambers are separated by a porous filter coated with ECM components. Cells are plated on top of the ECM and invasion

is measured by counting the number of cells that pass through the ECM to the bottom side of the porous filter (Fig. 1.6). In these assays, inhibition of invasion is marked by a negative readout (ie. a reduction in the number of cells on the bottom filter). Although Boyden chamber assays provide accurate measurements of cellular invasive potential, the laborious task of processing filters and counting cells makes these assays incompatible with the high throughput requirements of a drug screening project. Furthermore, the negative readout is an undesirable aspect when drug screening because of the high occurrence of false hits that arise due to the general cytotoxic effect of many compounds.

High-throughput cell based assays for tumour invasion have only recently been established (Maliakal, 2002; Roskelley *et al.*, 2001). As an undergraduate student working in the laboratories of Dr. Calvin Roskelley and Dr. Michel Roberge, I developed an invasion assay with a positive read-out for invasion inhibition that has the capability to be used for high-throughput drug screening (Roskelley *et al.*, 2001). This assay identifies compounds that inhibit invasion while maintaining cell viability and cellular adhesions to the ECM. Cells are plated on ECM in a 96-well plate format and invasion is quantified by measuring the number of cells that do not invade, but remain attached on top of the matrix. The non-invasive cells are removed from the ECM and quantified using a colorimetric cell viability assay, thus generating the positive-readout (Fig. 1.7). Positive hits in this assay can be identified visually; wells with a strong blue color contain active compounds, whereas, wells that are yellow contain non-active chemicals or the negative control. Optical density values can also be measured with a spectrometer and used in smaller scale hypothesis based

experiments to reproducibly quantitate differences in the invasive capability of cells under specific treatment conditions.

A ‘forward chemical genetics’ project was initiated using this high-throughput invasion assay to screen a natural extract library collected from the coast of Papua New Guinea. After screening approximately 500 extracts as an initial proof of principle, two extracts from the organisms *Petrosia (Strongylophora) corticata* and *Xestospongia exigua* were identified as anti-invasive. Subsequent assay-guided fractionation (in collaboration with chemists in the laboratory of Dr. Raymond Andersen) led to the purification of two invasion inhibitors with chemically distinct structures; motuporamine C (MotC) (Williams *et al.*, 2002) and strongylophorine-26 (STP-26) (Warabi *et al.*, 2004).

1.5. Drug Target Identification: Using Yeast as a Model Organism in a Genome Wide Drug-induced Haploinsufficiency Screen

When taking a forward chemical genetic approach, target identification can pose a major problem because it is the least systematic step in the process of drug discovery (Lokey, 2003). Classical methods include, for example, to purify the target from cellular extracts by using immobilized or radiolabeled versions of the chemical (Lokey, 2003). However, it is often difficult to chemically modify small molecules without affecting the biologically active portion of the compound. Alternatively, the candidate approach can be used if there is an extensive background of knowledge that supports the election of possible candidate drug-targets. Candidates would then need to be tested one by one in binding or functional assays.

Chemical structure can be an indicator of possible target interactions, however, without prior knowledge of the pathways affected by the drug, these approaches have met with little success. Thus, systematic genomic and proteomic methods are needed to test a wide range of drugs against all possible targets in a cell.

The budding yeast *Saccharomyces cerevisiae* has been proposed as a tool for identifying human drug targets because ~40% of yeast proteins share some conserved sequence with at least one known or predicted human protein, including several hundred genes implicated in human disease (Hughes, 2002; Parsons *et al.*, 2003). Using yeast instead of human cells has many technical advantages. The life cycle is rapid and therefore, cells can be grown quickly, and cost effectively in liquid media or as colonies on solid agar. Yeast cells are easy to modify genetically, and genome-wide sequence information has made possible the creation of genome-wide sets of yeast deletion or overexpression mutants that can be utilized for various applications (Sturgeon *et al.*, 2006). Recent technological advances in yeast genomics, including gene expression profiling, chemical-genetic synthetic profiling, and drug-induced haploinsufficiency, show promise as tools to study proteins and pathways affected by drugs at a genome-wide level (Hughes, 2002; Parsons *et al.*, 2003).

Drug-induced haploinsufficiency occurs when lowering the dosage of a single gene from two copies to one copy in diploid cells results in a heterozygote that displays increased drug sensitivity compared with wild-type strains (Giaever *et al.*, 1999). In yeast, quantitative assessment of drug sensitivity can be easily obtained by conducting liquid or solid agar growth assays. Giaever *et al.* (Giaever *et al.*, 1999) pooled 233 ‘‘genetically bar-coded’’

heterozygous yeast strains, grew them competitively in the presence of a drug whose target in yeast cells was known, and successfully used DNA microarrays to identify the heterozygous drug target strain whose growth was compromised in the presence of the drug.

In a collaborative project between the laboratories of Dr. Michel Roberge and Dr. Phil Heiter, we developed a genome-wide drug induced haploinsufficiency screen that used colony formation on solid agar as the phenotypic readout to determine drug-induced sensitivity. We asked if this genome-wide assay could facilitate target identification of lead compounds that are identified in the 'forward chemical genetic' cancer drug discovery project. We screened the yeast haploid deletion set for sensitivity to the anti-invasive motuporamine analogue dihydromotuporamine C.

1.6. Thesis Goals and Summary of Results

A forward chemical genetics project was initiated with the discovery of two novel invasion inhibitors, strongylophorine-26 and motuporamine C. The goal of this project was to pursue an understanding of the mechanism of action of these comounds for the purpose of furthering the development of the compounds as potential cancer therapies. Novel inhibitors can also be extremely useful as tools to probe a specific biological process. In order to guide the forward chemical genetics approach, three general objectives were set. Firstly, one objective was to evaluate the effects of these molecules on phenotypes related to cell migration and tumour invasion. The second objective was to assess the structure-activity relationship of the inhibitors. The third objective was to test the role of intracellular signaling

molecules, in an effort to determine the target pathways that are affected by the invasion inhibitors. Objectives one and two could be performed independently of each other, in contrast to objective three which partially relied on the results of objectives one and two to guide the formation of hypotheses. Independent, systematic means of acheiving objective three were also pursued, for example, the genome-wide drug induced haploinsufficiency screen was used to identify target molecules involved in drug mechanism of action.

In Chapter 3, the results of the initial evaluation of drug-induced phenotypes, and some structure-activity studies are presented. In particular, both STP-26 and the synthetic analogue dihydromotuporamine C (dhMotC) alter the organization of the actin cytoskeleton and induce the formation of large focal adhesions. Furthermore, Rho was identified as a physiological target of both molecules. It is shown that Rho activation, at least in part, is responsible for the anti-invasive activity of these inhibitors. Increased adhesion strength and loss of polarity are two outcomes of Rho activation which likely mediate their anti-migratory effects on tumour cells.

dhMotC is potent and easy to synthesize. Synthesis of STP-26, however, is not easy. The lack of an abundant source of STP-26 prevented further mechanistic studies on this molecule and thus limited the potential of this compound as a future drug candidate. Therefore, drug-target identification was pursued for the motuporamines. Structure-activity studies for the motuporamine were conducted prior to the intiation of the thesis research. Results from these studies are presented in the introduction to Chapter 4. In the results section of Chapter 4, a second phenotypic outcome of motuporamine treatment is presented,

one which was identified based on cues from the cationic amphiphilic structure of motuporamine analogues. It has been reported that many cationic amphiphilic drugs affect the trafficking and degradation of cellular membranes, a phenotype termed drug-induced lipidosis. It was found that motuporamines cause membranes to accumulate inside cells and also inhibit the degradation of the internalized ligand bound epidermal growth factor receptor. This phenotypic outcome of motuporamine treatment correlates well with the invasion activity of motuporamine analogues, which suggests that the disruption of normal vesicular trafficking and lysosomal degradation activity may be an important aspect of the mechanism for invasion inhibition by motuporamines.

Finally, presented in Chapter 5 is the results of a novel genome-wide haploinsufficiency yeast screen that was designed and performed in an effort to systematically identify protein targets of drug candidates with unkown mechanism of action. dhMotC was used as a pilot molecule in a proof-of-principle study for this novel screen. The resulting data from this screen highlighted the sphingolipid metabolism pathway as a target of dhMotC primarily in yeast cells. Further investigations in human cells revealed that motuporamine affects ARF1 (ADP ribosylation factor 1) function. Abrogation of ARF1 activity with the small molecule inhibitor brefeldin A reduced the morphological and anti-invasive effects of motuporamine treatment, thus indicating that dhMotC is an ARF1 activator. The advantages and pitfalls of using genome-wide yeast screens as a tool to identify drug mechanism of action of in human cells is also discussed.

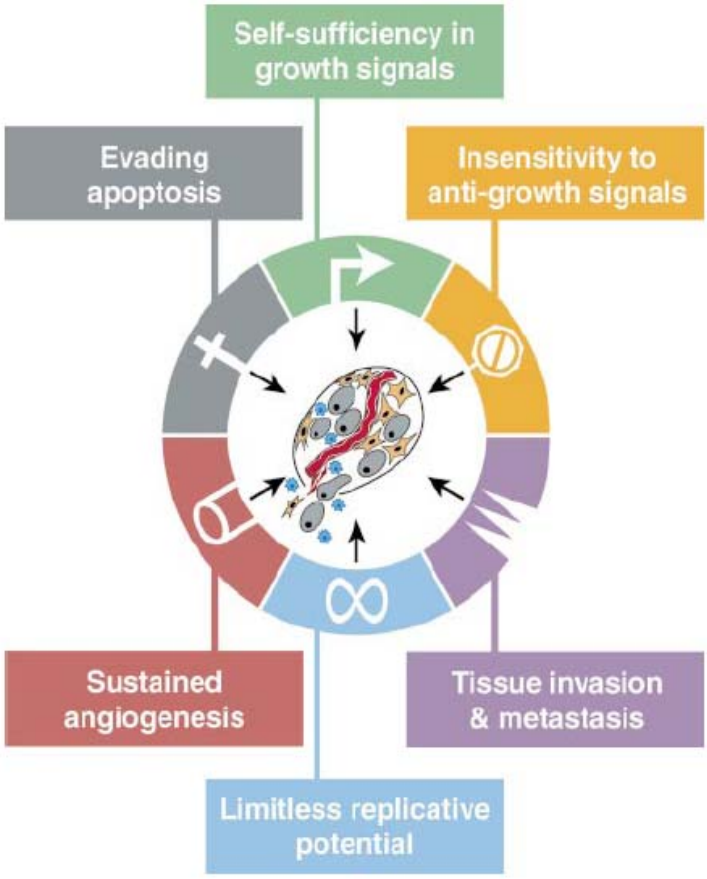

Figure 1.1. Acquired capabilities of cancer. Hanahan and Weinberg suggest that most if not all cancers have acquired the same set of functional capabilities during their development. (Adapted from Hanahan & Weinberg, 2000)

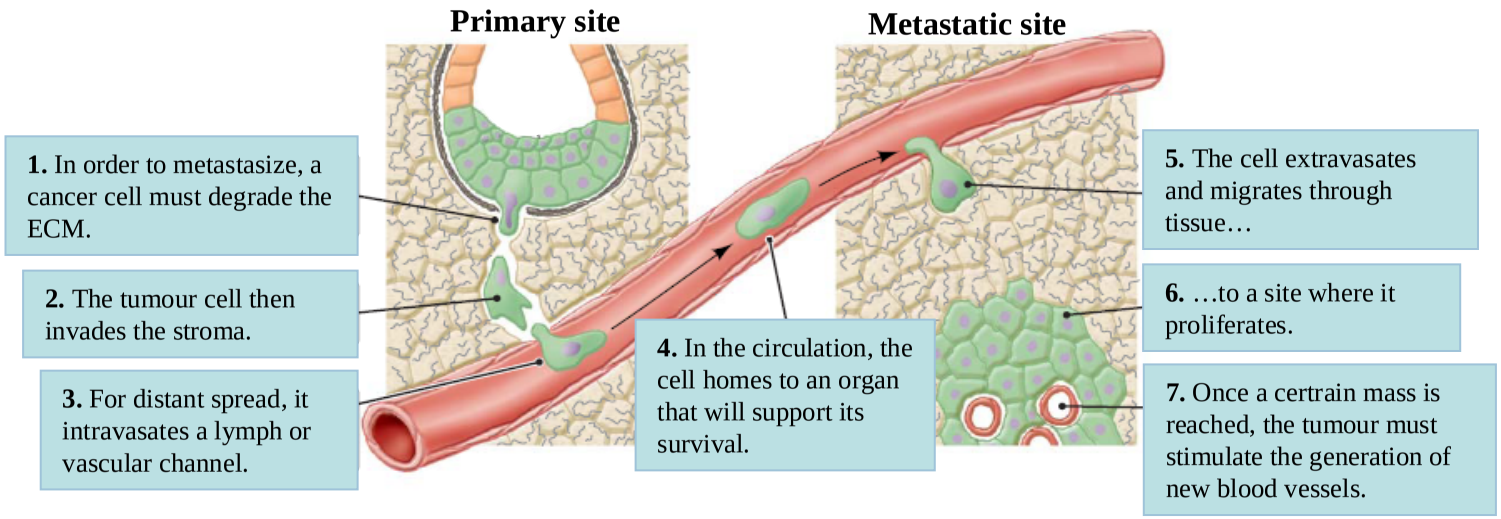

Figure. 1.2. The metastatic sequence.
(Adapted from Geho *et al*. 2005.)

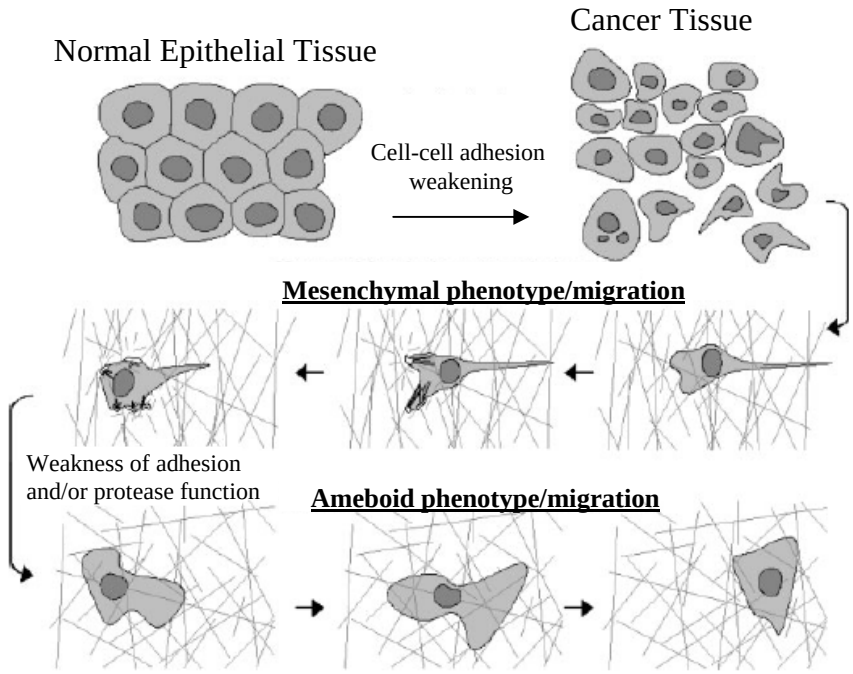

Figure 1.3. Transitions in the cell migration process occurring in cancer cell de-differentiation. Cell-cell adhesion is lost during epithelial-mesenchymal transition, a phenomenon which enables tumour cells to detach themselves from the collective and migrate using a mesenchymal mode. This mode essentially consists of cell polarization followed by the extension of cytoplasmic protrusions which adhere to the ECM through adhesion sites. After the local degradation of the matrix by tumour-cell-associated proteases, the cell moves forward into the region of the proteolysis-modified matrix by means of cell contraction due to the shortening of the actin filaments. Mesenchymal-amoeboid transition occurs after the weakening of the cell-ECM adhesion and/or protease functions. Ameoboid migration essentially consists of rapid cycles of morphological expansion and contraction. (Decaestecker *et al*., 2007.)

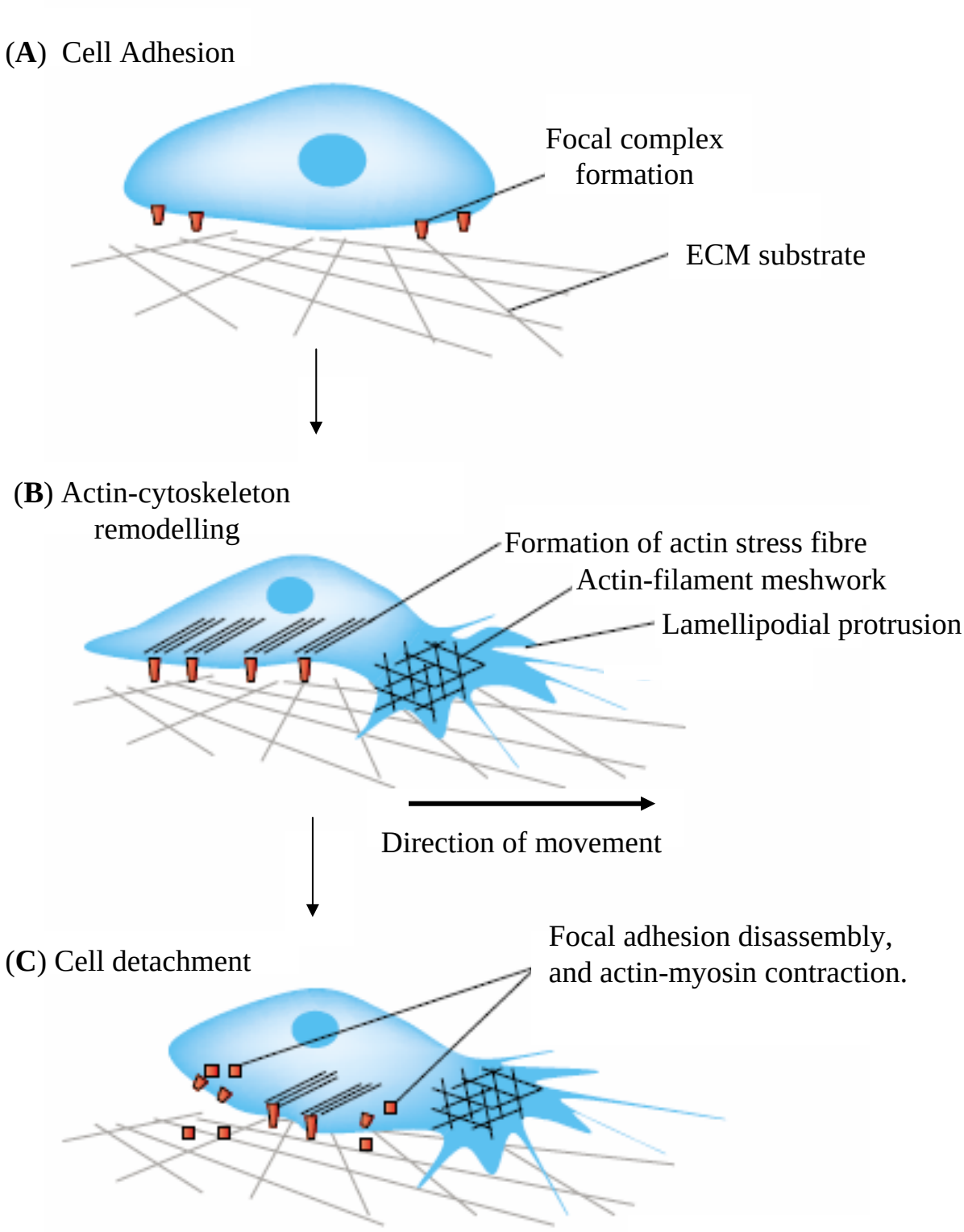

Figure 1.4. Cell motility. A dynamic cycle of (**A**) adhesion assembly, (**B**) actin remodelling and (**C**) adhesion disassembly. (Adapted from Carragher, 2004)

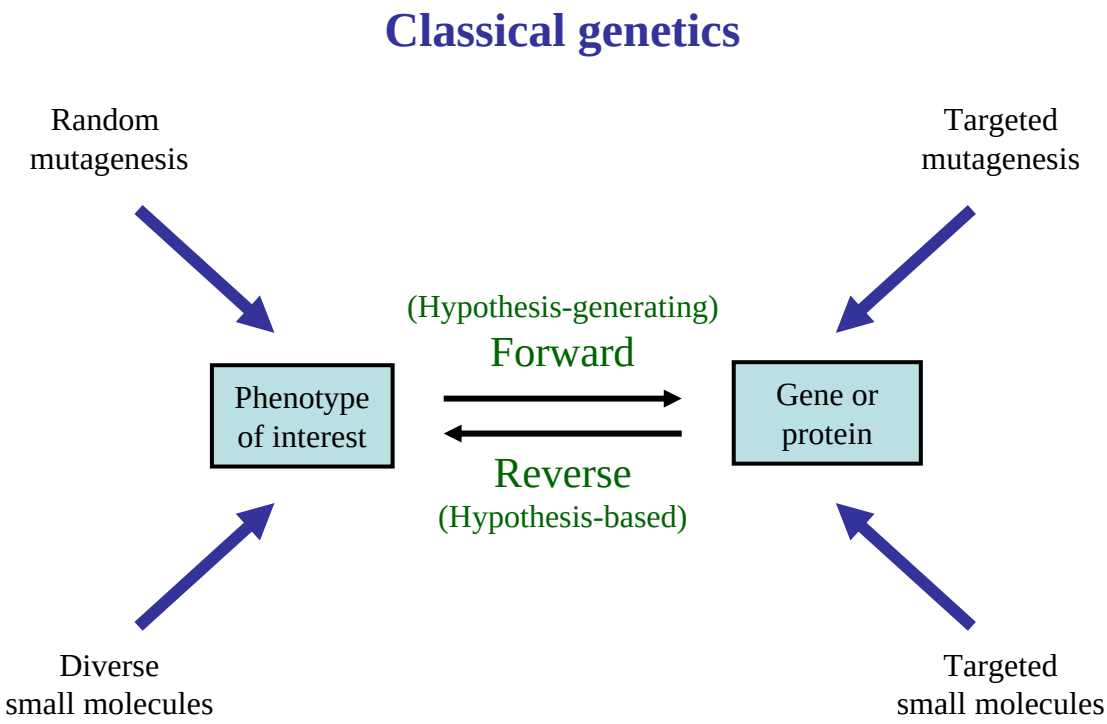

Figure 1.5. Classical and chemical genetic approaches. Classical genetics uses mutagenesis as a means of elucidating the relationship between genes and phenotypes, whereas chemical genetics employs small-molecule compounds to achieve the same general goals. A forward genetic study is a hypothesis-generating approach through which the gene responsible for the affected phenotype is identified. A reverse genetic study is a hypothesis-based approach in which genes or proteins are manipulated to characterize their role via identifying the resulting phenotype. (Adapted from Kawasumi *et al*. 2007)

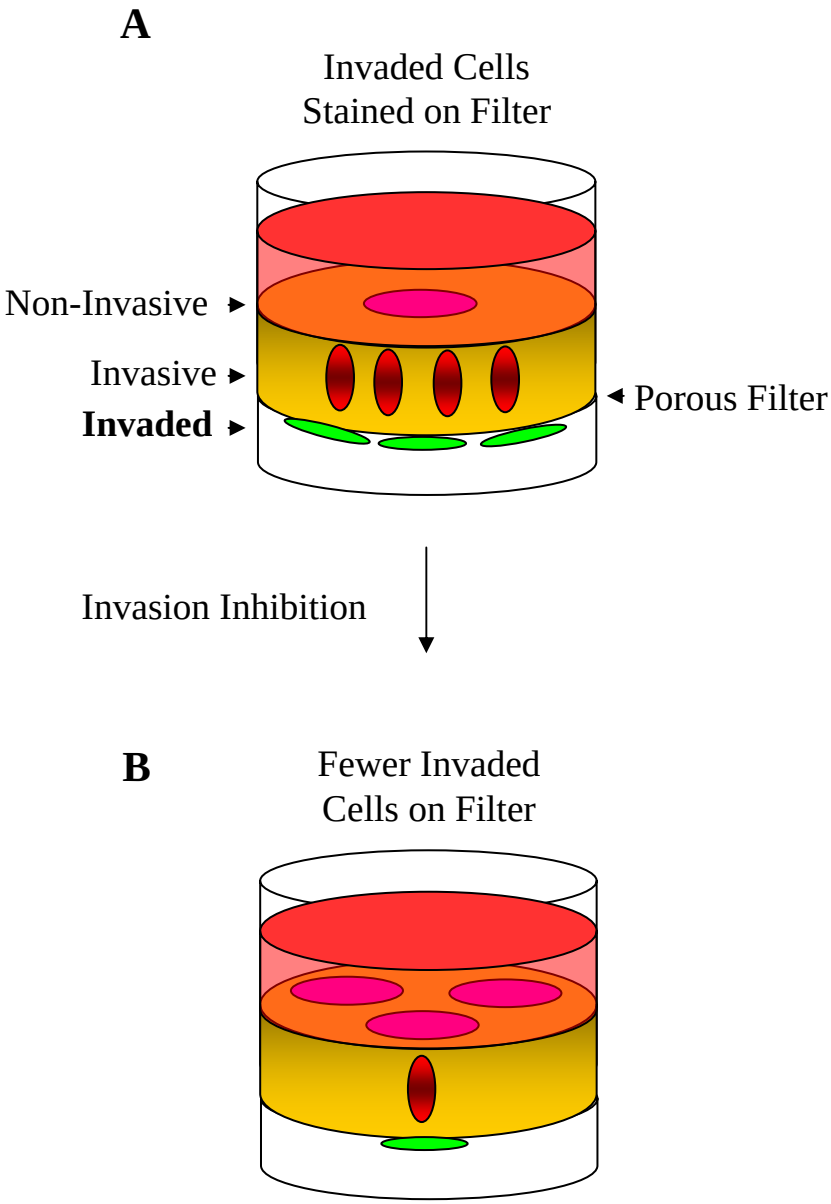

Figure. 1.6. Classical assay for invasion inhibition.
A, Cells are plated on a porous filter coated with an extracellular matrix. Invasive cells pass through the matrix to the underside of the porous filter. Invasion is quantified by removing the filter, staining cells, and counting the number of cells on the bottom side. **B,** When an invasion inhibitor is present, fewer cells will be present at the bottom side of the filter. Thus invasion inhibition has a negative readout in this assay. Pitfalls of a negative readout include false positives due to cell detachment or cytotoxicity.

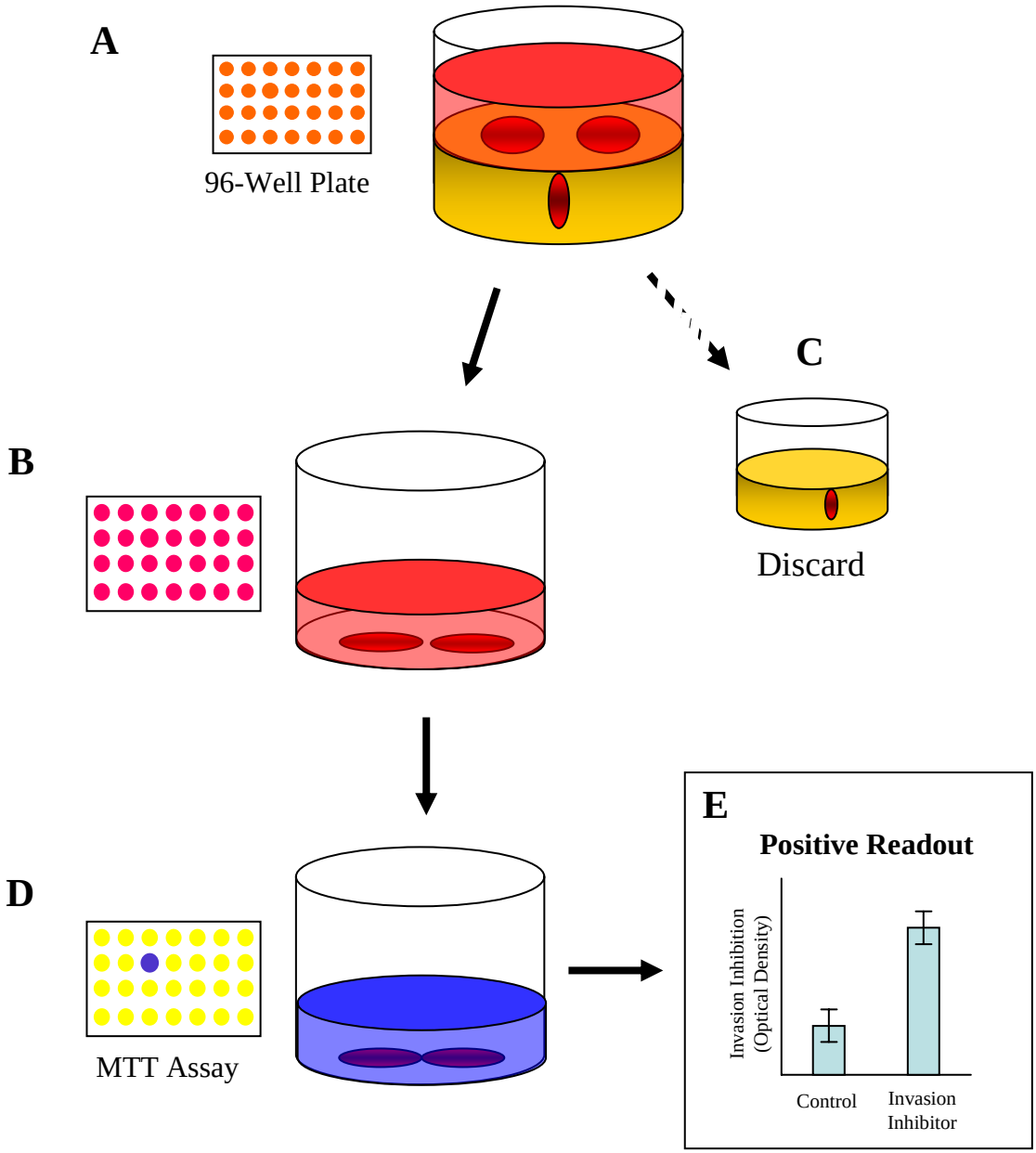

Figure. 1.7. High-throughput screen for invasion inhibitors.
A, Highly invasive MDA-MB-231 cells are plated on top of matrigel in a 96-well tissue culture dish. Crude extracts or a negative control are added at the time of plating and cells are incubated while invasion occurs. **B,** Non-invasive cells are trypsinized from the top of the matrigel and transferred to an uncoated 96-well plate. **C,** Invasive cells are discarded with the original matrix coated plate. **D,** After attachment, non-invasive cells are quantified by measuring the optical density of the media after performing an MTT assay. **E**, Invasion inhibition has a positive readout, and thus, this assay eliminates false postitives that would arise from cytotoxicity.

Chapter 2: Materials and Methods

2.1. Inhibitors and Biocompounds. Strongylophorine-26 was isolated from a methanol extract of the marine sponge *Petrosia (Strongylophora) corticata* as described recently (Warabi *et al.*, 2004). Motuporamine analogues were synthesized as described previously (Williams *et al.*, 2002). Because of slight differences between batches, optimal activity was found to range between 5 and 10 μM. Thus, these two concentrations were used interchangeably throughout the study. C6-ceramide, dihydrosphingosine, sphingosine, sphingosine-1-phosphate, Y-27632, tricyclic antidepressants and brefeldin A were purchased from Sigma (St. Louis, MO).

2.2. Mammalian Cell Culture. MDA-MB-231 breast carcinoma cells were routinely maintained in DMEM/F12 medium (Invitrogen, Carlsbad, CA) supplemented with 5% fetal bovine serum (FBS; Invitrogen) and 5 μg/ml insulin (Sigma). Mouse Swiss 3T3 fibroblasts and MCF-7 $p53^{-/-}$ cells were maintained in DMEM medium (Invitrogen) supplemented with 10% FBS.

2.3. Three-step Matrigel Invasion Assay. *Briefly*, MDA-MB-231 cells were plated on reconstituted basement membrane gels (Matrigel; BD Biosciences, Mississauga, Canada) in the absence or presence of various compounds for 1–3 h, and elongated, invasive morphology was assessed by phase contrast microscopy. The number of viable cells that did not invade the gel was then determined quantitatively; noninvasive cells were removed from the top of the gel by light trypsinization, allowed to reattach to tissue culture plastic for 18 h

in separate wells, and viable cells were quantified using a colorimetric cytotoxicity assay. Thus, unlike "classical" Transwell/Boyden chamber assays, this quantitative assay uses a positive readout for invasion inhibition that eliminates false positives caused by cytotoxicity.

In detail, reconstituted basement membrane (Matrigel; Collaborative Biomedical Products) was diluted 1:1 in ice cold DMEM:Ham's F-12, and 50 µl was distributed into each well of ice-cold 96-well cell culture plates. The plates were transferred to a 37°C incubator overnight to allow the Matrigel to polymerize and adhere to the plastic. On top of the Matrigel was added 100 µl of growth medium warmed to 37°C. When conducting experiments to test mechanism of action, various cocktails of inhibitors were added at this stage depending on the experimental conditions. Following the addition of inhibitors, 100 µl of medium containing 60,000 highly invasive MDA-MB-231 cells was added to each well. DMSO served as a negative control. The cells were then incubated for 1-3 h (depending on experimental conditions) to allow invasion to take place. After incubation, cells had either invaded the Matrigel or failed to invade and settled on the surface of the Matrigel. The cell culture medium was then removed without disturbing the cells using the aspiration function of a Bio-Tek ELx405 96-well plate washer with the aspiration needles positioned about 2 mm above the surface of the Matrigel. The attached cells that failed to invade were recovered by detaching them from the surface of the Matrigel by incubation with 200 µl of 0.125% trypsin in HBSS for 30 min at 37°C. The cells were then suspended by pipetting up and down three times using the 100-µl setting of a hand-held pipettor, and 100 µl were withdrawn and transferred to fresh plates without Matrigel containing 100 µl of medium supplemented with 30% FBS. The cells were then incubated overnight to allow attachment of

cells to the plastic surface, and live cells were measured using the 3-(4,5- dimethylthiazol-2-yl)-2,5-diphenyltetrazolium bromide (MTT) (Sigma) assay (Mossman, 1983). Thus, invasion inhibition is proportional to the number of live cells detected in the MTT. The positive readout for invasion inhibition eliminates false positives caused by cytotoxicity. For experiments involving serum starvation, cells in subconfluent monolayer culture were maintained in unsupplemented medium for 18 h before the initiation of the described procedures.

2.4. Cell Migration Assays. Confluent MDA-MB-231 cell monolayers were wounded with a sterile toothpick and cells were allowed to migrate into the wound over a 12-24 h period in the presence of inhibitors or the vehicle control. Migration was assessed by taking phase contrast photographs of the wound at a fixed location in the tissue culture wells. Photographs of control and drug treated cells were compared for various timepoints.

2.5. Fluorescence Microscopy of Mammalian Cells. For tubulin immunostaining, cells were fixed (3.7% formaldehyde in PBS, 15 min at 25°C), simultaneously permeabilized and blocked (0.1% Triton X-100 and 1% BSA for 30 min at 4°C), and then incubated with mouse monoclonal antibodies against β-tubulin (1 μg/ml; Developmental Studies Hybridoma Bank, University of Iowa). For immunostaining of vinculin, EGFR, LAMP2, Transferrin Receptor, PDI and GM-130, cells were fixed (3.7% formaldehyde in PBS, 15 min at 25°C), permeabilized (0.6% Triton X-100 in PBS for 5 min at 25°C), blocked (10% FBS, 2% BSA in PBS for 30 min at 25°C), and then incubated with the appropriate primary antibody for 60 min at 25°C. Source and dilutions of primary antibodies were as follows: mouse monoclonal

anti-vinculin (460 ug/ml; Sigma), mouse monoclonal anti-EGFR (3 μg/ml; Merck), AC17 mouse monoclonal anti-LAMP2 (1/100, gift from Dr. Robert Nabi (Nabi *et al.*, 1991)), mouse monoclonal anti-transferrin receptor (5 μg/ml, Zymed), mouse monoclonal anti-PDI (5 ug/ml, Stressgen), mouse monoclonal anti-GM130 (2.5 μg/ml, BD Transduction Laboratories). Primary antibody binding was detected using CY3-conjugated goat anti-mouse IgG, F(ab')2 fragment-specific antibodies (Jackson Laboratory, West Grove PA). F-actin was visualized after fixation (3.7% formaldehyde in PBS, 10 min at 25°C), acetone extraction (100%, 5 min at -20°C), and air drying followed by staining with rhodamine-labeled phalloidin (0.5 units/ml; Molecular Probes, Eugene OR). For phospholipid or GM-1 staining, cells were fixed (3.7% formaldehyde in PBS, 15 min at 25°C), permeabilized (0.1% Triton X-100 in PBS for 5 min at 25°C), and stained with Nile Red (diluted 2 μg/ml, for 30 min) (Sigma) or FITC-conjugated cholera toxin (10μg/ml, for 45 min) (Sigma). Images were generated using a Nikon Eclipse E400 microscope equipped with an Imaging Microimager II digital camera.

2.6. Rho Activation Assays. Activated, GTP-bound Rho proteins were isolated by coprecipitation with the Rho-binding domain of rhotekin and quantified by Western blotting according to the manufacturer's instructions (Upstate Biotechnology, Lake Placid, NY) using reagents and protocols originally developed by Ren *et al.* (Ren *et al.*, 1999). Neither the coprecipitation with the recombinant rhotekin fragment nor the antibody used for Western blotting is specific for individual Rho isoforms. Thus, these experiments were designed to assess the aggregate activation state of all mammalian Rho isoforms. Blotting of unprecipitated whole cell lysates with the pan-Rho antibody was carried out to demonstrate

that observed changes in activation state were not caused by changes in steady-state Rho protein levels.

2.7. C3 Exoenzyme Loading into Live Cells. The Rho inhibitor C3 exoenzyme from *Clostridium botulinum* (Calbiochem, San Diego, CA) was introduced into cells using the method of Renshaw *et al.* (Renshaw *et al.*, 1996). Briefly, to load cells, 5–20 μg/ml C3 exoenzyme (from 500 μg/ml stock reconstituted in DMEM/F12 base medium) were mixed with 5 μg/ml lipofectin (Invitrogen) 1:1 in medium lacking FBS and incubated with either MDA-MB-231 or Swiss 3T3 cells for 14 h at 37°C before initiating the experiments described. The Rho activation assay was used to demonstrate that C3 loading effectively inhibits activity of RhoGTPase.

2.8. Transmission Electron Microscopy. 50,000 MDA-MB-231 were plated 12-well plate filter inserts (Falcon) and allowed to adhere over night before addition of Mot#20 or DMSO for 6 h. Cells were fixed (1.5% paraformaldehyde, 1.5% gluturaldehyde in 0.1M Na Cacodylate buffer (pH7.3, 37°C) for 2h at room temperature. Cells were washed three times (10 min each) in 0.1M Na Cacodylate buffer (pH 7.3), post-fixed (1% osmium tetroxide in 0.1M Na Cacodylate buffer for 30 min on ice), washed again, three times in ddH_2O (10 min each) before labeling with 1% uranyl acetate (30min, room temp). Cells were washed in ddH_2O (3 times, 5 min each) before dehydration in an ascending ethanol series (30%, 50%, 70%, 95% (10 min each) and finally 100%, 3 times 10 min). This treatment was followed by two incubations of 15 min each in propylene oxide. The cells were then left in a 1:1 solution of propylene oxide: Polybed overnight for 30 min before embedding in 100% Polybed. The

resin polymerized at 60°C for 24 h. Sections were viewed and photographed in collaboration with Dr. Wayne Vogl, on a Philips 300 electron microscope operated at 60 kV.

2.9. EGF Trafficking and Degradation Assay. MDA-MB-231 cells were plated on glass cover slips in 6-well tissue culture plates and grown until they were approximately 60% confluent. To image EGF binding to receptors on the cell surface without internalization, cells were incubated at 4°C for 1h with FITC-conjugated EGF (0.4 μg/ml, Molecular Probes) in binding medium (normal growth medium supplemented with 2 mg/ml BSA (Sigma)). Cells were then washed two times in cold binding medium before addition of inhibitors in normal growth medium. To allow internalization of receptor bound EGF, cells were incubated at 37°C for various time periods and then fixed in 3.7% formaldehyde for 15 min, washed 2 times in PBS and mounted on cover slips for viewing and imaging using confocal microscopy, or a Nikon Eclipse E400 microscope equipped with an Imaging Microimager II digital camera.

2.10. Lysotracker Red Assay to Indicate Lysosomal pH. MCF-7 $p53^{-/-}$ cells were plated on coverslips overnight and the pretreated with 100nM lysotracker red for 25 min before the addition of motuporamine or DMSO for 35 min. Cells were fixed in 3.7% formaldehyde for 15 min, washed and then DNA was stained with Hoechst 33342 for 2 min. Cells were washed again two times and then mounted on glass slides for viewing with a fluorescence microscope.

2.11. Mammalian Cell Survival Assays. MDA-MB-231 cells were plated at 10,000 cells per well in 96-well culture dishes and were allowed to grow overnight. They were subsequently exposed to motuporamines and/or various sphingolipids for 24 h. Cell survival was measured by using the MTT assay (Sigma).

2.12. Yeast Strains, Media, and Genetic Manipulations. The diploid heterozygous deletion mutants generated by the International Deletion Consortium (Winzeler *et al.*, 1999) were obtained from Research Genetics/Invitrogen. BY4743 was used as the diploid wild-type control. TDY2037 (wild-type) and TDY2038 (*csg2*Δ) *MAT*α haploid strains were described (Beeler *et al.*, 1998). Yeast was grown on/in standard rich medium [1% yeast extract, 2% peptone, 2% dextrose (YPD)] with or without 2% agar at 30°C.

2.13. Drug-Induced Haploinsufficiency Screen. The deletion mutant arrays (DMA) were propagated on rich liquid medium containing G418 (200 mg/litre, GIBCO/BRL). The DMA were transferred by hand with a model VP408FH 96-floating pin replicator (V & P Scientific, San Diego) and a VP380 colony copier (V & P Scientific) into 96-well plates containing 100 μl of liquid YPD and were grown overnight at 25°C to saturation. Replicator sterilization procedures were as described (Tong *et al.*, 2001). Saturated cultures were used to compensate for differences in growth rate between strains and ensure that roughly equal amounts of cells were deposited on the agar plates. After 24 h, the DMA were pinned onto plates (OmniTray, Nunc) containing YPD-agar and DMSO (6 μl/ml) or 60 μM dhMotC and DMSO (6 μl/ml). DMA were arrayed at high density by using a BioRobotics TAS1 robot with a 0.4-mm diameter 96-pin tool that spots ≈20 nl or ≈250 cells. Strains were pinned in

duplicate with a density of 1,536 per plate. Pins were sterilized by agitating for 30 s in 10% bleach followed by 95% ethanol for 15 s and drying with warm air for 15 s. Plates were grown at 25°C and strains were scored for growth, slow growth, or no growth, compared with no drug over a period of 4 days.

2.14. Growth Rate Analysis of Individual Yeast Strains. Growth rates of strains were measured under various drug conditions essentially as described (Giaever *et al.*, 1999). Cells were diluted from an overnight culture to an OD_{600} of ≈0.01 and were allowed to grow until the OD_{600} reached ≈0.05 (t = 0) to ensure that cells were in logarithmic phase. Drug was added and growth rates were measured by determination of OD_{600} as a function of time by using a Pharmacia Biotech Ultrospec 3000 or a Tecan Sunrise plate reader. Growth curves were carried out in triplicate and curves shown are averages of three experiments with error bars representing 1 SD.

2.15. Integrative Growth Curve Difference (IGCD) Analysis. The growth of 29 strains without drug and in the presence of 20 μM dhMotC was analyzed over time. OD_{600} measurements of cell density were taken hourly for 10 time points. The typical level of replication was three growth curves per strain per condition, for a total of six curves per strain. The cultures underwent exponential growth during the time points and conditions studied. Therefore, a log-transformed linear model was used to relate growth to time by using the model: $\log OD_{600\ g}(t) = \beta_{0g} + \beta_{1g} M + \beta_{2g} t + \beta_{3g}\ tM + \varepsilon_g$ where g indicates the strain, M indicates the presence of dhMotC, and t indicates time. The intercept of this model, equal to $\beta_{0g} + \beta_{1g} M$, captures early growth and β_{1g} is the adjustment due to dhMotC. The slope, equal

to $\beta_{2g} + \beta_{3g} M$, reflects the steady-state doubling time and β_{3g} is the adjustment due to dhMotC. Both the intercept and the slope were modified by the presence of dhMotC, indicating early and persistent effects on growth, respectively. The dhMotC effect on growth was highly statistically significant ($P < 10^{-11}$) for all 29 strains evaluated, when quantified by using an *F* test for a restricted model that does not include the dhMotC terms. Strains were ranked according to the cumulative dhMotC effect or IGCDs, denoted D_g, as measured by the area between the expected growth curves with and without drug. Because these curves were linear on the transformed scale, the integral has the following simple form $D_g = (-T\beta 1_{,g} - T^2/2)$ $\beta_{3,g}$. Therefore, the final quantitative measure of cumulative dhMotC effect on each strain is the estimated value of D_g, obtained by evaluating the above expression at the estimated dhMotC regression coefficients. (This method for statistical analysis of yeast growth rates was developed and performed by Jenny Bryan at Michael Smith Laboratories, UBC.)

2.16. Lipid Trafficking Assay in Yeast. EIS20-2B cells were grown overnight to saturation, then diluted and allowed to grow for 3-4 hrs until OD_{600} values reached approximately 0.05, indicating that cells were growing in log phase. Cultures were pelleted at 400g and re-suspended to an OD_{600} value of 3.0. For each assay condition, 100ul of concentrated culture was aliquoted to an eppendorf tube. Yeast cells were pre-incubated at room temperature with motuporamine or DMSO for 45 min. 40 μM FM4-64 was added to each tube and cells were incubated for a further 30 min on ice to prevent internalization of the dye. To remove unbound dye, cells were pelleted in a benchtop microcentrifuge (1 min, 3000 rpm), washed in YPD medium two times and then incubated in YPD (replenished with inhibitors) for 1 h at room temperature. For live cell fluorescent microscopy, 5 ul of resuspended culture was

dropped on a glass slide and covered with a glass cover slip. Cells were photographed and counted manually to quantify the percentage of cells displaying a defect in the trafficking of FM4-64 bound lipids to the yeast vacuolar membrane.

2.17. Database. For further information, refer to the *Saccharomyces* Genome Database, which can be accessed at www.yeastgenome.org.

Chapter 3: Characterization of the Anti-invasion Activity of the Novel Tumour Invasion Inhibitors: Dihydromotuporamine C and Strongylophorine-26

3.1. Introduction

The goal of this forward chemical genetics project was to identify small molecules that target tumour invasion and to use these molecules as tools to uncover the underlying biological processes that are involved in this disease event. Using the phenotypic tumour invasion screen that I developed, I screened a library of crude natural extracts for invasion activity. A small number of active extracts were identified. In collaboration with members of Dr. Raymond Andersen's laboratory in the Department of Chemistry at UBC, I participated in the assay guided fractionation of two of these extracts from marine organisms that were collected off the coast of Papau New Guinea, *Xestospongia exigua* and *Petrosia (Strongylophora) corticata.* This effort led to the identification of two novel inhibitors of tumour invasion, motuporamine C (MotC) and strongylophorine-26 (STP-26) (Fig. 3.1).

MotC was identified as the most abundant anti-invasive molecule in the extract from *Xestospongia exigua*, however, other naturally occurring motuporamine analogues were also present in smaller quantities. Purification and testing of these natural analogues determined

that they had weaker activity. Thus, the earliest characterization of motuporamine anti-invasion activity was conducted with the naturally abundant MotC. This work was a collaborative effort between the laboratories of Dr. Raymond Andersen, Dr. Shoukat Dedhar, Dr. Aly Karsan, Dr. Michel Roberge, and Dr. Calvin Roskelley (Roskelley *et al.*, 2001) that was conducted prior to the initiation of my thesis research. We found that MotC inhibited tumour cell invasion into matrigel at low micromolar concentrations without disrupting attachment of cells to the extracellular matrix (Fig 3.2A). MotC also inhibited *in vitro* angiogenesis in an endothelial cell sprouting assay. *In vivo,* it blocked the formation of blood vessels in a chick choriallantoic membrane assay (Fig. 3.3). MotC subtly affected cell shape and actin organization on cells attached to tissue culture plastic in the presence of serum, but did not cause complete cell rounding at these low concentrations (Fig 3.2B). Additionally, MotC blocked the formation of actin-rich leading lamellae (Fig 3.4A). Ultimately, motuporamine causes significant inhibition of directed cell migration on two-dimensional tissue culture plastic (Fig 3.4B), which is likely a direct result of the subtle effects motuporamine has on cell morphology and leading lamellae.

In collaboration with members of Dr. Raymond Andersen's laboratory, I participated in a larger structure-activity study of the motuporamine family of macrocyclic amides, which was I also conducted prior to entering the PhD program. The results from this study will be discussed in more detail in the introduction to Chapter 4. However, dihydromotuporamine C (dhMotC) (Fig. 3.5), a saturated version of the naturally occurring MotC, was identified as a promising analogue based on its increased potency, its ease of synthesis, water solubility, and stability (Williams *et al.*, 2002).

Thus, this preliminary work forms the basis for my thesis project which begins with the results presented in Chapter 3. This chapter focuses on the basic characterization of the anti-invasion properties of STP-26, as well as a parallel investigation of the mechanism by which the synthetic motuporamine analogue, dhMotC, and STP-26 inhibit cell migration and tumour invasion.

Cell migration is fundamentally linked to tumour invasion. The cell's cytoskeleton and cell-substrate adhesions are important cellular structures that mediate cellular movement and changes in cellular shape. Rho GTPases are key signaling molecules that regulate the actin cytoskeleton and formation of focal adhesions. Thus, I investigated the effect of dhMotC and STP-26 on the cytoskeleton, cellular adhesions, and on Rho. I found that both molecules induced an increase in cellular adhesions and induced changes in the actin cytoskeleton, although, the effect on actin was different for the two molecules. This difference likely contributes to the observation that these inhibitors alter cellular shape in different ways. Motuporamines induced non-polarized cell contraction, whereas, STP-26 induced non-polarized spreading of the cell membrane. Nonetheless, both dhMotC and STP-26 activate Rho, and it is shown that the inhibition of invasion by both molecules is dependent on this increase in Rho activity.

3.2. Results: Motuporamines

3.2.1. dhMotC Induces the Formation of Stress Fibers and Adhesion Complexes. Characterization of dhMotC mode of action began by examining its effects on the major components of the MDA-MB-231 cytoskeleton. Cells were treated with dhMotC and then stained with primary antibodies against microtubules or intermediate filaments and then fluorescently-conjugated secondary antibodies. A fluorescently-conjugated actin probe was used to stain actin filaments. Then the cytoskeletal compartments were visualized by fluorescence microscopy. dhMotC treatment of MDA-MB-231 cells maintained in monolayer culture slightly decreased the density of the perinuclear microtubule cage (Fig. 3.6A, *a* and *b*) but otherwise had little observable effect on cytoplasmic microtubule distribution. Additionally, there were no readily discernible differences in the vimentin intermediate filament cytoskeleton between untreated and treated cells (Fig. 3.6, *c* and *d*). These observations suggested that dhMotC was not a general disruptor of the cytoskeleton, a tentative conclusion that was further supported by an examination of the actin cytoskeleton. Specifically, dhMotC treatment appeared to increase the number and thickness of cytoplasmic actin-containing stress fibers (Fig. 3.6, *e* and *f*). As stress fibers often terminate in adhesion complexes (Burridge & Chrzanowska-Wodnicka, 1996), the latter structures were also examined. Indeed, dhMotC treatment appeared to increase both the number and size of adhesion complex-associated accumulations of vinculin (Fig. 3.6, *g* and *h*) and paxillin (data not shown). Dynamic changes to the actin cytoskeleton and regulated assembly and disassembly of adhesion complexes help mediate the advancement of the leading edge and the retraction of the trailing edge of motile cells in monolayer culture (Webb *et al.*,

2002). These two processes have been very well characterized in serum-starved mouse fibroblasts (Ridley & Hall, 1992). Therefore, to unequivocally determine whether dhMotC specifically affects these processes, the effect of the compound in the Swiss 3T3 mouse fibroblast line was examined. After they had been serum-starved for 18 h, Swiss 3T3 cells in subconfluent monolayer culture exhibited very few F-actin-containing stress fibers or vinculin-containing adhesion complexes (Fig. 3.7, *a* and d), but, as expected (Ridley & Hall, 1992), both were induced by the readdition of FBS (Fig. 3.7, b and e). As was the case with MDA-MB-231 cells, dhMotC treatment also induced stress fiber formation and focal adhesion formation in the serum-starved Swiss 3T3 cells. This induction was rapid (*i.e.,* initiated within 15 min) and long lived (*i.e.,* still maintained after 2 h of treatment). There were also qualitative differences between the serum- and dhMotC-induced structures: (i) dhMotC induced stress fibers were generally thicker than those induced by serum (compare Fig. 3.7, b with *c*); and (*ii*) although serum-induced adhesion complexes were concentrated at the leading (Fig. 3.7e *arrows*) and trailing (Fig. 3.7e *arrowheads*) cell edges, dhMotC-induced focal adhesions were rarely polarized and instead dispersed around the entire cell periphery (Fig. 3.7f). dhMotC-induced focal adhesions also tended to be thicker and blunter than those induced by serum (compare Fig. 3.7, e with f).

3.2.2. dhMotC Strongly Activates Rho. A number of agents present in serum induce stress fiber and adhesion complex formation in Swiss 3T3 cells by transiently activating RhoA (Ridley & Hall, 1992), and various Rho isoforms have been implicated in cell migration (Ridley, 2001). Therefore, the effect of dhMotC on aggregate Rho activity was assessed

using the rhotekin-based pulldown assay. Rhotekin is a Rho effector protein which binds only to Rho in its active, GTP-bound, conformation. In this pulldown assay, rhotekin-conjugated agarose beads are added to cell lysates and the mixture is incubated for a brief period to allow for binding. RhoGTP is then purified from lysates by centrifugation of the RhoGTP-rhotekin-agarose complex. Rho activity levels are measured by conducting SDS-PAGE on the purified lysates and performing a western blot using a pan-Rho antibody. Clearly, dhMotC stimulated Rho activity in Swiss 3T3 (Fig. 3.8) cells. The activation occurred within 20 min, and it was sustained for ≥2 h (Fig 3.8A).

The C3 exoenzyme from *C. botulinum* inhibits the activation of all three mammalian Rho isoforms by ADP ribosylation (Wilde & Aktories, 2001). Using liposomal delivery, Swiss 3T3 cells were preloaded with C3 exoenzyme, which was found to inhibit baseline Rho activity in serum-starved cells (Fig. 3.8B). It also strongly blocked the dhMotC-induced stimulation of aggregate Rho activity (Fig. 3.8B) and stress fiber formation (Fig. 3.9). Therefore, the ability of dhMotC to alter the actin cytoskeleton in Swiss 3T3 cells is mediated, at least in part, by its ability to stimulate Rho activation.

3.2.3. dhMotC-Mediated Inhibition of Tumour Cell Invasion Is Rho Dependent. When they are plated on top of Matrigel, highly invasive MDA-MB-231 breast carcinoma cells rapidly elongate and send out processes (*i.e.,* "invadopodia") that move into the gel within a few hours (Fig. 3.10A-a). The formation of these elongated invadopodia, which helps facilitate the movement of MDA-MB-231 cells into the basement membrane matrix, was not

affected by preloading with the C3 exoenzyme (Fig. 3.10A-b). This finding supports the observation that Rho inhibition does not block elongated cellular invasion in other tumour lines (Sahai & Marshall, 2003). In contrast to the ineffectiveness of C3 exoenzyme, elongated cellular invasion is blocked by dhMotC (Fig. 3.10A-c). As a result, MDA-MB-231 cells treated with dhMotC remained rounded and noninvasive on top of the basement membrane matrix. Strikingly, this morphological effect of dhMotC was prevented by preloading the cells with C3 exoenzyme (Fig. 3.10A-d). The ability of C3 exoenzyme to abrogate the anti-invasive effects of dhMotC was confirmed in our quantitative anti-invasion assay (Fig. 3.10B). Taken together, these data demonstrate that dhMotC's ability to activate Rho is a critical component of its anti-invasive activity.

3.3. Results: Strongylophorine-26

STP-26 was identified in our anti-invasion screen subsequent to the initial characterization of dhMotC mechanism of activity. Thus, procedures developed and obtained from the characterization of dhMotC provided a template for the initial characterization of STP-26. It was found that the mechanism of action of STP-26 also involves involves Rho activation. However, there are distinct differences in the way STP-26 and dhMotC alter actin organization.

3.3.1. STP-26 Inhibits Tumour Cell Invasion. STP-26 is new meroterpenoid consisting of a diterpenoid fragment fused to a methoxy-*p*-quinone (Fig. 3.11A - #**1**). In order to determine the optimum concentration for invasion inhibition, an STP-26 dilution series was tested in the anti-invasion screen. It was found that 0.5 – 2.5 μg/ml STP-26 prevents MDA-MB-231 cells from invading Matrigel (Fig. 3.11C). Without STP-26, cells attached and extended elongated invadopodial membrane protrusions into Matrigel as early as 2 hours after plating (Fig. 3.11B-a). When treated with 1 μg/ml STP-26, the cells attached, but remained rounded on top of the gel, and did not form invadopodia (Fig. 3.11B-b). This morphological effect was readily apparent at 2 hours and was lasting, as a one time treatment with STP-26 inhibited morphological invasion for at least 12 hours (data not shown). The concentration of 1 μg/ml (equivalent to 2μM) was selected for use in most experiments in this report because invasion inhibition at this concentration was easily quantified in the anti-invasion assay (Fig. 3.11C). Of note, STP-26 caused no detectable cytotoxicity at concentrations lower than 5 μg/ml during 24h treatment (data not shown).

3.3.2. Structure-activity Study of STP-26. A basic structure activity study of STP-26 activity was done by comparing its invasion inhibiting properties with that of two other strongylophorine analogues that differ by the presence or absence of a methoxy group on the quinone (Fig. 3.11A - #**2**), and by the quinone oxidation state (Fig. 3.11A - #**3**). The structurally related bioactive quinone, ilimaquinone (Fig. 3.11A -#**4**) was also assayed for anti-invasion activity. Results from the assays indicated that the hydroquinone **3** and the corresponding quinone **2** were both active in the assay, but were significantly less potent than

STP-26 (**1**). STP-26 had an IC_{50} for invasion inhibition of approximately 1μg/ml. The observation of identical IC_{50}'s for **2** and **3** (approximately 7μg/ml) suggests that hydroquinone **3** may be oxidized to quinone **2** during the assay. Ilimaquinone was found to be completely inactive at concentrations less than 50μg/ml. Taken together, the bioassay results for **1**, **2**, and **3** show that the methoxy substituent on the quinone fragment of STP-26 enhances the potency. The observed inactivity of ilimaquinone in the assay implies that the diterpenoid fragment of **1**, **2**, and **3** also plays an important role.

3.3.3. STP-26 Inhibits Two-dimensional Cell Migration. In addition to inhibiting invasion, STP-26 also prevented the migration of MDA-MB-231 cells in an *in vitro* wound closure assay. Confluent monolayers of cells grown on tissue culture plastic were scraped and then treated with or without STP-26. After 6 h, untreated cells began to move into the wound and after 12 h, the wound was closed due to the influx of highly migratory cells (Fig. 3.12, left column). In comparison, treatment with STP-26 almost completely inhibited cell migration - after 12 h in the presence of the compound, the size of the wound had not decreased appreciably (Fig. 3.12, right column). Importantly, STP-26 did not exert its effects by preventing cell adhesion to the plastic substratum, as cells remained adherent after 12 hours of treatment with STP-26. (Fig. 3.12b,d,f).

3.3.4. STP-26 Induces Cell Depolarization and Spreading. Next, STP-26 was examined for its effect on the morphology of MDA-MB-231 cells grown on tissue culture plastic.

Compared to untreated cells which displayed a migratory, fibroblast-like morphology (Fig. 3.13a), STP-26 treated cells contracted and became depolarized rapidly, within 30 min (Fig. 3.13b). However, in contrast to the effects of dhMotC, after 2 hours of STP-26 treatment, the cells began to spread again and they formed a flattened apron that completely encircled the cells in a radial fashion (Fig. 3.13c). Phase contrast-dark membrane ruffles were prominent along the cell periphery, and the cells extended lamellipodia in all directions. After 6 h treatment, the cells were completely flat and not polarized and the radial apron remained (Fig. 3.13d). This flattened, ruffled phenotype is markedly different from the observed morphological effects of dhMotC.

3.3.5. STP-26 Induces Reorganization of the Actin Cytoskeleton and Formation of Cell-substrate Adhesions. In order to further characterize the differences between STP-26 and dhMotC-induced shape changes, the cytoskeleton and focal adhesions were examined by fluorescence microscopy in a comparable study to that conducted for dhMotC. As expected, the shape changes induced by STP-26 also corresponded with significant alterations in the actin cytoskeleton and focal adhesion. There was, however, a striking difference between the effect of STP-26 on the actin cytoskeleton, compared to the effect of dhMotC. STP-26 caused a significant decrease in F-actin-containing stress fibers which was apparent within 30 min (Fig. 3.14, compare a to c). This contrasts with dhMotC which induced stress fibre formation. After longer incubation times with STP-26, many cells displayed a dense meshwork of unpolarized actin filaments around the cell periphery (a 6 h time point is shown

in Fig. 3.14e). Notably, this biphasic response to treatment was not observed in the dhMotC study.

Focal adhesions were visualized by staining cells with antibodies against the focal adhesion protein, vinculin. Similar to dhMotC, STP-26 induced a dramatic increase in the size and number of focal adhesions at the cell periphery, which became increasingly prominent during longer incubation (Fig. 3.14, compare b,d, and f). Also like dhMotC, STP-26 had little effect on microtubules (not shown).

3.3.6. Invasion Inhibition by STP-26 Requires Rho Activity. Given the phenotypic effect of STP-26, the influence of STP-26 on Rho activity was assessed using the rhotekin-based pulldown assay. STP-26 induced a strong increase in Rho activity at 30 min, but this effect was transient, Rho activity diminished to basal levels within 6 h (Fig. 3.15A).

Anti-invasion assays were next used to determine whether the anti-invasive activity of STP-26 could be abrogated by the Rho inhibitor C3 exoenzyme. Cells were preloaded with or without C3 exoenzyme and then plated on Matrigel in the presence or absence of STP-26. Quantitative assessment of non-invasive cells revealed that treatment with C3 exoenzyme blocked STP-26 activity (Fig. 3.15B). Cells that had been simultaneously treated with STP-26 and C3 exoenzyme extended protrusions into the Matrigel, whereas, cells treated with STP-26 alone remained rounded (Fig. 3.15C, compare c to d). These results indicate that Rho activation is required for the anti-invasion activity of STP-26.

Interestingly, there was a morphological difference in the protrusions of cells treated with C3 exoenzyme alone compared to those of cells treated with STP-26 and C3 exoenzyme together. In the latter condition, the membrane extensions were broader and less extensive, whereas, in the former, cells had elongated spindle-like protrusions that are characteristic of low levels of active Rho (Sahai & Marshall, 2003) (Fig. 3.15C, compare b to d). C3 exoenzyme was able to restore invasive characteristics to cells in the presence of STP-26 (Fig. 3.15C), but the cells showed a different morphology than control cells, indicating that complete abrogation of STP-26 effects did not occur.

3.4. Summary and Discussion

Metastatic progression of tumour cells requires the acquisition of a motile and invasive phenotype. Thus, inhibiting tissue invasion by interfering with cell motility is a promising approach to anti-metastasis therapy. I developed previously a high-throughput, quantitative variation of the classical Matrigel/Transwell/Boyden chamber assay to guide the purification of MotC and STP-26 from marine sponge extracts. Subsequently, this assay was used to identify dhMotC as a potent, easily synthesized anti-invasive analogue (Williams *et al.*, 2002). Characterization of the anti-invasion effect of dhMot C and STP-26 determined that both molecules inhibit two-dimensional cell motility and that they both activate Rho. Both dhMotC and STP-26 induce focal adhesion formation, however, the two compounds induce distinct effects on actin filaments, and therefore cause distinct rearrangements in cell

shape that are morphological manifestations of these underlying changes in the cytoskeleton. These morphological effects are represented diagrammatically in Fig. 3.16.

The original characterization of the motuporamines suggested that they cause subtle changes to the cytoskeleton, but otherwise, these initial studies provided no clues about their mode(s) of action. It has now been demonstrated that dhMotC does not globally disrupt microtubules, intermediate filaments, or actin microfilaments but instead induces the formation of stress fibers caused by its ability to activate Rho.

Rho activity, stress fibers, and focal adhesions are all required for contractility-mediated traction events that pull the cell forward during directed migration in monolayer culture (Etienne-Manneville & Hall, 2002; Ridley, 2001; Webb *et al.*, 2002). However, hyperactivation of Rho, which can be initiated by directly manipulating Rho activity (Arthur & Burridge, 2001), misregulating chemoattractant-mediated receptor activation (Sugimoto *et al.*, 2003), altering integrin-mediated adhesion (Cox *et al.*, 2001; Vial *et al.*, 2003), or knocking out the focal adhesion kinase (Ilic *et al.*, 1995; Ren *et al.*, 2000), can inhibit migration. Under these conditions, the cells rarely form leading lamella or trailing edges but instead often form extensive stress fiber networks and large, stable, peripherally located focal adhesion complexes (Arthur & Burridge, 2001; Cox *et al.*, 2001; Ilic *et al.*, 1995; Ren *et al.*, 2000; Sugimoto *et al.*, 2003; Vial *et al.*, 2003), which is precisely the phenotype observed in dhMotC-treated cells maintained in monolayer culture.

At early time points, treatment with STP-26 induces Rho activation, cell contraction and rounding. However, after longer treatments, Rho activity diminishes and STP-26 induces radial non-polar lamellipodial protrusions in cells on tissue culture plastic. In contrast to dhMotC, induction of stress fibers by STP-26 was not observed. One explanation might be that signaling cascades induced by STP-26 and dhMotC feed through distinct Rho effectors. ROCK (Rho-kinase) and mDia are two Rho effectors that cooperate to organize the formation and alignment of actin stress fibers (Watanabe, 1999). Activation of ROCK leads to actin stabilization and the formation of thick centrally located stress fibers (Amano *et al.*, 1997; Leung *et al.*, 1996), whereas, mDia reduces central stress fibers and induces actin polymerization (Vicente-Manzanares *et al.*, 2003; Watanabe *et al.*, 1997), a process required for lamellipodial extension. In the case of STP-26, it is possible that signaling cascades through mDia and feed back to activate Rac, as seen in a study by Tsuji *et al*. (Tsuji *et al.*, 2002) where ROCK signaling in lysophosphatidic acid-treated Swiss 3T3 cells was abrogated using the inhibitor Y-27632. Cells under these conditions exhibited membrane ruffles and focal complexes, and stress fiber formation was suppressed. The phenotype was shown to be dependent on Rac1. A similar feedback mechanism through mDia to Rac could explain the delayed cell flattening and lamellipodial extensions that were observed in this study. Another important aspect of the migration process is the subcellular localization of actin regulators. In addition to the well characterized role for Rho as a regulator of stress fibre formation and rear-end contractility, recent studies utilizing FRET-based GTPase probes have shown that small amounts of active RhoA localize to leading edge lamella and are required for lamellipodial formation (Kurokawa & Matsuda, 2005; Pertz *et al.*, 2006). In contrast, regulation of RhoA activity at the leading egde is controlled by localized

degradation by the E3 ubiquitin ligase Smurf1 (Bose & Wrana, 2006; Wang *et al.*, 2003) (Sahai *et al.*, 2007). Loss of this regulation also results in increased contractility and loss of leading edge protrusions. Thus, it is clear that balanced levels of Rho signaling, in terms of activation and localization, is necessary to maintain a migratory phenotype. This balanced control is likely disrupted by both STP-26 and dhMotC. Furthermore, the RhoB isoform has been shown to regulate actin filament organization withing the cell body when localized to endosomal membranes (Fernandez-Borja *et al.*, 2005; Sturge *et al.*, 2006; Wallar *et al.*, 2007). The Rhotekin-pull down assay that was used in the study of dhMotC and STP-26 did not distinguish between the common Rho isoforms; RhoA, RhoB, and RhoC. Thus, divergent signaling downstream of Rho, as well as subcellular localization and isoform specific activity are three factors which might lead to the distinct morphological outcomes that result from dhMotC and STP-26 treatments.

Classically, the literature reports that lamellipodial protrusions increase in rapidly migrating cells. So, why then, does STP-26 inhibit cell migration? It was observed that STP-26 induced lamellipodia in a non-polarized manner. The entire cell periphery is extended and flattened with increased ruffling throughout. Cells also exhibited numerous, large focal adhesions at the cell periphery (Fig. 3.16C). In the case of dhMotC, treated cells also exhibit a non-polarized phenotype. Although ruffling is inhibited, the cells also have large focal adhesions throughout the cell periphery (Fig. 3.16B). Effectively, both STP-26- and dhMotC-treated cells are “stuck”. Distinct signaling events in both cells lead to an unpolarized phenotype which, on a more macroscopic level, is likely the explanation for inhibition of cell motility. Cdc42 is a third GTPase of the Rho family that has been well characterized for its

central role in establishing cell polarity in all eukaryotic cells (Etienne-Manneville, 2004). In both cases, it is possible that these compounds are affecting cdc42 activity or localization, which could result in the loss of polarity. Thus, further experimentation is needed to understand more thoroughly, the effect of these compounds on the larger family of RhoGTPase proteins.

MDA-MB-231 breast carcinoma cells extend protrusive invadopodia on Matrigel. This is an example of "elongated" tumour cell invasion (Hauck *et al.*, 2002; Sahai & Marshall, 2003). Like directed cell migration in two dimensional monolayer culture, elongated tumour cell invasion in three-dimensional culture is prevented by dhMotC and STP-26. As a result, dhMotC- or STP-26-treated cells remain rounded, but attached and viable, on top of the gel. Importantly, the abilities of these inhibitors to prevent tumour cell elongation and quantitatively inhibit tumour cell invasion were both abrogated by preloading of cells with the Rho-inhibiting C3 exoenzyme. This indicates that the ability to activate Rho blocks invasion, at least in part, by preventing the tumour cells from extending elongated protrusions into the basement membrane matrix.

Is Rho activation desirable from a therapeutic perspective? In a number of cases, Rho overexpression and/or pathway activation has been positively correlated with malignant progression (Fritz *et al.*, 1999; Kamai *et al.*, 2003; Preudhomme *et al.*, 2000; Suwa *et al.*, 1998; van Golen *et al.*, 2000), which suggests that Rho inhibitors, rather than Rho activators, might show anti-metastatic activity. However, the efficacy of either approach may be tumour specific. As was described above, MDA-MB-231 breast carcinoma cells must elongate to

invade. The same is true of BE colon and S2962 squamous carcinoma cells (Sahai & Marshall, 2003). Importantly, all three of these tumour cell lines continue to invade when Rho signaling is downregulated (Fig. 3.10, Fig. 3.15 and (Sahai & Marshall, 2003)). Thus, metastatic tumours which use "elongated" invasion may be sensitive to Rho activation by pharmacological agents. This may explain the selective antitumour activity of farnesyl transferase inhibitors, which, although originally designed to attenuate the action of Ras proteins, are now believed to act, at least in part, by activating RhoB (Du & Prendergast, 1999). Conversely, metastatic tumours whose cells invade using a rounded, amoeboid movement are clearly susceptible to inhibition of Rho/Rho Kinase signaling (Sahai & Marshall, 2003) (Carragher *et al.*, 2006; Gadea *et al.*, 2007; Torka *et al.*, 2006; Wilkinson *et al.*, 2005). Differences in invasion morphology also confer a differential sensitivity to protease inhibition (Sahai & Marshall, 2003; Wolf *et al.*, 2003). Interestingly, the parental MotC compound was also able to block the invasion of PC-3 prostate carcinoma cells (Roskelley *et al.*, 2001), which invade with a rounded morphology. This suggests that the motuporamines elicit additional anti-invasive effects that are not mediated by Rho activation alone. When Rho alone is activated in tumour cells that use the elongated mode of invasion, these cells undergo a phenotypic switching and begin to invade basement membrane matrices with a rounded morphology (Sahai & Marshall, 2003) (Gadea *et al.*, 2007; Sahai *et al.*, 2007). dhMotC and STP-26 only partially induced this phenotype switch. As mentioned above, elongated MDA-MB-231 cells become rounded but not invasive. This further implicates additional signaling events in the anti-invasive activity of both molecules.

It is possible that dhMotC and/or STP-26 activates the Rho pathway by directly targeting Rho regulators. This does occur in nonmigratory focal adhesion kinase knockout fibroblasts where Rho signaling is activated because of an inhibition of the negative regulator p190RhoGAP (Ren *et al.*, 2000). Alternatively, these inhibitors could impinge on downstream signaling end points of parallel pathways that then feedback to modulate Rho activity with functional consequence. An example of such a modulator is the Fos family member Fra-1, which is a mitogen-activated protein kinase pathway end point that, when lost, stimulates integrin signaling, which then activates Rho to inhibit tumour cell motility (Vial *et al.*, 2003). Regardless its direct target(s), it is clear from the present study that the ability of dhMotC and STP-26 to functionally activate Rho is a critical component of its anti-invasive properties *in vitro* and, presumably, its anticancer activity *in vivo*.

Strongylophorine-26

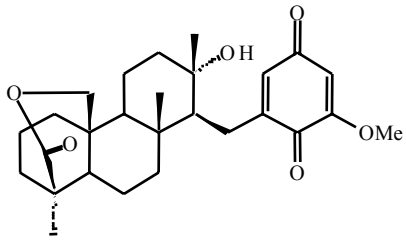

Motuporamine C

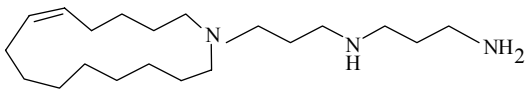

Figure 3.1. Chemical structure of Strongylophorine-26 and Motuporamine C.

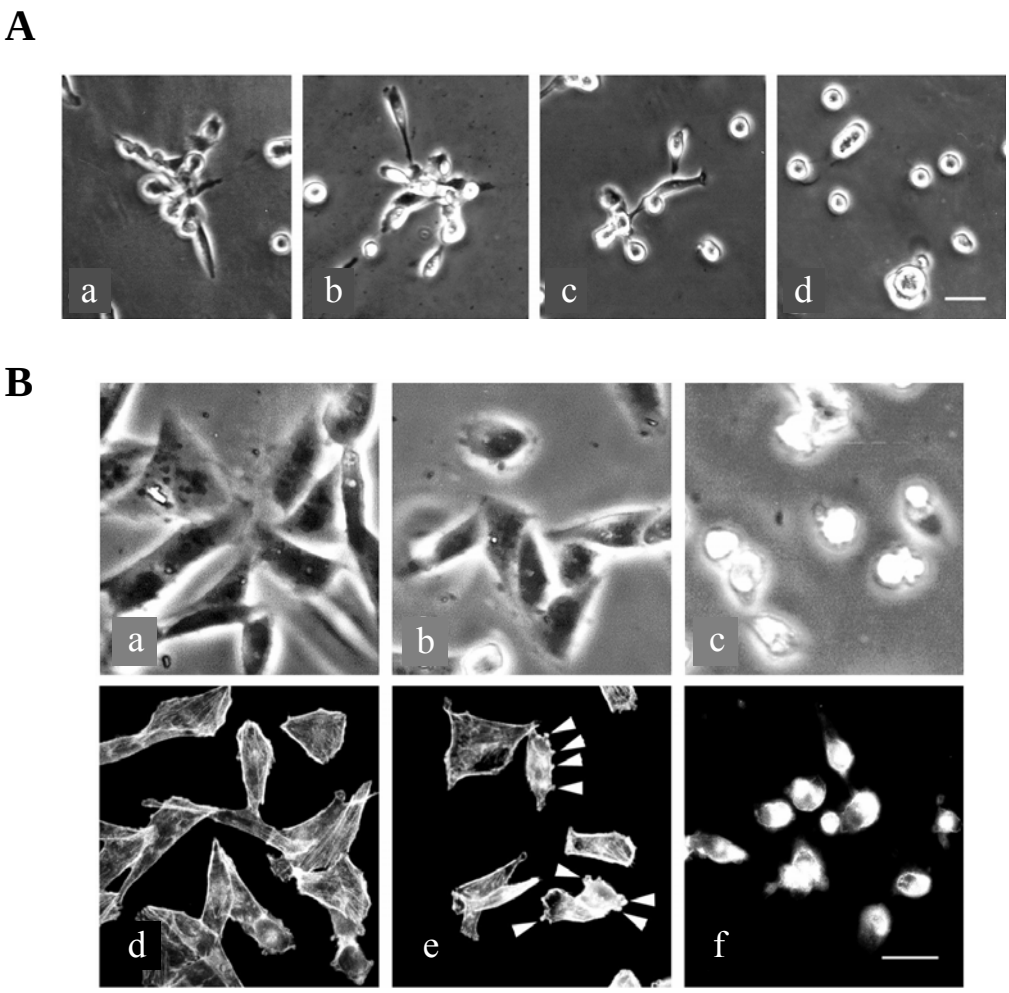

Figure 3.2. Motuporamine C inhibits invasion of basement membrane gels and subtly affects cell morphology in monolayer culture. A, MDA-MB-231 cells were plated on Matrigel in the presence of the vehicle control, DMSO (*a*), 1.25 μM (*b*), 2.5 μM (*c*) or 5 μM MotC (*d*) for 4 h (*bar*, 20 μm). **B**, MDA-231 cells were pre-spread in monolayer culture after attachment to tissue culture plastic and then treated with the vehicle control DMSO (*a,d*) or 5 μM MotC (*b,e*) or 1 μg/ml cytochalasin D (*c,f*) for 4 h. Cell morphology was then assessed by phase contrast microscopy of live cultures *(parts a–c),* and actin was visualized by rhodamine-phalloidin staining (*parts d–f*; *arrowheads*, small discontinuous aggregations of actin at cell edges; *bar*, 15 μm).

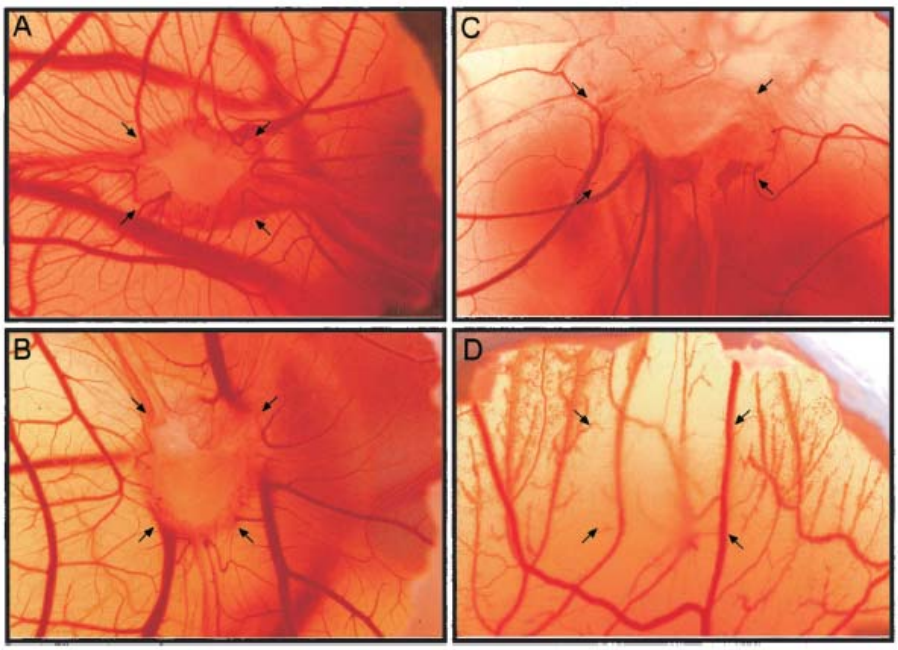

Figure. 3.3. Motuporamine C inhibits angiogenesis *in vivo*.
Photographs of developing CAMs incubated for 2 days with VEGF (*A*) or VEGF and motuporamine C at 2.5 μM (*B*), 5 μM (*C*), or 10 μM (*D*). The *arrows* indicate the corners of the gelatin sponges containing VEGF and the compounds.

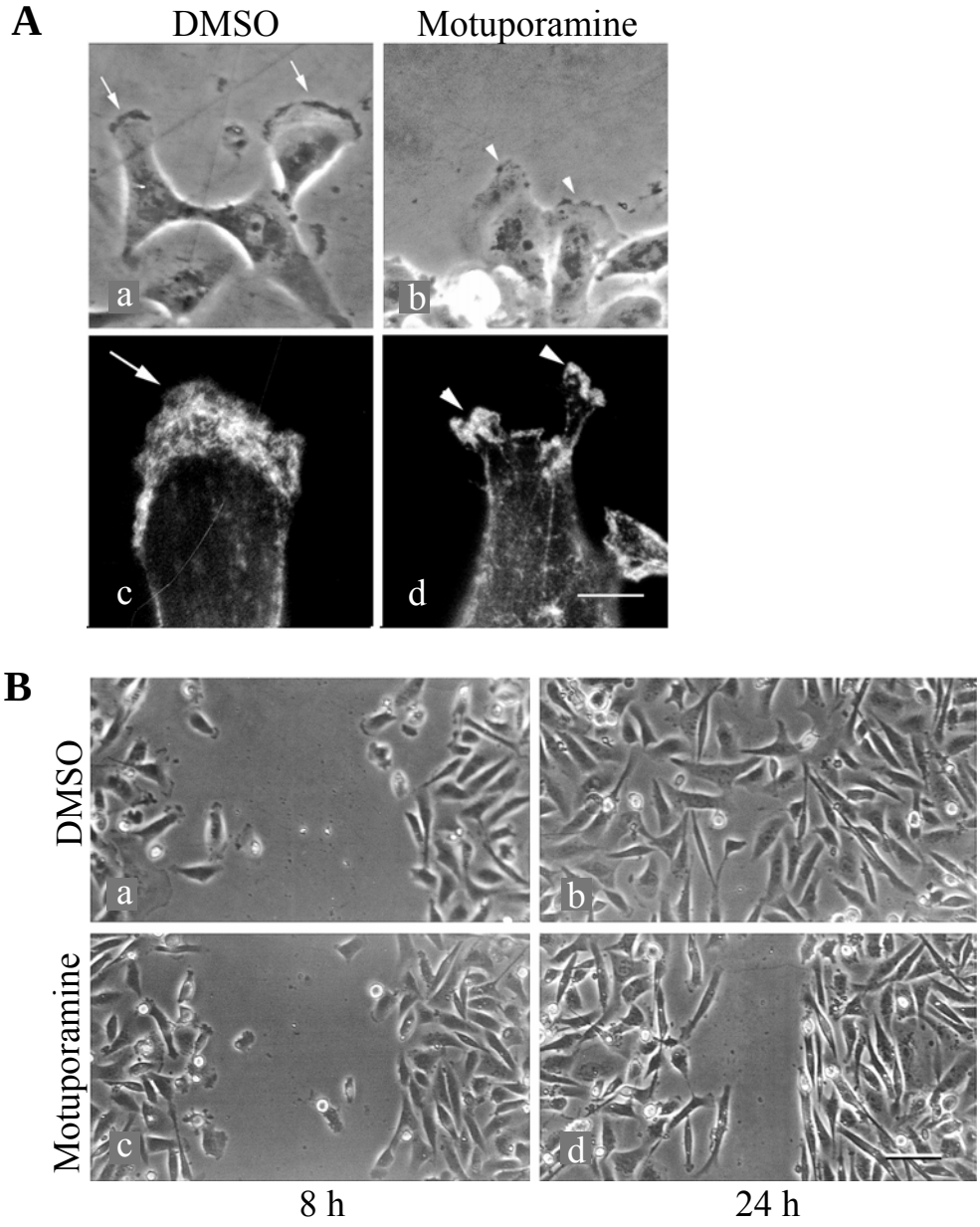

Figure 3.4. Motuporamine C inhibits cell migration and perturbs actin ruffling in leading lamellae. A, MDA-MB-231 monolayers were wounded and maintained for 8 h in the presence of DMSO or 5 μM motuporamine C and then photographed live by phase contrast microscopy or stained for filamentous actin with rhodamine phalloidin. The wound is located in the *top* portion of each photomicrograph. The *black arrow* on the *right* indicates the direction of cell migration (*white arrows*, continuous membrane ruffles in control cultures; *white arrowheads*, discontinuous ruffles in motuporamine treated cultures; *bar*, 20 μm for *parts a* and *b* and 10 μm for *parts c* and *d*). **B**, Confluent MDA-MB-231 cell monolayers were wounded with a sterile toothpick (*vertical orientation* in the micrographs), and cells were allowed to migrate into the wound over a 24-h period in the presence of the vehicle control (*DMSO*) or 5 μM motuporamine C (*MP*; *bar*, 30 μm).

Motuporamine C

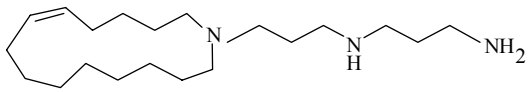

Dihydromotuporamine C

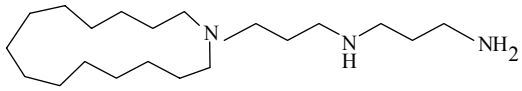

Figure 3.5. Structure of the synthetic dihydromotuporamine C analogue compared to naturally occuring motuporamine C.

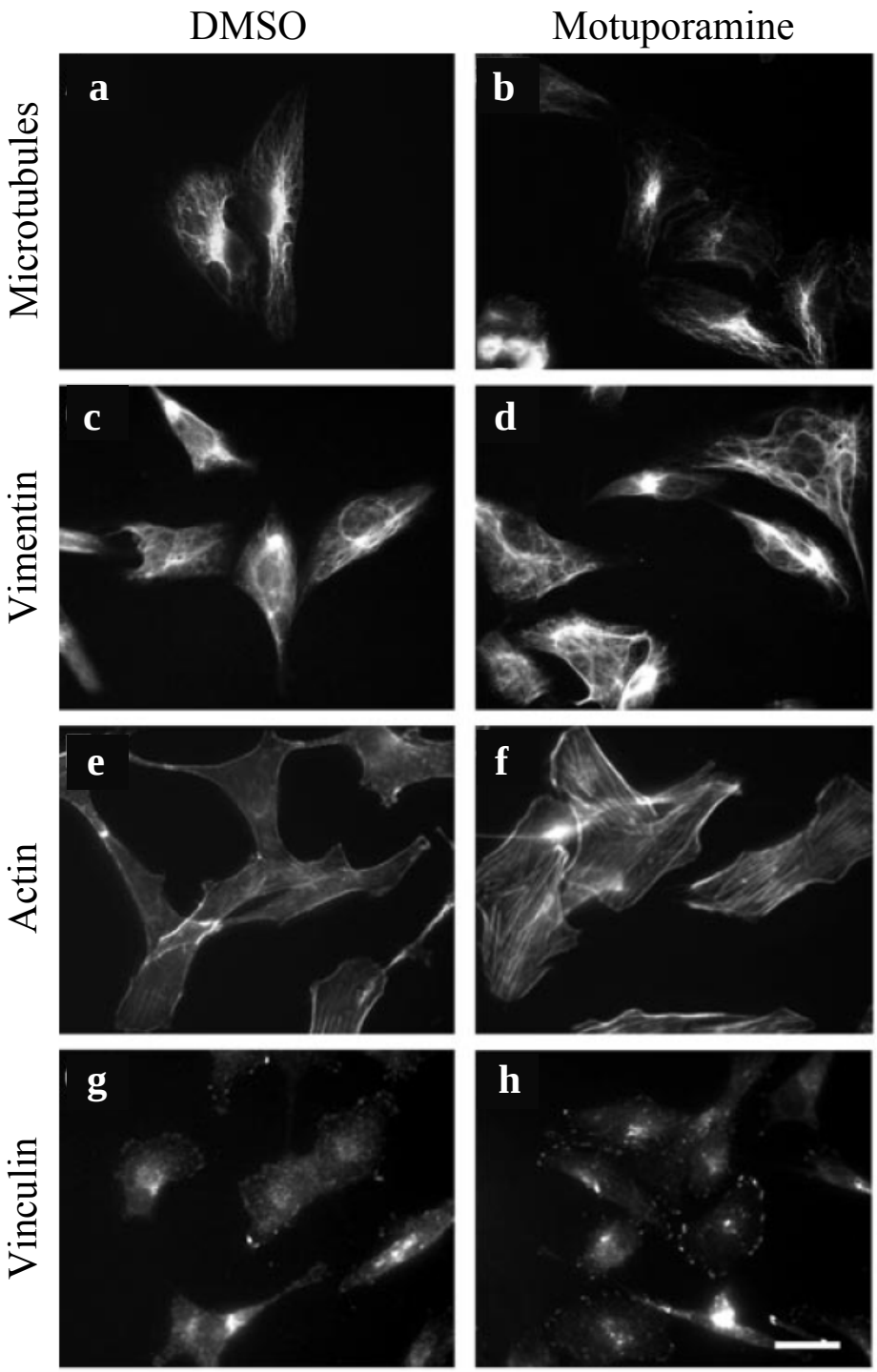

Figure 3. 6. Motuporamine alters cytoskeleton and adhesion complexes. Serum starved MDA-MB-231 cells in monolayer culture were treated without or with dhMotC for 40 min. Cytoskeletal elements were assessed by fixing and and fluorescently staining for β-tubulin (microtubules; a,d), vimentin (intermediate filaments; c,d) or f-actin (microfilaments; e,f). Adhesion complexes were assessed by immunostaining for vinculin clustering (g,h) (bar, 10 μM).

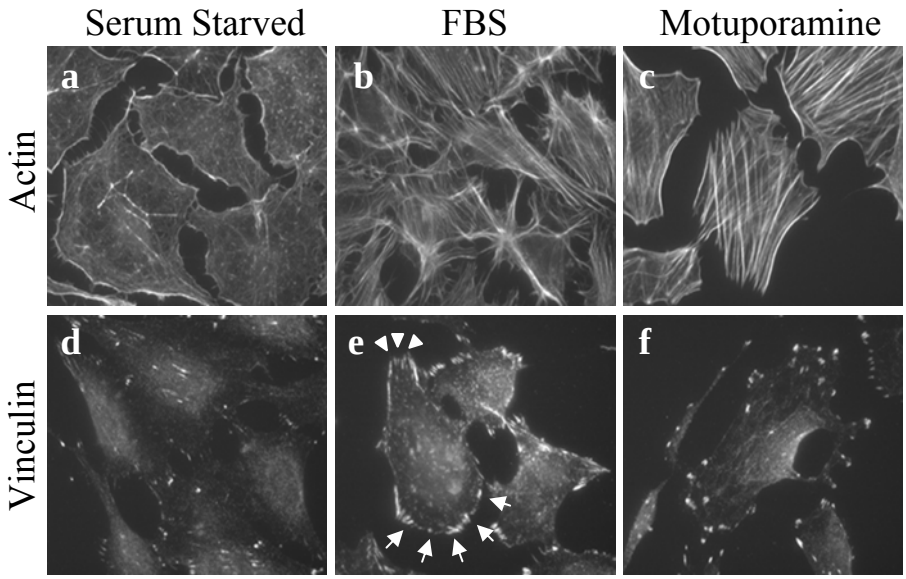

Figure 3.7. DhMotC induces stress fibre and adhesion complex formation in Swiss 3T3 fibroblasts. Swiss 3T3 cells in monolayer culture were left untreated (*serum starved*; a,d), or they were treated with fetal bovine serum (*FBS*; b,e) or dhMotC (c,f) for 30 min and stained for f-actin (microfilaments, stress fibres) and vinculin (adhesion complexes). Notice that dhMotC induced stress fiber and adhesion complex formation. In addition, in dhMotC-treated cells, the adhesion complexes were large and located around the entire cell periphery in contrast to the polarized anterior (*arrows*) and posterior (*arrowheads*) complexes often observed in migratory FBS-treated cells.

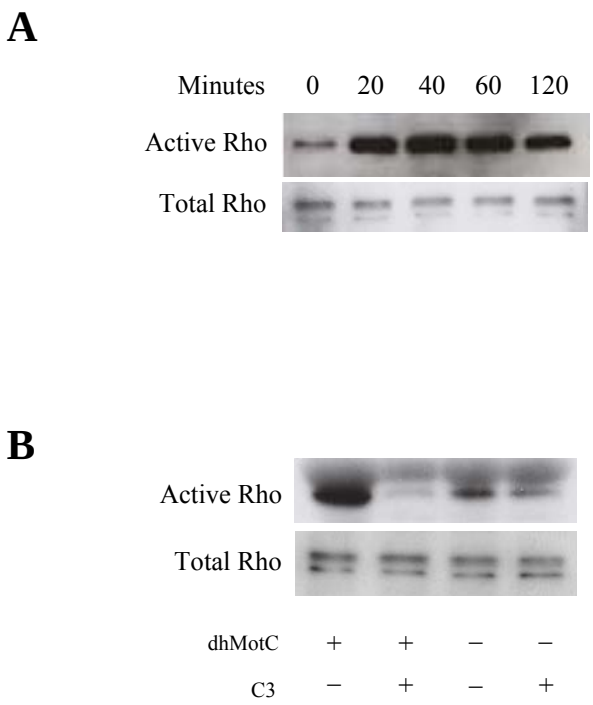

Figure 3.8. DhMotC activates Rho.
A, Serum-starved Swiss 3T3 cells were treated with dhMotC for the indicated times, and Rho activation was assessed. Note that Rho activity remained sttrongly stimulated, even after 2 h of treatment. **B,** Swiss 3T3 cells were preloaded without (-) or with (+) C3 exoenzyme and treated without or with dhMotC.

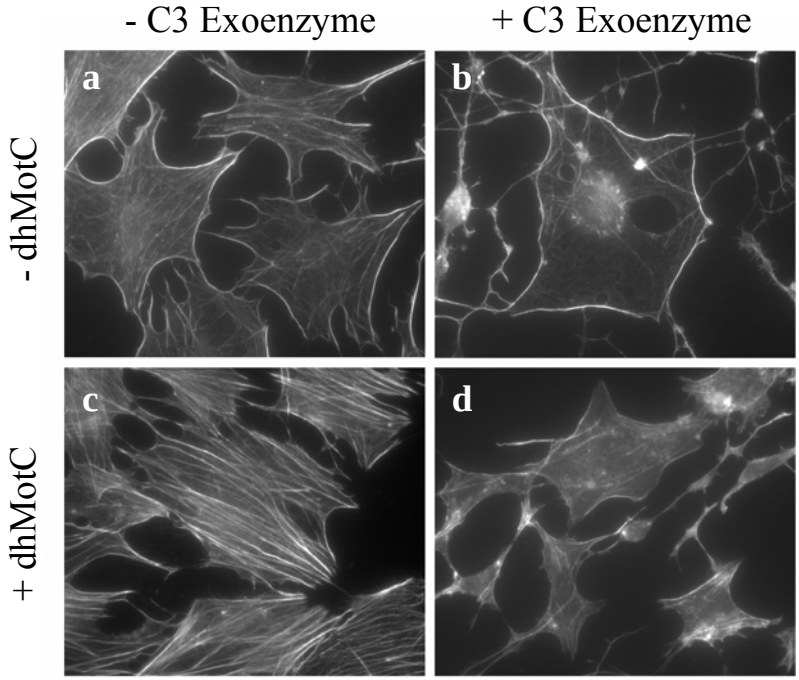

Figure 3.9. DhMotC-induced stress fiber formation is Rho dependent. Serum-starved Swiss 3T3 cells preloaded with (b,d) or without (a,c) C3 exoenzyme were treated with (c,d) or without (a,b) dhMotC for 60 min. Cells were then stained for F-actin. Note that preloading with C3 exoenzyme prevented dhMotC-mediated stress fiber formation.

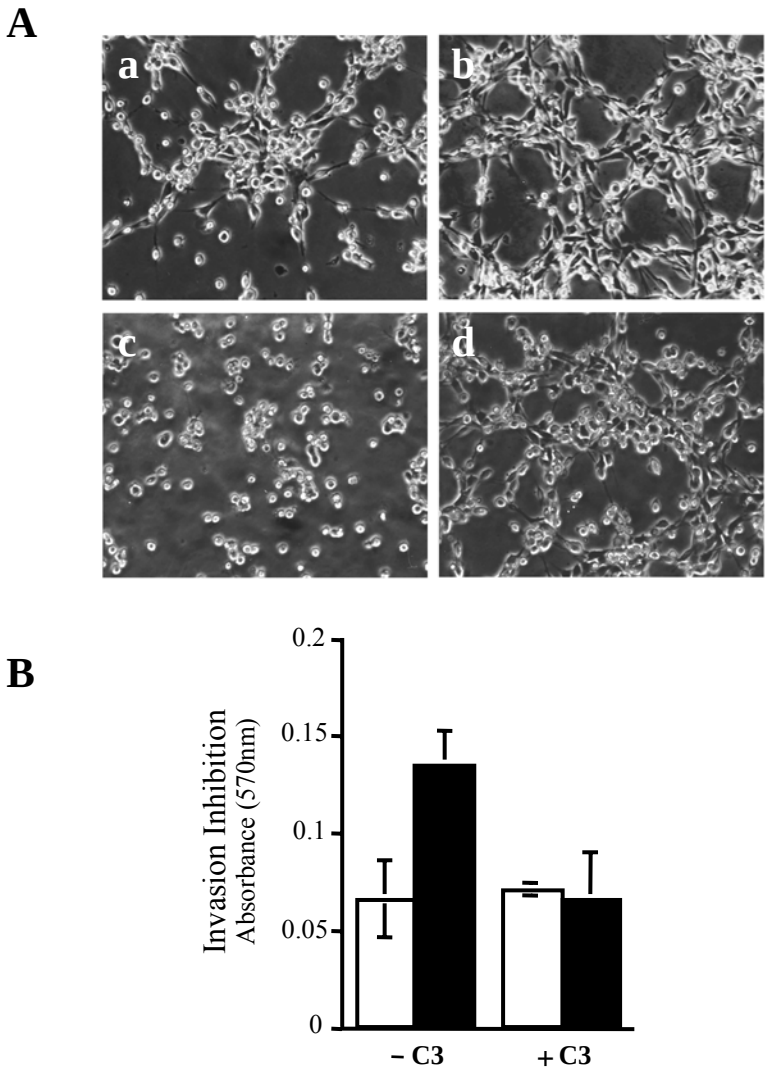

Figure 3.10. DhMotC-mediated inhibition of MDA-MB-231 invasion is Rho dependent. A, MDA-MB-231 cells preloaded with or without C3 exoenzyme were treated with or without dhMotC, plated on basement membrane gels for 3h, and photographed live by phase microscopy. Untreated cells without or with C3 exoenzyme elongated and invaded the gel (a,b). This morphological invasion was inhibited by dhMotC treatment but only in the absence of C3 exoenzyme (compare c with d). **B,** MDA-MB-231 cells were treated as described in A, and invasion was assessed quantitatively. Note that the abiltiy of dhMotC (*white bars*, untreated; *black bars*, treated) to inhibit invasion was abrogated by preloading the cells with C3 exoenzyme.

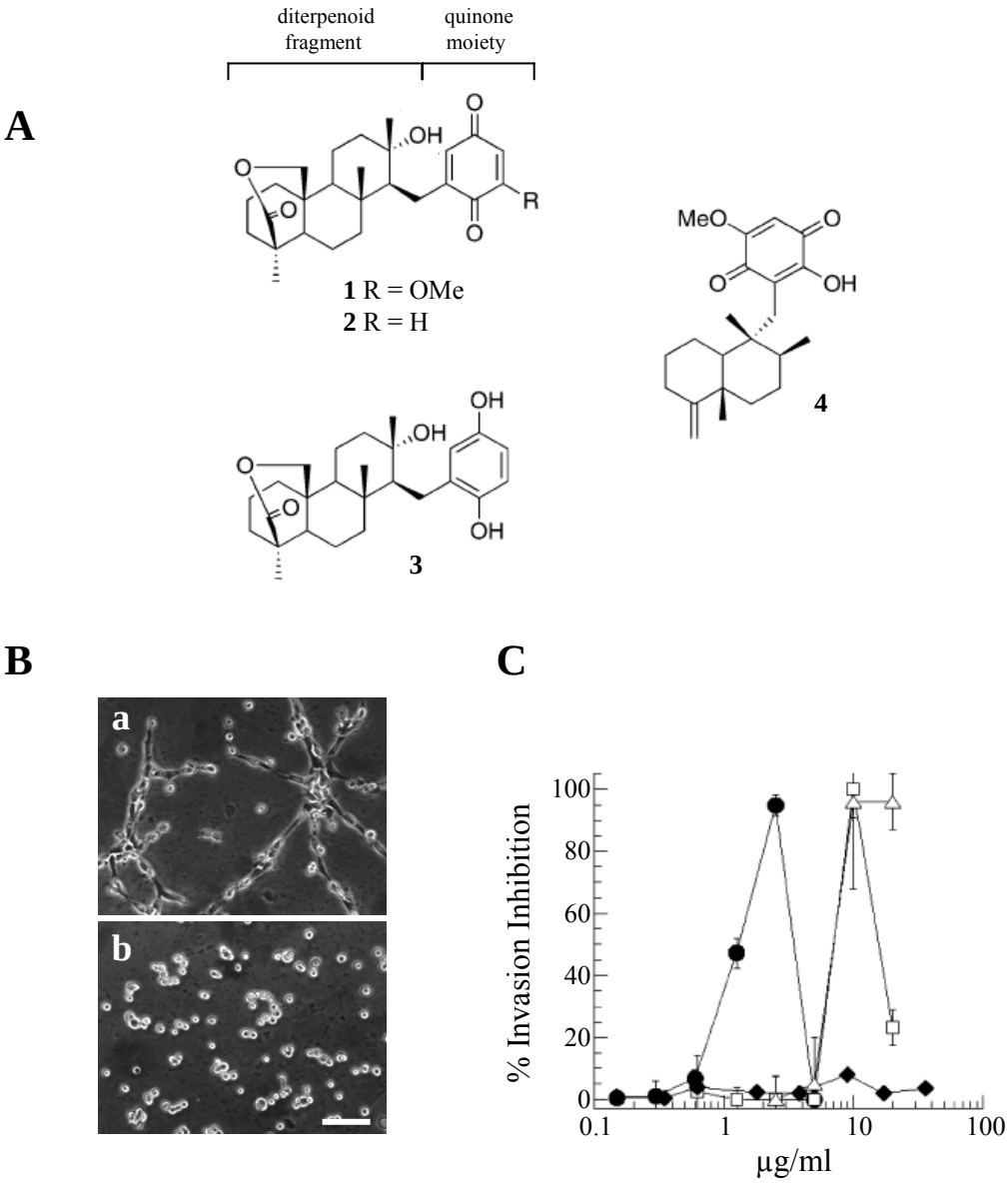

Figure 3.11. Anti-invasive activity of Strongylophorine-26 and analogues. **A,** Structure of strongylophorine-26 (1) and analogues (2 and 3), with ilimaquinone (4). **B,** MDA-MB-231 cells were plated on Matrigel in the presence of DMSO (a) or 1 µg/mL strongylophorine-26 (b) for 2 h, and photographed live by phase contrast microscopy (bar, 60 µm). **C,** Cells were treated as in (B) with strongylophorine analogs. (1) (●), 2 (□), 3 (△), and ilimaquinone (◆) and inhibition of tumor invasion was assessed quantitatively. The assay was done in triplicate and error bars represent SEM.

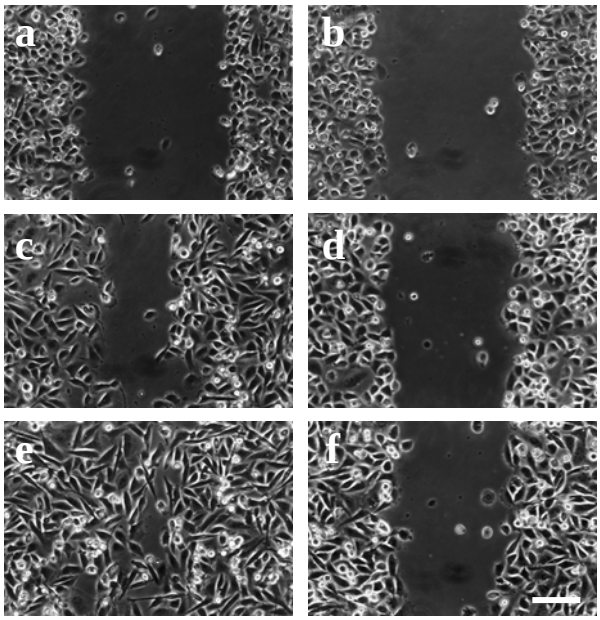

Figure 3.12. **Strongylophorine-26 inhibits cell migration.**
A confluent monolayer was scraped with a sterile toothpick and migration into the wounded monolayer was assessed by phase contrast microscopy after 1 (a and b), 6 (c and d), and 12 h (e and f) in the presence of DMSO (a, c, and e) or 1 µg/mL strongylophorine-26 (b, d, and f; bar, 45 µm).

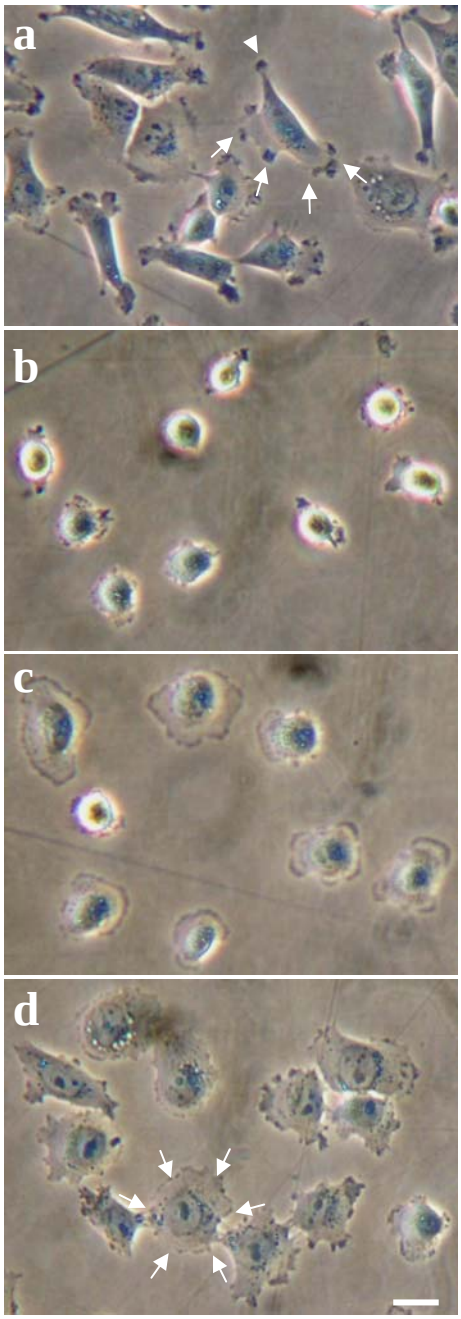

Figure 3.13. **Strongylophorine-26 induces cell depolarization and spreading.** Cells were treated with DMSO (a) or strongylophorine-26 for 30 min (b), 2 h (c), or 6 h (d) and phase contrast photographs were taken of live cells. Notice the polarized lamella at the leading membrane (arrows) and the narrow retracting membrane (arrowhead) of an untreated cell in (a). In contrast, strongylophorine-26-treated cells seem flattened and spread, and exhibit nonpolarized lamellar extensions around the entire cell periphery in (c and d), shown with arrows in (d; bar, 15 µm).

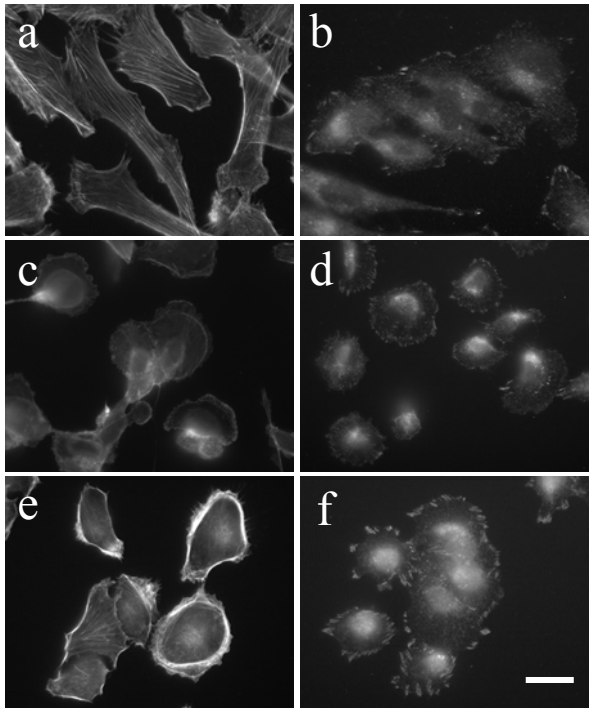

Figure 3.14. **Strongylophorine-26 induces peripheral actin bundling and adhesion complex formation.** MDA-MB-231 cells were treated with DMSO (a and b) or 2 μg/mL strongylophorine-26 for 30 min (c and d) or 6 h (e and f). They were fixed and stained for F-actin (a, c, and e) and the focal adhesion protein vinculin (b, d, and f; bar, 10 μm).

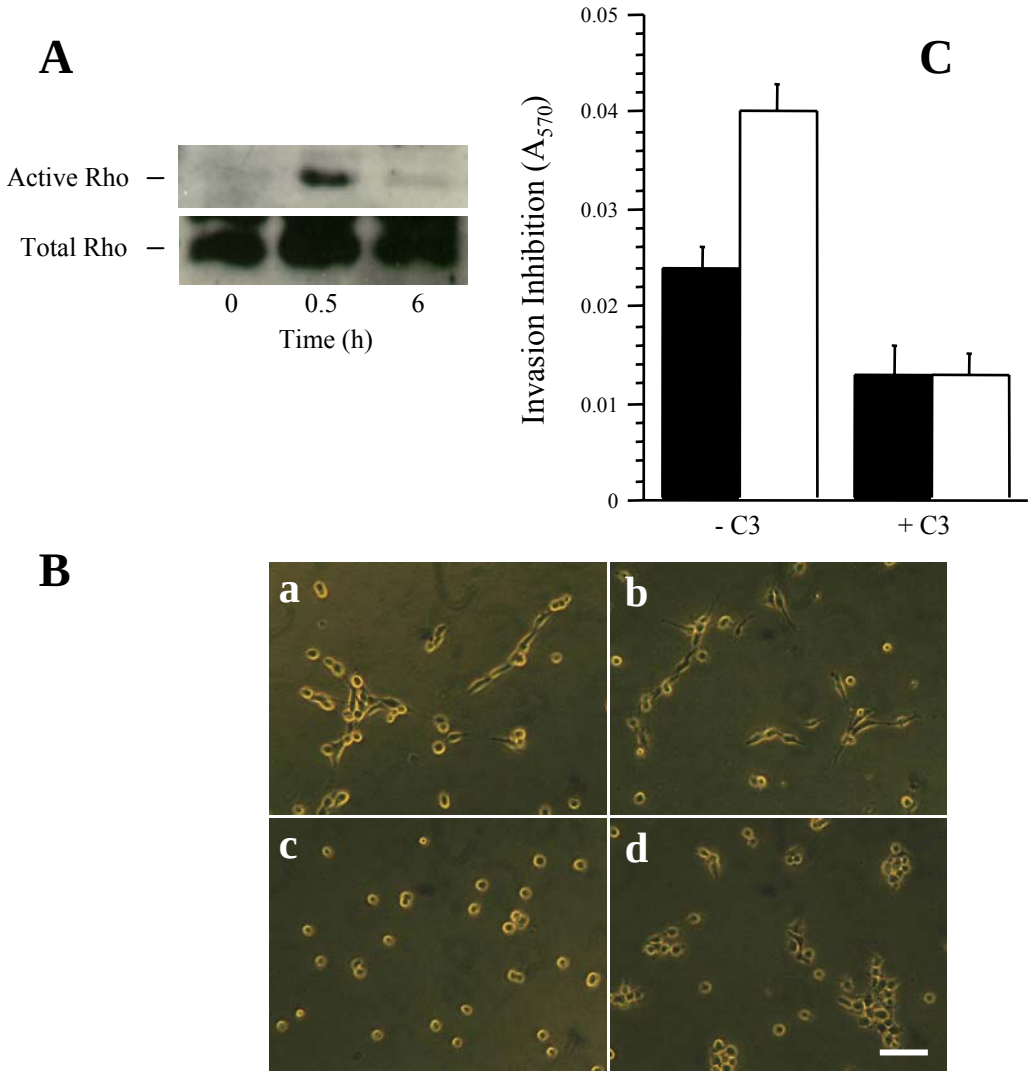

Figure 3.15. **Strongylophorine-26 activates Rho and inhibits invasion in a Rho-dependent manner. A**, MDA-MB-231 cells were treated with 2 µg/mL strongylophorine-26 for the indicated times and Rho activation was assessed. **B**, MDA-MB-231 cells were preloaded with or without the Rho inhibitor C3 exoenzyme, and cells were plated on Matrigel in the presence of DMSO (black column) or 1 µg/mL strongylophorine-26 (white column). Invasion inhibition was quantified as described in Materials and Methods. The assay was done in triplicate; bars, SEM (strongylophorine-26 versus strongylophorine-26 + C3 = $P < 0.001$). **C**, cells were treated as in (B) for 4 h and phase contrast photographs of live cells were taken. Untreated cells without (a) or with (b) C3 exoenzyme invaded the gel. Invasion was inhibited by strongylophorine-26 (c), but this effect was abrogated by pretreatment with C3 exoenzyme (d; bar, 60 µm).

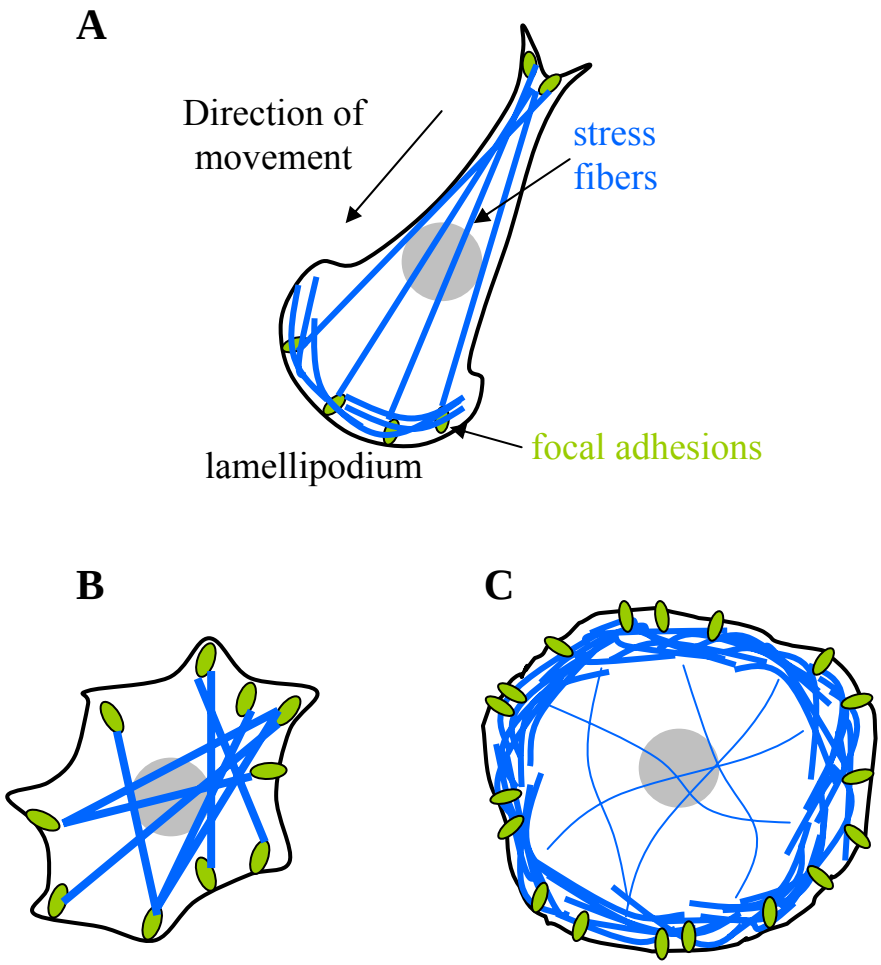

Figure 3.16. Diagram comparing the morphological effects of STP-26 with dhMotC. **A,** Migrating cells with a lamellipodium extending in the direction of cell migration, focal adhesions, a meshwork of lamellipodial actin filaments and actin stress fibers. **B,** DhMotC disrupts cell polarity and prevent cell migration by stabilizing focal adhesions and actin stress fibers. **C,** STP-26 disrupts cell polarity and prevents cell migration by stabilizing focal adhesions and inducing the formation of radial protrusions resembling lamellipodia that contain a dense meshwork of peripheral actin filaments and few stress fibers.

Chapter 4: Motuporamines: Cationic Amphiphilic Compounds that Induce the Formation of Membrane-rich Inclusions and Inhibit Degradation of Ligand Bound Epidermal Growth Factor Receptor.

4.1. Introduction

The motuporamine family of inhibitors are macrocyclic amides. Naturally occurring MotC consists of an unsaturated 15-membered cyclic amine fused to a diamine side chain. The simple structure of the motuporamine family makes these molecules relatively easy to synthesize. Because of this, drug supply is not an issue when planning mechanistic or drug development studies. With the invasion inhibitor STP-26, however, this was not the case. STP-26 could only be attained by extracting from the natural source, a process that requires the collection of large quantities of the marine organism that produces STP-26. Experimentation with STP-26 was limited by drug availablitiy, and therefore, the following work focuses completely on understanding the mechanism of activity of motuporamines.

In an effort to better understand the motuporamine structure-activity relationship, a panel of synthetic and naturally occurring motuporamine analogues was created by chemists

in the laboratory of Dr. Raymond Andersen (Williams *et al.*, 2002) (Fig. 4.1, Fig. 4.2). Prior to my thesis research, I tested these compounds for activity against tumour invasion, as well as cytotoxicity against the invasive MDA-MB-231 cells or the non-cancerous HUMEC cells (Williams *et al.*, 2002). Results from this study indicated that the size of the amide ring was important for the invasion activity of the molecule (Fig. 4.1). Analogues with a 15-membered ring were the most active, however, weaker activity was observed in rings consisting of 13 to 18 carbons. Also of importance was the saturation state of the ring. The presence of double bonds in the ring structure reduced the level of activity of the analogues. When the double bond of the naturally occurring MotC was reduced to create the 15-membered saturated ring of dhMotC, an increase in potency was observed. Interestingly, the 14-membered ring with a double bond had no activity. A complete loss of activity was also observed for the 15-membered ring analogue with two double bonds. Other factors that influenced activity were the presence of positively charged amine groups in the carbon side-chain, as well as the number of carbons separating these amine groups in the chain (Fig. 4.2). MotC has two amines in the side-chain fragment. Three carbons separate the first amine in the side-chain from the nitrogen in the ring structure. The second amine in the side-chain is separated from the first by an equal number of carbons. Side-chains with 2 or 4 carbons between the amine groups had reduced activity, and side-chains with amines that were separated by 5 carbons or more were no longer active. Shorter chains that terminated after the first amine group also had no activity. The importance of the positive charge on the nitrogen is indicated by the complete loss of MotC invasion activity after acylation of both amines in MotC (Roskelley *et al.*, 2001).

Tricyclic antidepressants (TCAs) are a class of cationic amphiphilic drugs (CADs) which have structural similarities to the motuporamines. The TCA desipramine consists of a triple ring structure fused to an amine side-chain. TCAs have been used to treat depression since the early 1960's, and thus a vast body of literature exists which reports their clinical efficacy and toxicities (for review: (Boyce & Judd, 1999; Nierenberg, 1994)). However, the exact mechanism for their biological activity is still unknown. TCAs are thought to act by desensitizing neurotransmitter receptors at the synaptic membrane (Stahl, 1998). For example, the tricyclic antidepressant desipramine has been shown to cause downregulation of β-adrenoceptors (Burgi *et al.*, 2003) by a mechanism that involves inhibition of trafficking and recycling of receptors to the plasma membrane. CADs have also been reported to induce multi-lamellar body (MLB) formation (Anderson & Borlak, 2006), a phenomenon in which cellular membranes accumulate intracellularly at the peri-nuclear region of cells. Over 50 CADs have been shown to induce MLBs, although within this group, many of the drugs have other distinct effects on cellular behavior (Anderson & Borlak, 2006). The hydrophobic amide ring and the hydrophilic amine tail of the motuporamines give them a cationic amphiphilic property. There is also a strikingly close similarity in structure between one of the active motuporamine analogues, Mot#49, and the tri-cyclic antidepressant desipramine (Fig. 4.3). This similiarity led to the hypothesis that desipramine and motuporamines might have similar mechanisms for activity. It was therefore investigated whether motuporamines also affect trafficking of cellular membranes. Indeed, in this section, it was found that motuporamines, like desipramine, induce the intracellular accumulation of membranes and that trafficking and degradation of the epidermal growth factor receptor, a model trans-membrane protein, is altered by motuporamine treatment. TCAs have weak anti-migratory

activity and therefore one could hypothesize that membrane trafficking is involved in the mechanism of migration inhibition by both TCAs and motuporamines.

4.2. Results

4.2.1. Motuporamine Causes Intracellular Accumulation of Lipids. In order to determine whether dhMotC affects the organization of cellular membranes, a strong lipophilic fluorophore, nile red (Greenspan & Fowler, 1985; Greenspan *et al.*, 1985), was used to stain cellular lipids and membranes in MDA-MB-231 cells after long term treatments with dhMotC. Cells were treated for 24 hours in the presence of 10 μM dhMotC, DMSO, or 50 μM desipramine which was used as a positive control because it is known to induce multi-lamellar body formation. Cells were then fixed, permeabilized and stained with nile red. In control cells, a diffuse staining pattern that resembled the cellular morphology of untreated MDA-MB-231 cells was observed (Fig. 4.4a). These cells had a slight increase in the peri-nuclear staining intensity, which likely represents the concentration of cellular organelles such as the endoplasmic reticulum, Golgi apparatus and organelles of the endosomal-lysosomal system which localize to that region. In cells treated with the positive control desipramine, abnormally large brightly staining punctate structures were also observed in the peri-nuclear region (Fig. 4.4b). These structures were not observed in control cells. Furthermore, cells treated with the invasion inhibitor, dhMotC, also exhibited brightly staining structures (Fig. 4.4c) that were similar in size and location to that of the positive control.

A panel of motuporamine analogues that have varying degrees of activity against tumour invasion were tested for their ability to induce the punctate lipid rich structures that were observed in dhMotC treated cells. In a blind experiment, cells were treated with the motuporamine analogues, stained with nile red, and then given a score between 0 and 6 for their increasing ability to induce the intracellular accumulation of lipids. A relative score for invasion inhibition was also given to the analogues based on the IC_{50} values reported previously in Williams *et al* (Williams *et al.*, 2002). These scores are represented symbolically in Table 1. Interestingly, a correlative trend was observed between the induction of intracellular lipid accumulation and the activity against tumour invasion (Table 1). Mot#4 and Mot#5 are two motuporamine analogues that have a similar structure to dhMotC (Mot#13) (Fig. 4.1) but differ by the presence of two double bonds in the 15-membered ring of Mot#4 and one double bond in the smaller 14-membered ring of Mot#5. Table 1 indicates that the slight alteration in the structure of the hydrocarbon ring can confer inactivity in the invasion assay as well as the inability to induce lipid accumulations in these cells (see also Fig. 4.4B-d,e for nile red staining). Of note, it was also observed that analogue Mot#20, containing a saturated 16-membered carbon ring, had the strongest effect in the nile red assay (Table 1, see Fig. 4.1 for structure) and thus this analogue was used for some of the experiments relating to membrane trafficking.

4.2.2. Motuporamine Induces Intracellular Accumulation of Lipid Raft Associated GM1-ganglioside. Our observations of nile red-stained cells indicated that dhMotC caused the accumulation of cellular lipids. Eukaryotic cellular membranes are primarily made up of

phospholipids, although other types of lipids, such as sphingolipids and gangliosides also constitute a much smaller percentage of cellular membranes. Due to their rigid structure, sphingolipids aggregate into discrete regions of cellular membranes called membrane microdomains or lipid rafts. These microdomains play an important role in cell signaling because they act as anchoring points for many transmembrane receptor kinases and lipid anchored signaling proteins (Golub *et al.*, 2004). The ganglioside GM1 is a molecule that associates primarily with lipid rafts and has been used extensively as a marker for membrane microdomains. In order to determine whether the membrane inclusions induced by dhMotC contained lipid rafts, a fluorescently conjugated GM1 probe, FITC-cholera toxin B subunit, was used. MDA-MB-231 cells were treated with or without dhMotC for a timecourse of 40 min, 2 h, 6 h or 24 h and then fixed and stained with FITC-Cholera Toxin B subunit. After a 24 h treatment, distinct brightly staining clusters of ganglioside GM1 were observed at perinuclear regions in the cell (Fig. 4.5e). This staining pattern was not observed in untreated cells (Fig. 4.5a). Of note, 24 h treatment with desipramine also induced the relocation of GM1 to intracellular regions (Fig. 4.5f). In a timecourse experiment with dhMotC, the first appearance of GM1 accumulation was detectable as early as 2 hours after treatment and was clearly visible by 6 hours (Fig. 4.5b-d). These results suggest that dhMotC also affects the cellular location of lipid rafts.

4.2.3. Motuporamine Alters Staining Pattern of LAMP2 but not Other Markers of Cellular Organelles Involved in Vesicular Trafficking. It is possible that motuporamines induce the formation of the lipid rich bodies by interfering with vesicular trafficking. Thus, it

was asked whether motuporamines altered the organization of organelles involved in vesicular trafficking in the endocytic or secretory pathways. MDA-MB-231 cells were treated with or without Mot#20 for 24 hours before cells were fixed and stained with antibodies against markers for early endosomes (TfR (transferrin receptor)), late endosomes/lysosomes (LAMP2 (lysosomal membrane-associated glycoprotein)), Golgi apparatus (GM-130 (Golgi matrix protein of 130 kDa)) and endoplasmic reticulum (PDI (protein disulfide isomerase)). In TfR stained non-treated cells, the fluorescent pattern appeared granular and spanned the entire cytoplasm, with a general increase in staining intensity in the peri-nuclear region of the cell. The TfR staining pattern was not significantly affected by Mot#20 treatment (Fig. 4.6a,e). LAMP2 staining in non-treated cells was also granular and appeared to be concentrated in the peri-nuclear region where punctate LAMP2 associated vesicular structures were apparent. However, in contrast to the TfR staining, Mot#20 treatment did significantly alter the appearance of the LAMP2 staining pattern. In Mot#20 treated cells, the LAMP2-associated structures were significantly larger in size and more abundant compared to untreated cells (Fig. 4.6b,f). Neither the GM-130 nor PDI staining appeared to be significantly altered by treatment with Mot#20. Based on these results, one could hypothesize that the lipid rich bodies induced by motuporamines originate, at least partially, from late endocyctic or lysosomal vesicles.

4.2.4. Transmission Electron Microscopy Reveals Large Aberrant Multi-vesicular/multi-lamellar Bodies in Motuporamine Treated Cells. In order to further characterize the lipid rich bodies induced by motuporamines, transmission electron

microscopy was used to determine their ultrastructure. MDA-MB-231 cells plated on filters were treated with or without Mot#20 for 6 h before they were fixed and processed for viewing. Observation of treated cells revealed very large membrane-bound structures with a seemingly unorganized membranous interior. The structures were both multi-vesicular and multi-lamellar in nature. A representative photograph of one of these structures is shown in Fig. 4.7b. There were no organelles of a similar size or membranous organization in untreated cells. For comparison, a photograph of equal magnification (Fig. 4.7a) shows a normal multi-vesicular body/late endosome in untreated cells. Although, the results from immunostaining point to the late endosomes/lysosomes as probable candidates for the organelles of origin of the lipid bodies, the electron micrograph of a representative lipid body suggests that the structures induced by motuporamines are not simply enlarged versions of these organelles.

4.2.5. Motuporamine Inhibits Degradation of Internalized FITC-EGF and Causes Accumulation of Endogenous EGF Receptor. In order to further characterize the effect of motuporamines on intra-vesicular trafficking, the internalization, trafficking and degradation of a fluorescently conjugated epidermal growth factor (EGF) was assessed. In normal cells, binding of EGF to the EGF receptor (EGFR) at the plasma membrane leads to dimerization of EGFR, auto-activation of tyrosine kinase activity, and initiation of downstream signaling cascades. One important mechanism by which cells can downregulate signaling from transmembrane receptors is through endocytosis and trafficking of ligand-receptor complexes to the lysosome for degradation (for review; (Katzmann *et al.*, 2002).

For internalization and trafficking assays, MDA-MB-231 cells were pre-incubated at 4°C in the presence of FITC-EGF for 1h. Receptor-mediated endocytosis is inhibited at cold temperatures, therefore, this pre-treatment is done so that ligand binding can occur while internalization of the ligand/receptor complex is prevented. Thus, timecourse experiments can be performed where the zero timepoint corresponds to the addition of drug and to the return to physiological temperature. After allowing binding of FITC-EGF, MDA-MB-231 cells were treated with Mot#20 or DMSO and incubated cells at 37°C. Cells were then fixed at various time-points and the fate of the complex was determined by fluorescent microscopy. Our results showed that the majority of bound FITC-EGF is endocytosed in both control and Mot#20 treated cells. The distribution of FITC-EGF looked similar in control and treated cells after 10 min (data not shown), 30 min (Fig. 4.8A-b,e) or 1h (data not shown). Thus, Mot#20 does not inhibit endocytosis nor protein transport in the early endocytic pathway. Cells were also fixed after longer incubation times to assess the affect of Mot#20 on protein degradation. After three hours, the majority of FITC-EGF had disappeared in untreated cells, thus indicating protein degradation had occurred at the lysosome. However, in cells treated with Mot#20, there was a significant increase in the amount of FITC-EGF remaining in the cell (data not shown). The difference in amount of FITC-EGF between control and treated cells was even more apparent after 6 hours of incubation (Fig. 4.8Ac,f). After 24 hours, FITC-EGF still remained in Mot#20 treated cells whereas it was completely absent in untreated cells (data not shown). Of note, it was found that desipramine also inhibits the degradation of the internalized complex (data not shown).

In MDA-MB-231 cells, immuno-staining of the EGFR was carried out to determine the cellular location of EGFR after long term treatments with Mot#20. In untreated cells, there was a granular staining pattern that covered the entire cell while increased staining intensity was observed at the lamellipodial ruffles of the plasma membrane (Fig. 4.8B-a). In contrast, Mot#20 treated cells had punctate accumulations of the EGFR at intracellular locations. There was significantly less ruffling in Mot#20 treated cells and correspondingly less EGFR at the plasma membrane (Fig. 4.8B-b). Together, the results of these experiments suggest that Mot#20 prevents degradation of internalized EGF at the lysosome and alters the cellular location of EGFR by causing intracellular accumulation of the receptor.

4.2.6. Motuporamine Increases the pH of Lysosomes. Cationic amphiphilic drugs cause the luminal pH of lysosomes to increase and deacidification of the lysosome is one proposed mechanism for drug-induced accumulation of intracellular membranes (Anderson & Borlak, 2006). It is thought that the increase in pH at the lysosme inactivates lysosomal enzymes which normally function to degrade membranes and proteins that are trafficked to this cellular organelle. Therefore, the lysosomal pH indicator, lysotracker red, was used to assess the effect of motuporamine on lysosomal pH. Cells were pretreated with lysotracker red (25 min) and then treated with dhMotC (35 min) before they were fixed and viewed with a fluorescent microscope. The results showed a significant decrease in fluorescence intensity at the lysosomes of dhMotC treated cells (Fig. 4.9c). compared to the lysosomes in cells treated with DMSO (Fig. 4.9a). Fluorescence intensity correlates with acidity, thus, these results indicate that dhMotC reduced the acidity of the lysosomal lumen.

4.2.7. Inhibition of EGF Degradation by Motuporamine is Independent of Rho/Rho Kinase Signaling. Given that dhMotC is a Rho activator, it was asked whether the effect of the Mot#20 analogue on the degradation of FITC-EGF was a downstream result of Rho signaling. FITC-EGF degradation assays were carried out on cells preloaded with the Rho inhibitor C3 exoenzyme or a liposome control, and the effect of Mot#20 on FITC-EGF degradation was assessed by fluorescence microscopy. It was found that the C3 inhibitor did not abrogate Mot#20 induced inhibition of FITC-EGF degradation (Fig. 4.10A). A similar experiment was performed by pretreating cells with Y-27632, a small molecule inhibitor of the downstream Rho effector, Rho kinase/ROCK (Narumiya *et al.*, 2000). In agreement with the above results, pretreatment with Y-27632 did not abrogate Mot#20 induced inhibition of FITC-EGF degradation (Fig. 4.10B). Thus, Mot#20 induced inhibition of FITC-EGF degradation is not dependent on or downstream of Rho or Rho kinase/ROCK signaling.

4.2.8. Tricyclic Antidepressants are Weak Inhibitors of Cell Migration. Tricyclic antidepressants affect lipid storage and inhibit lysosomal degradation of cellular lipids. Motuporamines and desipramine have somewhat similar chemical structures and they both cause lipid body formation and inhibit degradation at the lysosome. Thus, it was hypothesized that tricyclic anti-depressants, like motuporamines, might also inhibit migration of tumour cells. Using the two-dimensional wound closure assay, a panel of six tricyclic antidepressants (amoxapine (100 μM), clomipramine (50 μM), imipramine (100 μM), amitriptyline (75 μM) fluoxatine (75 μM), and desipramine (50 μM)), was tested for their ability to inhibit migration of MDA-MB-231 cells. Photographs were taken 4 h after the

initial wounding of cell monolayers (Fig. 4.11a-h) and again 24 h after initial wounding (Fig. 4.11i-p) at the same location in the tissue culture well. After the 24 h incubation period, untreated cells had migrated to fill the wounded monolayer (Fig. 4.11i). dhMotC was added as a positive control (Fig. 4.11b,j) and significantly inhibited the migration into the wound after 24h. All of the tricyclic antidepressants that were tested in this experiment also inhibited cell migration into the wound, however, the size of the wound remaining after 24h was significantly smaller than the size of the wound in the dhMotC treated cells (Fig. 4.11k-p). Note also that concentrations of tricyclic antidepressants needed to partially inhibit cell migration were in the range of 5-10 fold higher than the concentration of dhMotC (10 μM) used in this experiment. At similar concentrations to those used in the migration assay, TCAs also inhibited MDA-MB-231 invasion of basement membrane (data not shown).

4.2. Summary and Discussion

Based on the cationic amphiphilic property of motuporamines, an investigation was conducted to determine whether motuporamines, like TCAs and other CADs, affect cellular lipids. It was found that long term treatments with motuporamines induced an intracellular accumulation of lipids at the peri-nuclear region in MDA-MB-231 cells. Transmission electron microscopy was used to further characterize the lipid bodies and revealed a relatively unorganized multi-vesicular/multi-lamellar ultrastructure. Fluorescent microscopy of cellular organelles involved in vesicular trafficking showed that motuporamine affects the staining pattern of late endosome/lysosomes, but not early endosomes, Golgi apparatus or

endoplasmic reticulum. Although, the results from immunostaining point to the late endosomes/lysosomes as probable candidates for the organelles of origin of the lipid bodies, the electron micrograph of a representative lipid body suggests that the structures induced by motuporamines are not simply enlarged versions of these organelles.

The major function of the endocytic pathway is the trafficking and sorting of endocytosed proteins from the plasma membrane. Activation of membrane receptors by ligand binding leads to endocytosis of the ligand-receptor complexes. Complexes are transported to early endosomes where they are sorted and can either be recycled back to the plasma membrane, or carried through the endocytic pathway via multi-vesicular bodies/late endosomes to lysosomes. Degradation of internalized transmembrane receptors is an important mechanism by which cells can downregulate signaling cascades initiated by extracellular stimuli (Katzmann *et al.*, 2002). In this study, endocyctosis of internalized EGF/EGFR complexes and trafficking of the complexes through the early endosomal pathway was not affected by motuporamines. However, degradation of the ligand-receptor complexes at the lysosome was significantly inhibited. This result suggests that motuporamines impinge on the function of lysosomes. Motuporamines could inhibit the trafficking of proteins from late endosomes to lysosomes or they could directly inhibit lysosomal degradative function. dhMotC treatment caused an increase in lysosomal pH, as indicated by the pH sensitive fluorophore lysotracker red. This phenotype is characteristic of other amine- containing drugs ((Kaufmann & Krise, 2007), and inhibition of phospholipase activity has been linked to CAD-induced lipidosis ((Hostetler & Matsuzawa, 1981; Hurwitz *et al.*, 1994; Kucia *et al.*, 2003). The inhibition of lysosomal enzymes by alteration in

lysosomal pH is an attractive hypothesis for the mechanism by which moturporamines affect degradation of EGF/EGFR complexes.

The interaction of CADs with cell membranes has been proposed to be one cause of the lipidosis phenotype (Albouz *et al.*, 1982; Albouz *et al.*, 1983; Albouz *et al.*, 1986; Geist & Lullmann-Rauch, 1994; Scuntaro *et al.*, 1996; Xia *et al.*, 2000). The major lipid constituents of cellular membranes are phospholipids. The hydrophobic fatty acid chains of these lipids contain polar head groups which create an amphiphilic environment in the fluid membrane. TCAs bind cellular membranes (Bickel & Steele, 1974; Romer & Bickel, 1979; Rothgeb & Oldfield, 1981; Sanganahalli *et al.*, 2000; Santos *et al.*, 2004; Seydel & Wassermann, 1976). The cationic amphiphilic structure of motuporamines suggests that these molecules may also be attracted to this amphiphilic environment because motuporamines have a hydrophobic amide ring and a positively charged amine tail, and both aspects of the motuporamine structure have been shown to be important for activity (Williams *et al.*, 2002). Although, further experimentation is needed to understand the mechanism by which motuporamines induced the formation of intracellular membrane inclusions, the chemical structure of these molecules is supportive of the hypothesis that it acts, similarly to other cationic amphiphilic drugs, by a mechanism that involves interaction with cellular membranes and alteration of lysosomal pH. It should be noted, however, that this hypothesis is likely an oversimplification of the mechanism, because some motuporamine analogues which are also cationic amphiphilic failed to induce the intracellular accumulation of membranes.

Although, many CADs induce the formation of membrane rich inclusions, these molecules still have distinct effects on cellular behavior, thus suggesting that they have distinct molecular targets. dhMotC is a strong Rho activator and Rho signaling is important for the mechanism of tumour invasion inhibition by dhMotC. By inhibiting rho signaling with C3 exoenzyme, it was shown that Rho activation does not cause EGFR degradation to be inhibited. It is not known, however, whether the opposite is true. Interestingly, the anti-tumour activity of motuporamines correlated well with the ability of motuporamine analogues to induce the formation of membrane rich inclusions. It was also found that TCAs inhibit cell migration. These two results are supportive of the hypothesis that lipidosis and tumour invasion inhibition may be causally linked. Furthermore, if motuporamines and TCAs have a similar mechanism of activity, the question arises whether motuporamines may also have efficacy as antidepressants. The latter being an interesting point for further investigation.

Immunostaining revealed that Mot#20 induced an intracellular accumulation of EGFR, and reduced localization of EGFR at the plasma membrane. It has been shown similarly, that desipramine inhibited the recycling of β_1-adrenoceptors (β1AR) to the plasma membrane after receptor internalization and trafficking to early endosomes (Burgi *et al.*, 2003). Interestingly, trafficking of the transferrin receptor was not affected by desipramine (Burgi *et al.*, 2003), neither did motuporamine significantly affect TfR staining. EGFR and β1AR are both transmembrane receptors which localize to lipid rafts when activated. Staining of GM1 ganglioside indicated that lipid raft microdomains accumulate intracellularly after motuporamine treatment. One could speculate that a side effect of

motuporamine or desipramine induced lipidosis is the mistrafficking of lipid raft associated membrane receptors to intracellular compartments. Because lysosomal degradation is inhibited, these receptors may be signaling from intracellular locations without downregulation. One could imagine a multitude of consequences resulting from such an aberrant state of signaling. In particular, sustained EGFR activation could be upstream of the Rho dependent inhibition of invasion by dhMotC. A similar mechanism might explain the inhibition of migration by TCAs that was observed in this study. Thus, an interesting point for further study would be to determine whether motuporamine-induced alterations of lipid organization is mechanistically connected with motuporamine-induced alterations in protein function. In particular, whether this connection could lead to sustained EGFR signaling, Rho activation, and subsequent inhibition of tumour invasion.

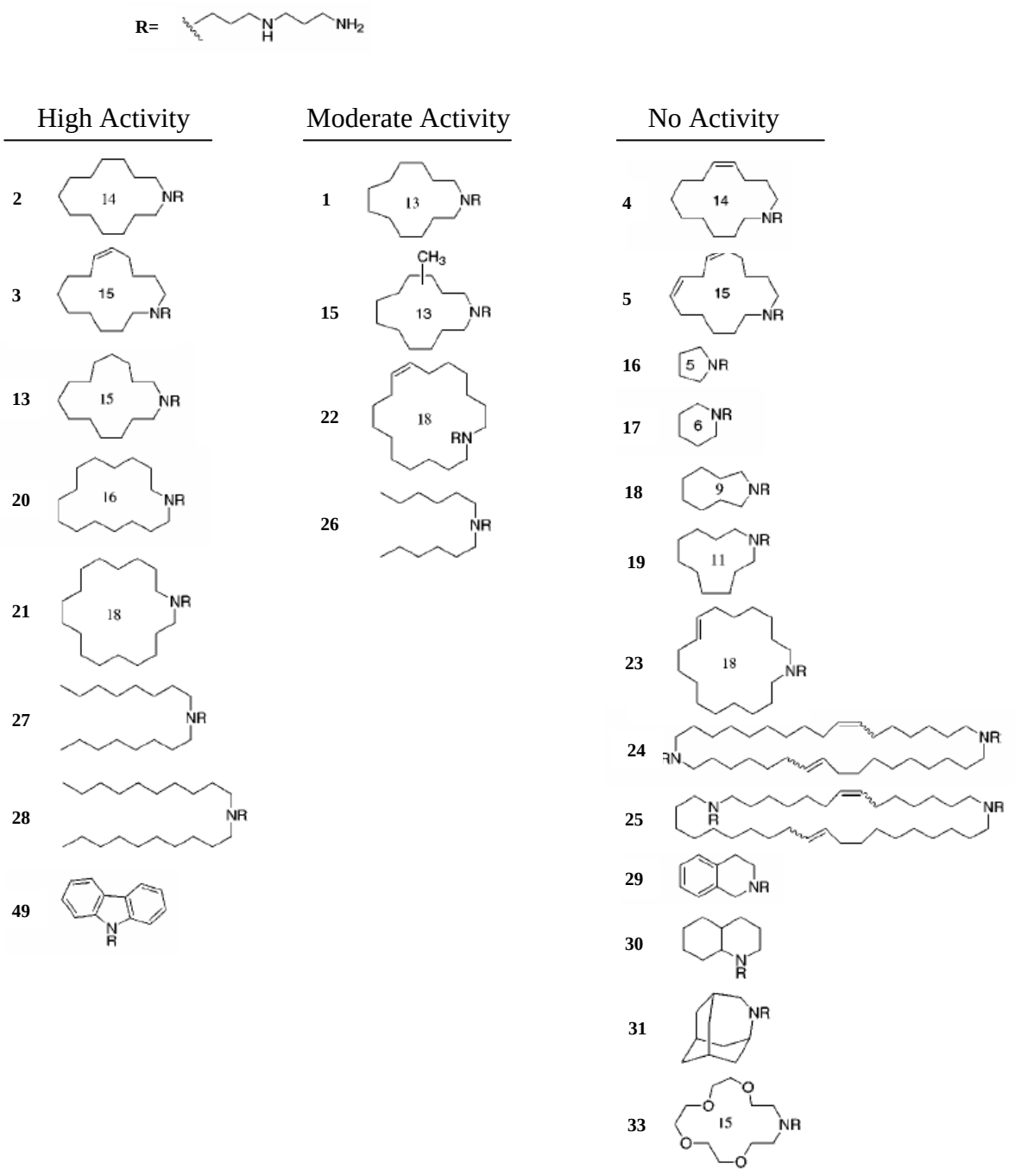

Figure 4.1. Variations in the cyclic amine fragment of motuporamine analogues. Ring size and saturation state are two characteristics of the ring fragment that influence anti-invasion activity of motuporamine analogues. Bold characters correspond to designated analogue numbers, while numbers inside the rings indicate the number of atomic constituents of the ring variations.

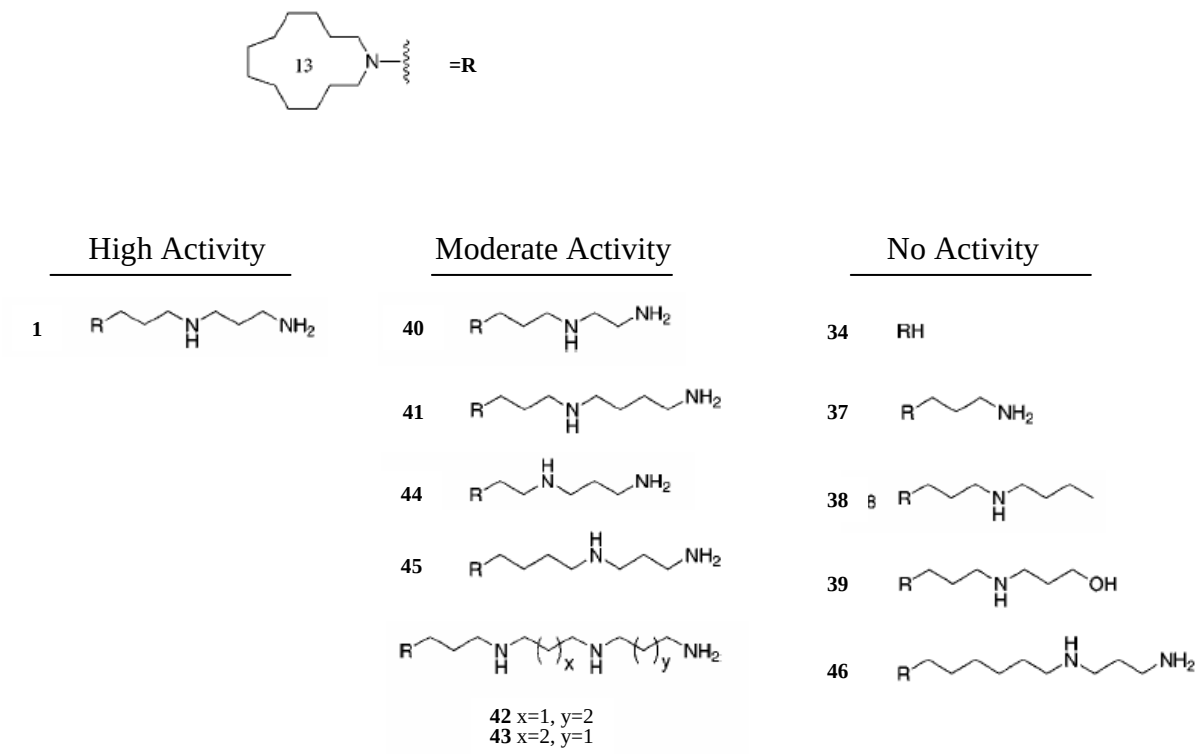

Figure 4.2. Variations in the side-chain fragment of motuporamine analogues. The presence of positively charged amine groups, and the length of the carbon chain between amines are two characteristics of the side-chain fragment that influence anti-invasion activity of motuporamine analogues. Bold characters correspond to designated analogue numbers.

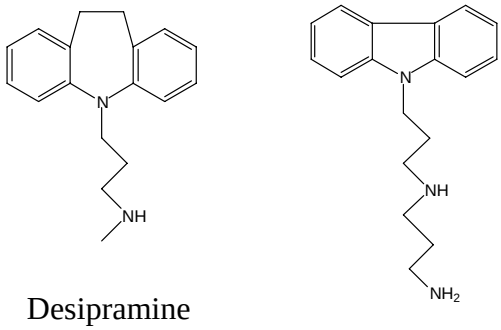

Desipramine

Mot. #49

Figure 4.3. The tri-cyclic anti-depressant desipramine and motuporamine analogue #49 have structural similarities. Notice that both molecules contain tri-cyclic rings fused to an amine tail. Mot. #49 has a longer tail which contains two amine groups separated by a three carbon chain, whereas the tail of desipramine is shorter and only contains one amine.

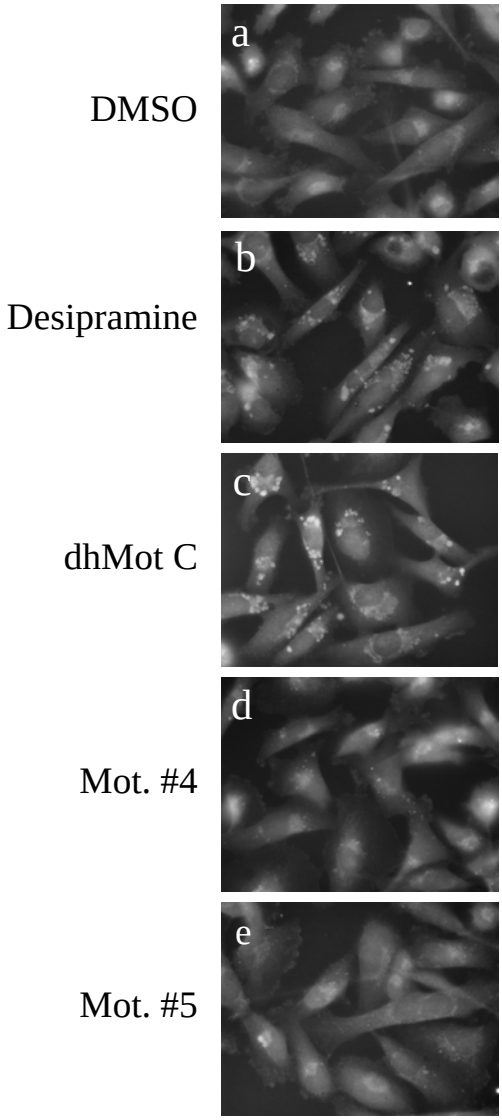

Figure 4.4. Lipids accumulate in the peri-nuclear region of mammalian cells after long-term treatment with active motuporamine analogues. DhMotC induces lipid accumulation in MDA-MB-231 cells. Cells were treated for 24h with DMSO (a), desipramine (b), dhMotC (c), Mot. #4 (d), or Mot. #5 (e) and then stained with the fluorescent lipid dye nile red.

Analog Number	Anti-Invasion Activity	Lipid Accumulation
4	0	0
5	0	0
13 (dhMotC)	6	4
16	0	0
17	0	0
18	0	0
19	0	0
20	4	6
22	4	4
23	0	2
24	0	0
26	1	1
29	0	0
30	0	0
31	0	0
33	0	0
38	0	1
40	2	2
42	2	1
44	1	2
45	2	1
46	0	0
49	3	1

Table 4.1. The invasion activity of motuporamine analogs correlates well with their ability to induce the intracellular accumulation of lipids. In a blind experiment, the activities of a panel of motuporamine analogues were given a score between 0 and 6 for their ability to induce the intracellular accumulation of lipids. A score of 6 is the largest effect that was observed. These ratings are charted next to a relative score for invasion activity determined from previously reported IC_{50} values.

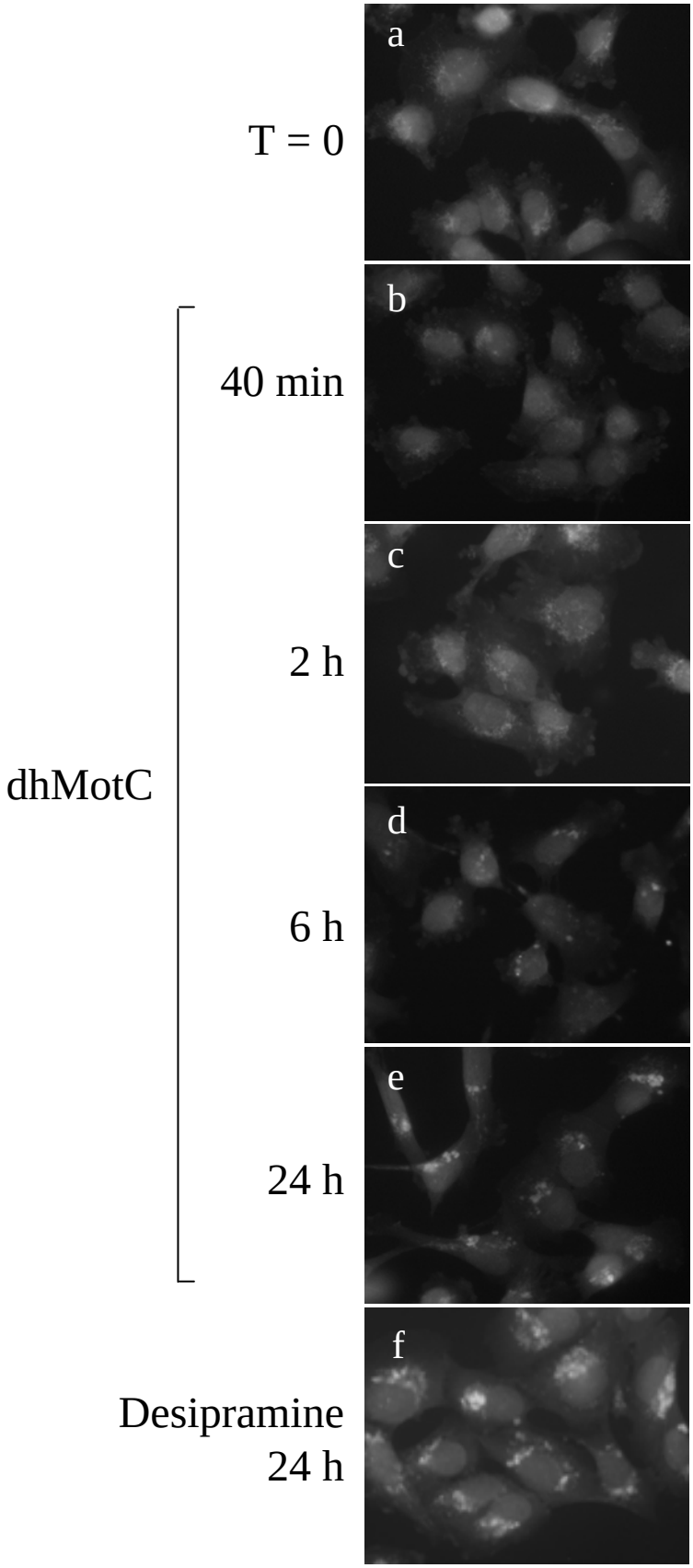

Figure 4.5. Motuporamine induces intracellular accumulation of lipid raft associated GM1-ganglioside. MDA-MB-231 cells were treated with dhMotC for 0 min (a), 40 min (b), 2h (c), 6h (d), or 24h (e), or with desipramine for 24h (f) and then fixed, permeabilized and incubated with FITC-cholera toxin.

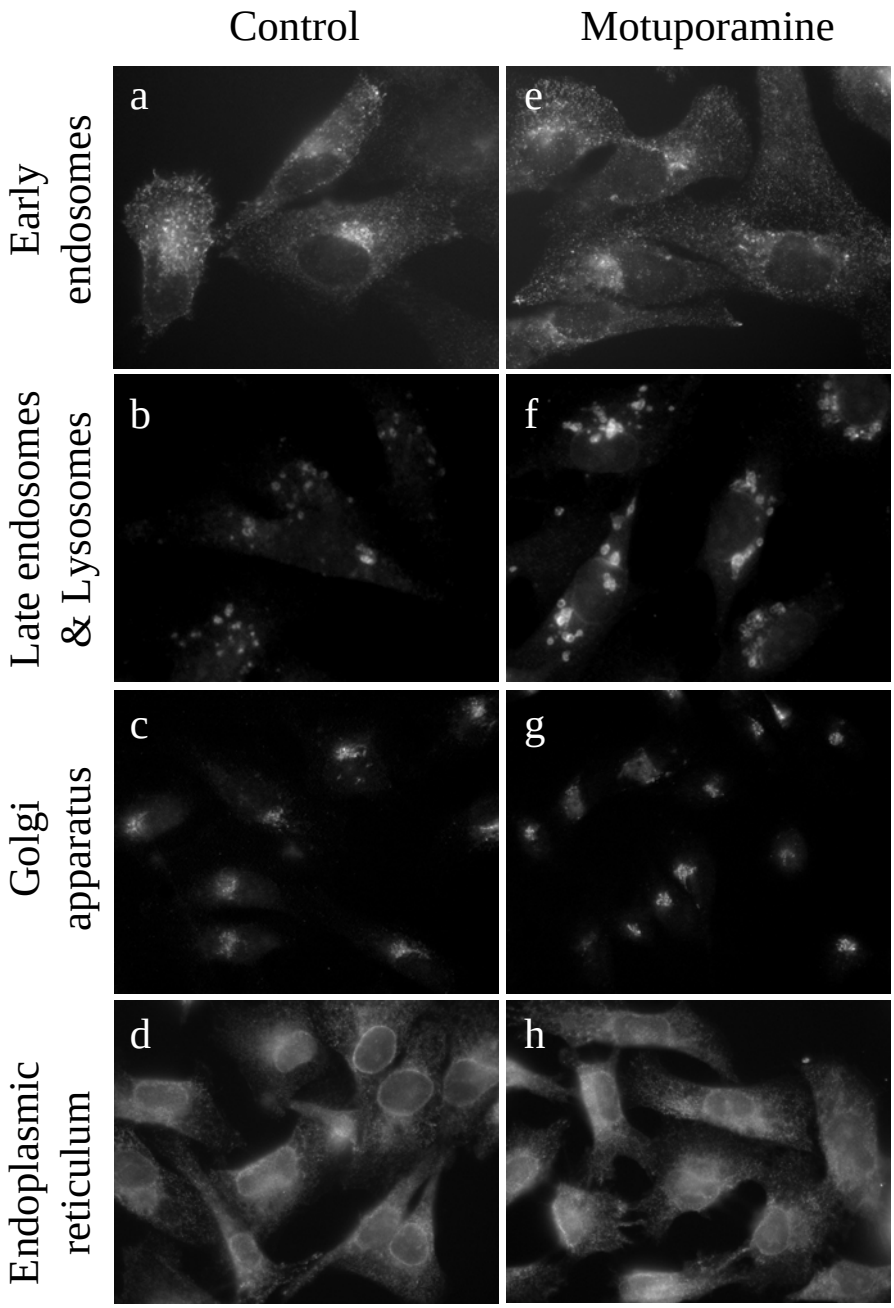

Figure 4.6. Fluorescent staining of organelles involved in vesicular trafficking. MDA-MB-231 cells were treated for 24h with DMSO (a-d) or Mot #20 (e-h) and then fixed and stained with antibodies against markers for early endosomes (transferrin receptor) (a,e), late endosomes/lysosomes (LAMP2) (b,f), Golgi apparatus (GM 130) (c,g) or the endoplasmic reticulum (PDI) (d,h).

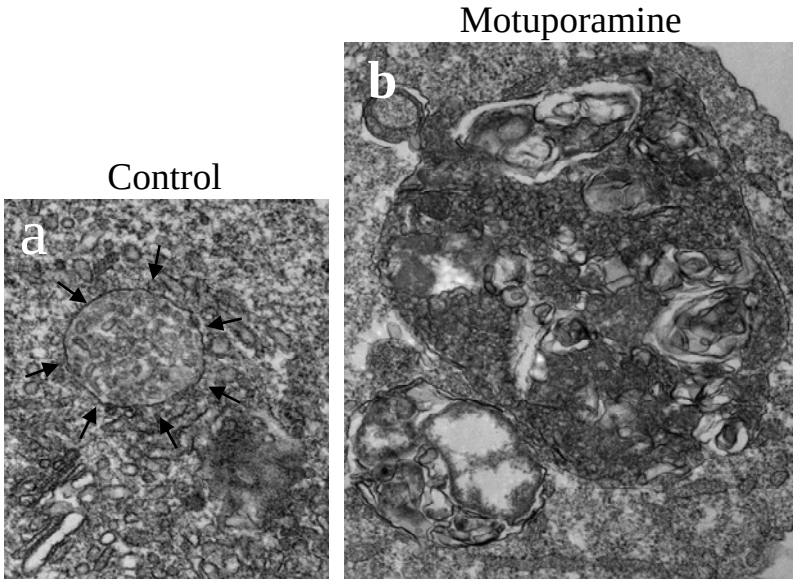

Figure 4.7. Motuporamine induces large aberrant multi-vesicular/ multi-lamellar bodies.
Transmission electron micrographs reveal large aberrant multi-vesicular/multi-lamellar bodies in cells treated with Mot #20 (b) for 6h which were not present in untreated cells (a). Notice the differences in size, shape, and membraneous structure compared to the multi-vesicular body (black arrows) shown in control cells. Note that photographs (a) and (b) are of equal magnification.

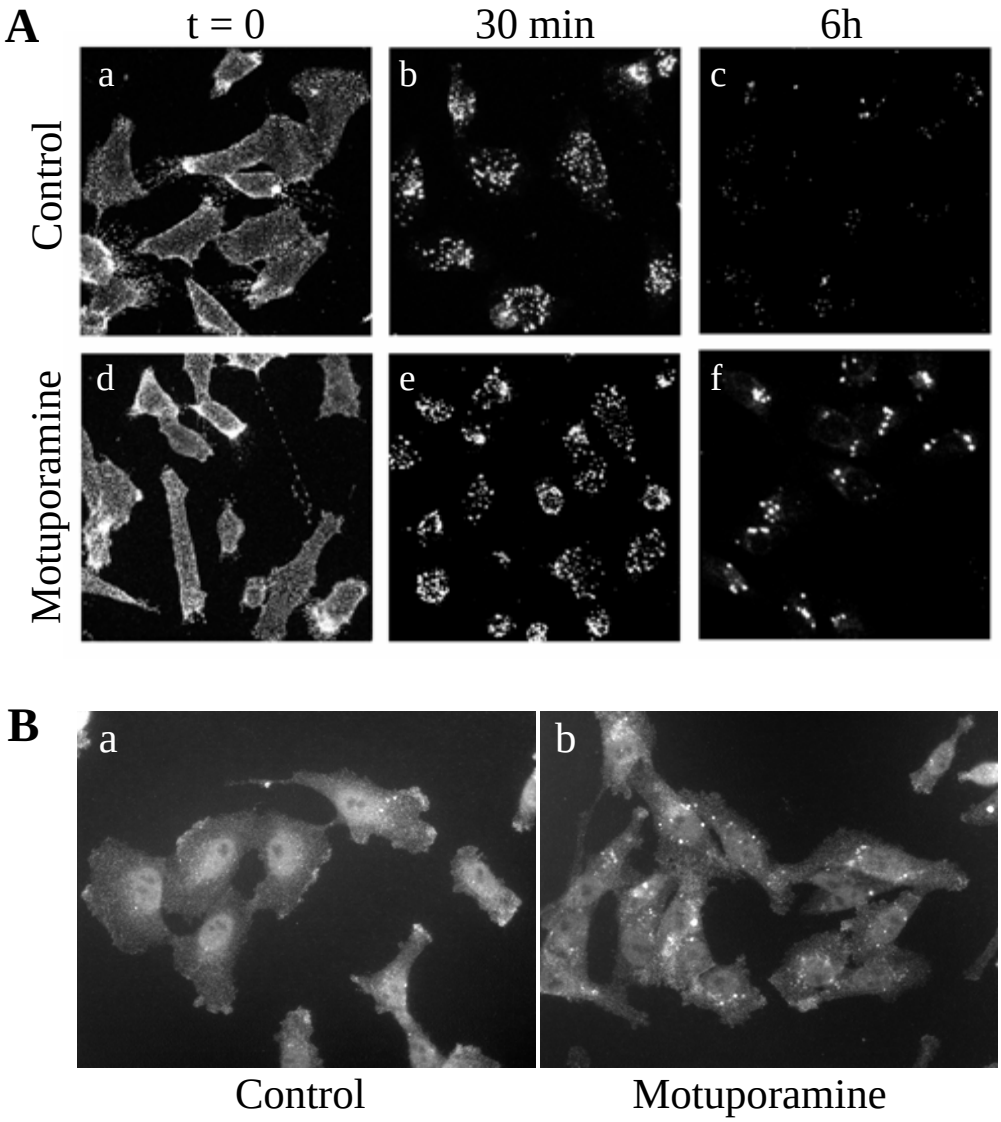

Figure 4.8. Motuporamine inhibits degradation of internalized FITC-EGF and induces intracellular accumulation EGFR.
A, MDA-MB-231 cells were exposed to FITC-EGF and then treated with DMSO (a,b,c) or mot#20 (d,e,f) before allowing endocytosis of FITC-EGF to proceed. Cells were fixed at time zero (a,b) and after 30 min (b,d) or 6 hours (c,f). FITC-EGF was visualized and photographed using confocal microscopy. **B,** MDA-MB-231 cells were treated with DMSO (a) or mot#20 (b) for 24h and then fixed, permeabilized and stained with antibodies against the EGF receptor.

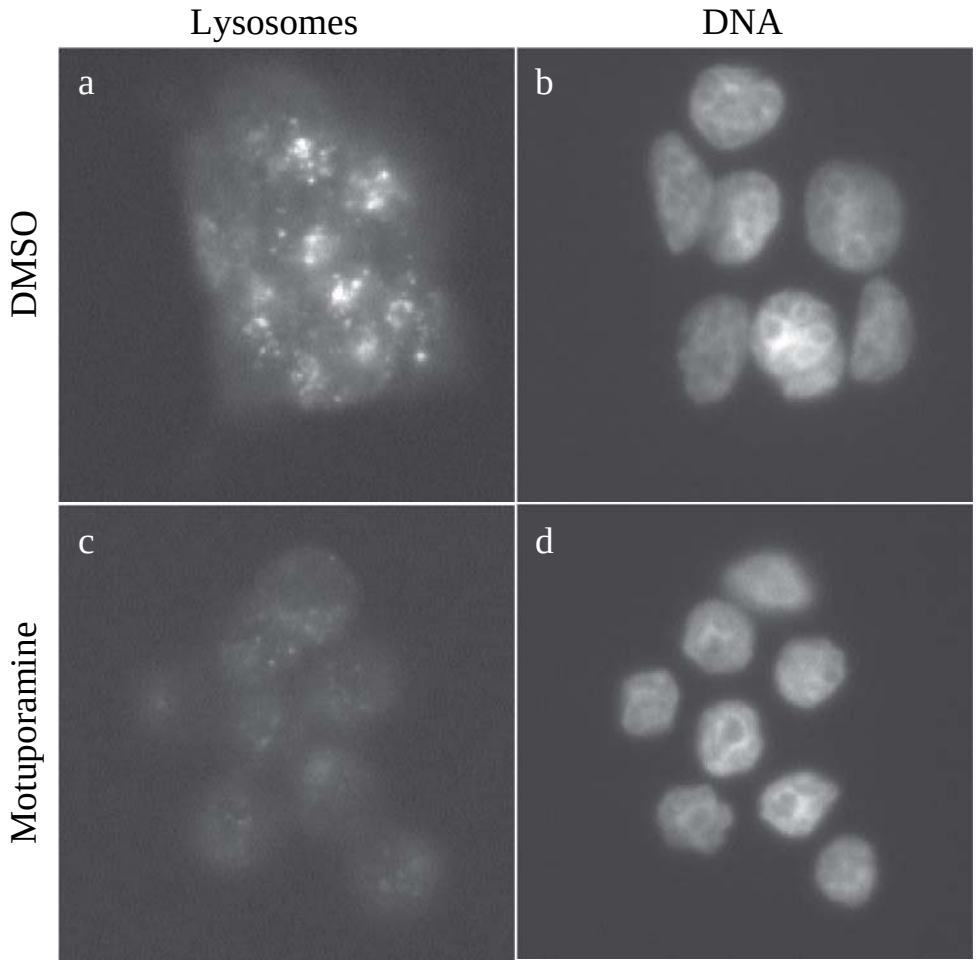

Figure 4.9. DhMotC increases lysosomal pH. Cells were treated with (c,d) or without (a,b) dhMotC for 35 min and lysosomal pH was assessed by lysotracker red fluorescence (a,c). Cellular nuclei are shown (b,d) for reference.

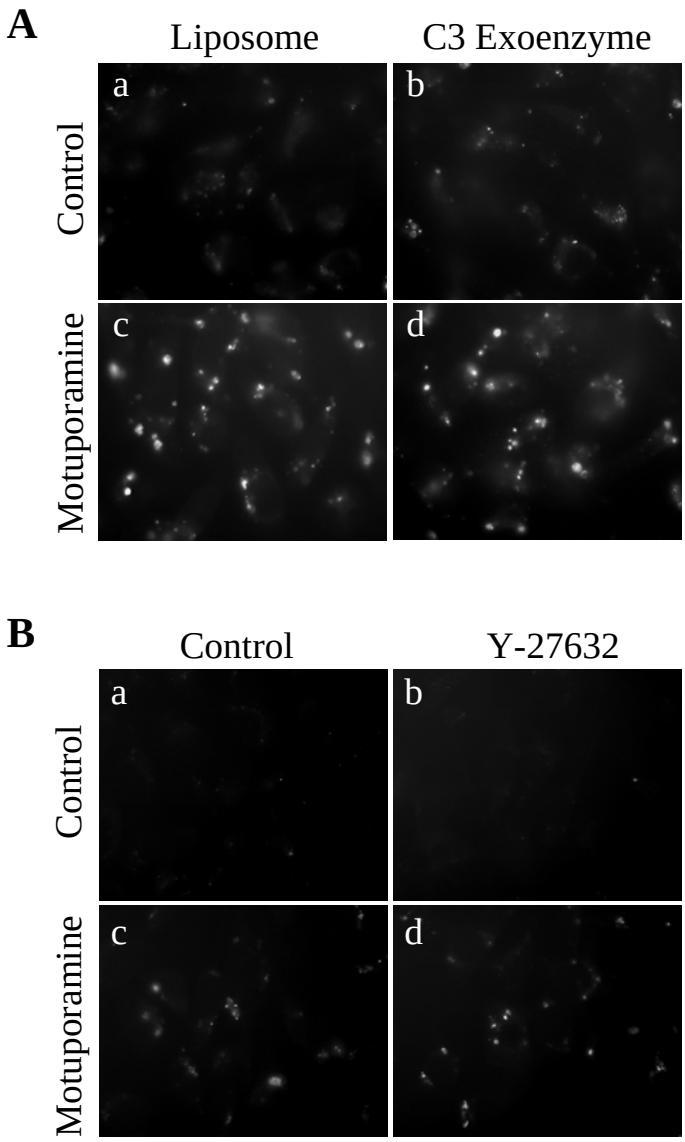

Figure 4.10. Inhibition of EFG degradation by motuporamine is independent of Rho/Rho kinase signaling. **A,** MDA-MB-231 cells were pre-treated with C3 exoenzyme (b,d) or liposome vehicle control (a,c) and then degradation of FITC-EGF was assessed after incubation with DMSO (a,b) or motuoporamine (c,d) for 6 hours. **B,** FITC-EGF degradation was assessed after treatment with DMSO (a,b) or motuporamine (c,d) in combination with (b,d) or without (a,c) Y-27632.

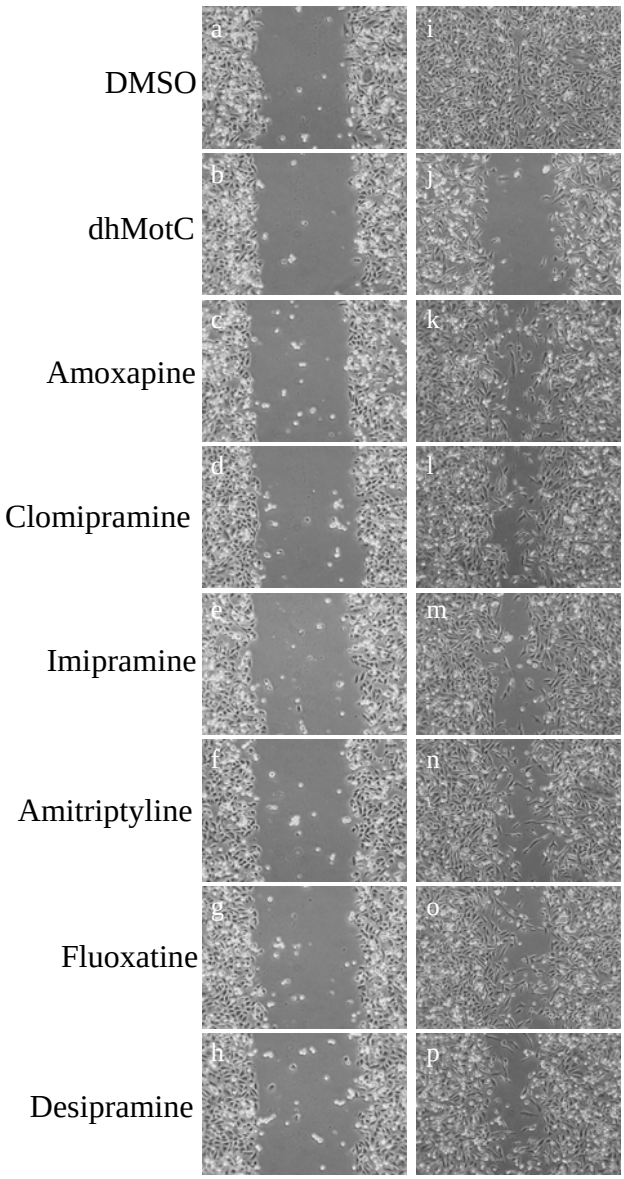

Figure 4.11. Tricyclic anti-depressants inhibit cell migration. Confluent monlayers of MDA-MB-231 cells were wounded and various tricyclic anti-depressants or controls were added; DMSO (a,i), 10 µM dhMotC (b,j), 100 µM amoxapine (c,k), 50 µM clomipramine (d,l), 100 µM imipramine (e,m), 75 µM amitriptyline (f,n) 75 µM fluoxatine (g,o), and 50 µM desipramine (h,p). Cells were then incubated for 24 hours until DMSO treated cells filled the wound. Photographs were taken at 4h (a-h) and at 24h (i-p).

Chapter 5: Yeast Genome-wide Drug-induced Haploinsufficiency Screen to Determine Drug Mode of Action.

5.1. Introduction

Drug target identification is a difficult task. Without knowledge of the primary target pathway, few tools exist to help decipher the direct target out of a choice of thousands of possible candidates. Drug-induced haploinsufficiency occurs when lowering the dosage of a single gene from two copies to one copy in diploid cells results in a heterozygote that displays increased drug sensitivity compared with wild-type strains (Giaever *et al.*, 1999). Screening for drug-induced haploinsufficiency is a novel method that was recently developed in yeast and showed applicability for use at the genome-wide level for drug target identification. Proof-of-prinicple studies have been carried out with drugs that have a known mechanism of action. However, successful target identification for drugs with unknown mechanisms of activity had not yet been achieved at the initiation of this study. Therefore, our group designed a genome-wide yeast haploinsufficiency screen in the hopes that we could achieve this goal.

dhMotC, as shown in previous chapters, alters actin filament organization and induces focal adhesion formation through the activation of RhoGTPase. dhMotC also affects trafficking and degradation of cellular membranes. However, the exact mechanism for these biological effects are still unknown. Understanding the mechanism for dhMotC activity is critical for evaluating its potential as a cancer therapy. dhMotC was therefore an intriguing candidate to be used in the pilot genome-wide yeast haploinsufficiency screen, and we asked whether this assay could be used to identify the target of dhMotC in human cells.

The screen was designed in a collaborative project between the laboratories of Dr. Phil Heiter and Dr. Michel Roberge. The initial screening was carried out by other members of the Roberge and Heiter laboratories, who identified a list of genes which showed increased drug sensitivity to dhMotC. From these data, the sphingolipid biosynthesis pathway was identified as a target of dhMotC in yeast. The results of their experiments will be presented at the beginning of this section (Fig. 5.1 – 5.5 and Table 1). Their work provided a basis for further research that I carried out in an effort to link the yeast screen data to a mechanism for dhMotC activity in human cells. Because this was a pilot study, there was no previously characterized method for achieving this task. The drug-induced haploinsufficiency study showed that sphingolipid metabolism is an important determinant of resistance to dhMotC. I was unable to show that sphingolipid synthesis is important for the mechanism of anti-invasion activity, however, sphingolipids did partially rescue drug-induced cell toxicity in mammalian cells. Subsequently, by returning to the yeast screen data and taking into consideration, the known phenotypic effects of motuporamine, I chose alternate target genes

to test. This resulted in the successful identification of ARF1, an important regulator of vesicular trafficking, as a mediator of dhMotC anti-invasion activity in human cells.

5.2. Results

5.2.1. Genome-wide Screen for dhMotC-induced Haploinsufficiency. As a prerequisite for yeast based genome-wide drug screening, treatment of yeast with a drug of interest must cause a phenotype that is easily scored, such as growth inhibition. dhMotC inhibited the growth of wild-type diploid yeast (BY4743) in liquid cultures in a concentration-dependent manner (data not shown). Concentrations >60 μM severely inhibited growth and resulted in a terminal phenotype that was not cell cycle- specific (data not shown). This result suggests that dhMotC targets at least one gene product involved in an essential function in *S. cerevisiae*. For high throughput phenotypic screening, a set of >5,000 heterozygous diploid deletion strains covering most yeast genes was robotically arrayed onto agar plates containing either DMSO (no drug control) or the sublethal dhMotC concentration of 60 μM. The plates were incubated at 25°C and strain growth on DMSO- and dhMotC-treated plates was compared over a period of 4 days (Fig. 5.1). An extended monitoring period was necessary for scoring of strains that grew slowly because of their intrinsic haploinsufficiency. The screen was carried out twice and strains displaying increased sensitivity to dhMotC in both screens are shown in Table 1. The list includes six essential genes and 15 nonessential genes implicated in a variety of functions.

5.2.2. Quantitative Identification of Supersensitive Strains. To confirm and quantitatively rank the sensitivity of the 21 strains, automated quantitative liquid growth measurements were carried out under no drug conditions or at a concentration of dhMotC (20 μM) that causes only a small degree of growth inhibition (Fig. 5.2a). Because many heterozygous yeast deletion strains exhibit a slow growth phenotype or haploinsufficiency in rich culture medium (Giaever *et al.*, 1999), it was necessary to compare growth profiles with and without drug for each strain. IGCDs (integrative growth curve differences) were used to rank strain sensitivity. This technique is unbiased by differences in growth rate between strains.

As expected, all 21 strains were more sensitive to 20 μM dhMotC than the wild-type control, but most showed only minor growth inhibition. However, two strains were clearly more sensitive than others: *lcb1*Δ/LCB1 and *tsc10*Δ/TSC10 showed an IGCD >2-fold over wild type and were defined as supersensitive (Fig. 5.2, c and d). Eight additional strains showed IGCD >1.5- fold greater than wild type (Fig. 5.3). Both *LCB1* and *TSC10* are essential genes required for the biosynthesis of the sphingolipid precursor sphingosine, suggesting that dhMotC targets a sphingolipid dependent process.

5.2.3. Sphingolipid Biosynthesis as a Target Candidate. Sphingolipids are essential components of all eukaryotic cells, playing both structural and regulatory roles (Dickson & Lester, 2002; Ohanian & Ohanian, 2001). The first committed step of sphingolipid synthesis is the condensation of serine and palmitoyl CoA to 3- ketodihydrosphingosine catalyzed by serine palmitoyl transferase, composed of subunits encoded by *LCB1* and *LCB2*. 3-

ketodihydrosphingosine is then reduced to DHS by 3-ketosphinganine reductase (Tsc10) encoded by *TSC10* and DHS is subsequently hydroxylated to phytosphingosine (PHS) by DHS hydroxylase encoded by *SUR2*. PHS is conjugated with C26-fattyacyl-CoA to form ceramide in a reaction requiring the homologous and functionally redundant *LAG1* and *LAC1* (Fig. 5.4). In mammalian cells, the predominant long chain base (LCB) is sphingosine (formed by desaturation of DHS) rather than PHS. In addition to *de novo* synthesis, LCBs and ceramide are produced both by this synthetic pathway and by catabolism of complex sphingolipids that are major components of cellular membranes. Sphingosine also plays an intracellular signaling function by activating a Pkh1- Ypk1 kinase cascade controlling the actin cytoskeleton (Fig. 5.4 and refs. (Ohanian & Ohanian, 2001) and (Dickson & Lester, 2002)). Pkh1 phosphorylates and activates several protein kinases, including Ypk1 and Pkc1 (Casamayor *et al.*, 1999; Inagaki *et al.*, 1999). *PKH1* is a nonessential gene that is genetically redundant with *PKH2*, and *pkh1*Δpkh2Δ double-deletion mutants are inviable (Casamayor *et al.*, 1999; Inagaki *et al.*, 1999), whereas $pkh1^{D398G}$*pkh2*Δ double mutants are viable and display actin polarization defects (Inagaki *et al.*, 1999). Although no genes of the sphingolipid metabolism pathway other than *LCB1* and *TSC10* were identified in the high-throughput screen, the supersensitivity of *lcb1*Δ/LCB1 and *tsc10*Δ/TSC10 to dhMotC motivated us to directly test the sensitivity of additional heterozygous mutants (indicated in Fig. 5.4). Whereas most strains did not display dhMotC sensitivity above wild type, the *ypk1*Δ/*YPK1* strain was supersensitive and lcb2Δ/*LCB2*, *sur2*Δ/SUR2, and *pkh1*Δ/PKH1 strains showed increased sensitivity to dhMotC when tested in the liquid growth assay (Fig. 5.3). The sensitivity of six mutants heterozygous for deletions of genes involved in sphingolipid metabolism strongly suggests that dhMotC either directly targets sphingolipid

metabolism or targets a pathway that is synthetically lethal in combination with compromised sphingolipid synthesis.

To determine whether interference with sphingolipid biosynthesis was important for growth inhibition by dhMotC, we asked whether increased levels of sphingolipid biosynthetic intermediates could rescue the dhMotC sensitivity of wild-type cells. Exogenous addition of DHS has been shown previously to rescue genetic disruption of *LCB1(Beeler et al., 1998; Zanolari et al., 2000)*. We therefore tested the effect of DHS addition to liquid growth medium and found that DHS did not affect the growth of wild-type yeast but nearly completely suppressed growth inhibition by dhMotC (Fig. 5.5*A*). Deletion of either *CSG1* or *CSG2*, genes required for mannosylation of inositolphosphorylceramide-C, has been shown to cause the accumulation of inositolphosphorylceramide-C and ceramide in cells (Beeler *et al.*, 1998; Zhao *et al.*, 1994). We found that *csg2*Δ mutant cells are almost completely resistant to dhMotC treatment, indicating that similar to exogenous DHS, elevated inositolphosphorylceramide-C and/or ceramide are protective against the effects of dhMotC (Fig. 5.5B). Our analysis suggests that dhMotC directly affects the biosynthesis of sphingolipids in yeast. Therefore, we carried out biochemical assays to determine which sphingolipid metabolic intermediate might be affected by dhMotC. To address whether dhMotC directly inhibits Tsc10, we analyzed sphingoid bases from drug-treated cells. Whereas *tsc10* mutants (with reduced function Tsc10) accumulate 3-ketosphinganine (Beeler *et al.*, 1998), treatment of cells with dhMotC did not cause 3- ketosphinganine to accumulate, nor did it alter the steady state levels of DHS and PHS (data not shown). Furthermore, *in vitro* activity of serine palmitoyl transferase was not inhibited by dhMotC (data not shown).

These data indicate that dhMotC is not directly inhibiting serine palmitoyl transferase or Tsc10. However, dhMotC reduced cellular ceramide levels (data not shown). To investigate this hypothesis further, we measured incorporation of ^{3}H-serine into ceramide during an 8 h labeling period with and without dhMotC (Fig. 5.5C) (for details regarding materials and methods, refer to Baetz *et al*., 2004). Wild-type cells treated with sublethal levels of dhMotC have roughly half as much ceramide per cell after 8 h as untreated wild-type cells. As expected, *csg2*Δ cells have elevated levels of ceramide, and although dhMotC treatment of *csg2*Δ cells also lowers ceramide levels, ceramide levels are still above normal, confirming that elevated ceramide levels protect *csg2*Δ cells from dhMotC. The fact that dhMotC lowers ceramide levels in wild-type cells indicates that dhMotC directly targets sphingolipid metabolism in yeast rather than a pathway that is synthetic lethal with compromised sphingolipid metabolism. If the mode of action of dhMotC is conserved between yeast and mammalian cells, then treatment of human cells with exogenous ceramide should rescue the effects of dhMotC. Exposure of breast carcinoma MDA-231 cells to high concentrations (10 μM) of dhMotC for an extended time (24 h) reduces their survival (Fig. 5.6). Addition of 10 or 50 nM C6-ceramide had no effect on the survival of cells not exposed to dhMotC, but 10 nM C6-ceramide slightly increased survival and 50 nM C6-ceramide increased by 4- to 5-fold the survival of cells exposed to dhMotC (Fig. 5.6). Higher ceramide concentrations reduced the extent of the rescue (data not shown), possibly because ceramide is known to induce apoptosis at higher concentrations (Ohanian & Ohanian, 2001; Ruvolo, 2003). These results indicate that modulation of ceramide levels by dhMotC is relevant to its mechanism of action in yeast and mammalian cells alike.

In order to determine whether the sphingolipid biogenesis pathway is involved specifically in the mechanism for invasion inhibition by dhMotC, we tested a panel of 5 different sphingolipid molecules for an effect on the invasive potential of MDA-MB-231 cells in the presence or absence of dhMotC. Dihydrosphingosine, sphingosine, sphingosine-1-phosphate, C6-ceramide, and C2-ceramide were tested at concentrations ranging from .01 – 10 μM. Interestingly, none of the above sphingolipids increased invasion of MDA-MB-231 cells in either the presence of absence of the invasion inhibitor dhMotC (data not shown).

5.2.4. SNF7 as a Target Candidate. We returned to the haploinsufficiency screen data (Table 5.1) to select a new candidate protein that might mediate dhMotC activity. Based on data suggesting that motuporamines affect vesicular trafficking, SNF7 became an intriguing target candidate. SNF7 functions as a subunit of the ESCRT-III complex involved in sorting and trafficking of protein cargos in the endosomal pathway (Babst *et al.*, 2002). SNF7 was characterized as a 'class E' VPS (vacuolar protein-sorting) gene because SNF7 mutants have an aberrant lipid compartment (the 'class E' compartment) adjacent to the vacuolar membrane (Raymond *et al.*, 1992). As a first step to determine whether dhMotC might be affecting the function of SNF7, we asked whether it also induced a class E-like compartment in wild type yeast cells. We used a lipid dye (FM4-64) to stain yeast membranes and track the internalization of lipids from the outer plasma membrane through the endocytic pathway to the yeast vacuole. Yeast cells were grown to log phase, pre-treated with dhMotC and then stained with FM4-64 at 4°C. The temperature was then raised to 25°C so that endocytosis and internalization of the stained lipids could occur. Cells were incubated for 1 h at room temperature and then viewed under a fluorescence microscope. In cells treated with a vehicle

control, the majority of stained lipids had accumulated at the vacuolar membrane and a large fluorescent ring was apparent inside the yeast cells (Fig. 5.7A-a). In cells treated with dhMotC, the vacuolar membrane was also fluorescent, however, there was an obvious accumulation of lipids adjacent to the vacuolar membrane (Fig. 5.,7A-b). In order to quantify this effect, yeast cells were counted manually and the percentage of cells exemplifying this phenotype was calculated. Results indicated that the phenotype induced by dhMotC was dose-dependent (Fig. 5.7B). This phenotype showed some resemblance to the class E phenotype (Raymond *et al.*, 1992), but did not appear identical to it. Of note, higher concentrations of dhMotC (60-100 μM) induced a more severe phenotype in a small percentage of cells (~ 10%). These cells had intensely staining spots in the cytoplasm and completely lacked fluorescently stained vacuolar membranes (data not shown).

Although the above observations were supportive of the hypothesis that dhMotC targets SNF7, it seemed unusual that other VPS mutants involved in vesicular trafficking were not identified in the screen for haploinsufficiency. To determine whether other VPS genes had been overlooked in the primary screen, we compiled a list of 15 'class E' VPS genes to retest for dhMotC-induced haploinsufficiency (Table 5.2). Yeast strains were grown in overnight cultures in the presence or absence of dhMotC and the OD_{600} was measured every hour for 16 hours. Fig. 5.8 shows the growth curves for each of the VPS mutant strains selected. In the absence of dhMotC, all of the happloinsufficient strains showed growth rates similar to that of the wild type yeast strain used as a control. As expected, dhMotC caused significant growth inhibition in the SNF7 (VPS32) happloinsufficient strain. However, no other strains had a similar increase in sensitivity to dhMotC compared to the wild type strain.

These results confirm the accuracy of the primary screen data, however, because none of the ESCRT III subunits, nor any other class E mutants were found to by hypersensitive to dhMotC, we concluded that these data do not provide strong enough support to warrant further investigation of SNF7 on the ESCRT III complex as a direct target of dhMotC.

5.2.5. ARF1 as a Target Candidate. ARF1 is a small GTPase that functions as a major regulator of vesicular trafficking in both the secretory and the endocytic pathways. ARF1 has also been shown to regulate actin dynamics through activation of RhoGTPases (for review; (D'Souza-Schorey & Chavrier, 2006; Donaldson *et al.*, 2005). We hypothesized that ARF1 might be involved in the mechanism for motuporamine anti-invasion activity because the ARF1 mutant was hypersensitive to dhMotC treatment in our haploinsufficiency screen (Table 5.1). Brefeldin A is a small molecule inhibitor of ARF1 which inhibits GDP/GTP exchange (Donaldson *et al.*, 1992; Helms & Rothman, 1992) by binding the molecular interface of ARF1 and the SEC7 domain of Arf GEFs (guanine nucleotide-exchange factors). Brefeldin A traps ARF1/SEC7 in an inactive conformation (Zeghouf *et al.*, 2005). Brefeldin A-induced inhibition of ARF1 causes rapid disassembly of the Golgi apparatus (Donaldson & Klausner, 1994). Thus, we first asked whether short-term treatments with dhMotC might also affect the structure of the Golgi apparatus. MDA-MB-231 cells were treated with DMSO, brefeldin A, dhMotC, or a combination of brefeldin A and dhMotC for 15 min. Cells were fixed and incubated with primary antibodies against the Golgi apparatus marker GM-130, and then stained with fluorescently-conjugated secondary antibodies. In control cells, the Golgi apparatus appeared relatively compact and was brightly stained in the peri-nuclear region (Fig. 5.9a), whereas in cells treated with brefeldin A, the staining became diffuse

throughout the cell and it appeared as if the Golgi apparatus was completely disassembled (Fig. 5.9c). We observed that treatment with dhMotC had little effect on Golgi structure or localization compared to the negative control (Fig. 5.9b), but surprisingly, when dhMotC was added in combination with brefeldin A, Golgi disassembly was partially inhibited (Fig. 5.9d). Although, the Golgi apparatus staining did not appear equivalent with the negative control, the staining intensity was more condensed to the peri-nuclear region in many cells.

The above results were somewhat unexpected because they imply that brefeldin A and dhMotC are acting antagonistically, and that dhMotC may be an activator and not an inhibitor of the ARF1 pathway. Therefore, it was next asked whether inhibition of ARF1 with brefeldin A could reverse the phenotypic effect of dhMotC on MDA-MB-231 cells. Cells were plated on plastic and allowed to adhere overnight before they were treated briefly (15 min) with either DMSO, dhMotC, brefeldin A, or a combination of both dhMotC and brefeldin A together. Then cell morphology was assessed by phase-contrast microscopy. Neither DMSO nor brefeldin A had a significant effect on cellular shape after the short treatment time (Fig. 5.10A-a,c). MDA-MB-231 cells remained elongated, adherent, and polarized; a characteristic phenotype of migratory cells. As expected, when cells were treated with a relatively high concentration of dhMotC (10 μM), significant effects on morphology were observed even after 15 minutes (Fig. 5.10A-b). Cells became contracted and many began to round up, completely losing their polarized shape. Some cells began to detach from the plastic dish. However, when brefeldin A was added to the media in combination with dhMotC, this rounding effect was significantly reduced (Fig. 5.10A-d). More cells remained attached and were significantly more spread on the dish. Furthermore, actin staining of cells

showed that brefeldin A also restored lamellipodial ruffling to the ruffling-inhibited dhMotC-treated cells (Fig. 5.10B- compare b with d). In the short time period of this assay, neither brefeldin A nor the vehicle control affected lamellipodial ruffling when added to the media alone (Fig. 5.10B-a,c).

Cell adhesions, membrane ruffling and polarity are important factors which influence migratory and invasive ability. Thus, if treatment with brefeldin A counteracts the morphological changes induced by dhMotC, it may also have an antagonistic effect on dhMotC-induced invasion inhibition. We therefore tested brefeldin A alone and in combination with dhMotC to determine if inhibition of ARF1 is involved in the mechanism of dhMotC anti-invasion activity. As expected, dhMotC inhibited MDA-MB-231 cell invasion into Matrigel compared to the negative control, DMSO (Fig. 5.11). Brefeldin A alone did not significantly affect invasion after the short time period used in this assay (1hr), however, the quantification of invasion inhibition showed that brefeldin A treatment made MDA-MB-231 cells more invasive in the presence of dhMotC compared to dhMotC alone. Although, brefeldin A did not completely abrogate the anti-invasion effect of dhMotC, this result supports the hypothesis that ARF1 is activated by dhMotC and this activation partially mediates the anti-invasion activity of dhMotC.

5.3. Summary and Discussion

We have applied a systematic approach for identifying candidate drug targets and pathways in yeast that should be applicable to any drug causing a scorable phenotype such as growth inhibition. Importantly, this study indicates that a physiological process that is affected by a drug in mammalian cells, in this case cancer cell invasion, need not be recapitulated in yeast for the technique to be considered. Of relevance is the cross-species conservation of biochemical pathway function and not the specific phenotypic consequence of pathway disruption in yeast versus human cells.

In this study, the initial high-throughput screen identified 21 heterozygous deletion strains that were more sensitive to dhMotC compared to wild type yeast cells. Heterozygous gene deletions that cause increased drug sensitivity are expected to comprise essential genes whose products are direct drug targets and essential or nonessential genes that exhibit synthetic interactions with the drug target. Quantitative ranking of dhMotC sensitivity in a subsequent liquid growth assay identified two members of the sphingolipid biosynthesis pathway, *lcb1Δ*/LCB1 and *tsc10Δ*/TSC10, as supersensitive strains, prioritizing this pathway as the candidate target. Direct measurements of cellular sphingolipid levels showed that dhMotC treatment lowers ceramide levels. Artificially elevating ceramide levels by adding exogenous sphingosine or preventing the incorporation of ceramide into complex sphingolipids through *CSG2* inactivation nearly totally rescued the effects of dhMotC on yeast growth. These results demonstrate that inhibition of sphingolipid metabolism is a major mechanism of the growth inhibiting activity of dhMotC in yeast.

Our screen did not identify all genes of the sphingolipid metabolism pathway. Further iterations of the primary screen might have revealed additional ones, such as the supersensitive *ypk1Δ/YPK1* strain found in follow up studies. However, functionally redundant genes such as *LAC1* and *LAG1* cannot be detected in simple haploinsufficiency screens, and other genes might escape detection because reduction in gene copy number does not manifest itself in compromised function. Despite these limitations, it is likely that at least a subset of heterozygous deletion strains of any given pathway will be gene dosage sensitive and show supersensitivity to drugs in this assay, and will be sufficient to expose the pathway.

To determine whether yeast drug-induced haploinsufficiency screening is relevant for finding drug mode of action in human cells, we sought a simple test with broad applicability. Most drugs are expected to affect the survival of human cells at high doses. By analogy to the yeast growth inhibition experiments, we determined whether the deleterious effects of dhMotC on human cell survival could be rescued by addition of exogenous ceramide. Indeed, ceramide provided significant protection from the effects of dhMotC. However, the extent of protection was not as high as observed in yeast. One explanation is that dhMotC might have additional targets in human cells that are not present in yeast. Alternatively, because ceramide has been implicated in the regulation of numerous cellular pathways including apoptosis, senescence and cell-cycle arrest (Ohanian & Ohanian, 2001; Ruvolo, 2003), it is possible that rescue by exogenous ceramide is limited by its intrinsic toxicity. Short-chain ceramides are often used in tissue culture because they pass easily through the plasma membrane, although endogenously synthesized ceramides have significantly longer carbon chains. Thus, the biological relevance of adding short-chained ceramides to cells remains

questionable, and it was difficult to assess conclusively whether or not dhMotC targets sphingolipid biosynthesis in human cells. Nonetheless, the addition of exogenous sphingolipids did not cause MDA-MB-231 cells to regain invasive characteristics in the presence of dhMotC. We therefore chose to return to the haploinsufficiency screen results and select another target candidate for further experimentation.

The strength of growth inhibition in yeast may not necessarily be the most important indicator when selecting a relevant target candidate for human cells. For this reason, we looked at the yeast strains that were moderately growth inhibited, and used a phenotype-based rationale to choose another target candidate. Our first inclination was to investigate SNF7 as a possible candidate because we have seen that motuporamines alter vesicular trafficking in human cells. SNF7 is a subunit of the ESCRT III complex involved in regulating vesicular trafficking and protein sorting in the endocytic pathway (Babst *et al.*, 2002). In yeast, we found that dhMotC causes endocytosed lipids to accumulate in a compartment adjacent to the yeast vacuole. This compartment somewhat resembled the previously characterized 'class E compartment' found in a group of vps mutants of which SNF7 is classified (Raymond *et al.*, 1992). However, none of the other class E mutants were growth inhibited by dhMotC. Therefore, we quickly questioned whether SNF7 was actually a valid target candidate. In a more recent study, Parsons *et al.* (Parsons *et al.*, 2004) performed haploinsufficiency screens on a panel of drugs with unknown mechanisms of activity. They identified a list of yeast mutants that showed multi-drug sensitivity. Interestingly, snf7Δ/SNF7 was identified in this list, which suggested to us that the sensitivity of this strain was not specific to dhMotC. Thus, we were deterred from continuing further experimentation

with this candidate. As genome-wide yeast screening is used more commonly, the characterization of multi-drug sensitive strains will facilitate the elimination of multidrug resistance that arise during the primary screening process.

ARF1 was selected as a third target candidate from the yeast haploinsufficiency data. ARF1 was attractive because it is involved in vesicular trafficking but has also been shown to regulate actin dynamics (Donaldson *et al.*, 2005). Both of these cellular processes are affected by dhMotC in human cells. The availability of the ARF1 inhibitor, brefeldin A, allowed for a simple method to perturb ARF1 function in cells and compare the phenotypic outcome with that of dhMotC. Interestingly, we observed that brefeldin A and dhMotC had antagonistic effects on MDA-MB-231 cells. dhMotC reduced brefeldin A-induced disassembly of the Golgi apparatus, while brefeldin A reduced dhMotC-induced cell contraction, lamellipodial ruffling, and matrigel invasion. It is not surprising that brefeldin A and dhMotC were only partially antagonistic because it is possible that either or both of the drugs have secondary target pathways. Direct assessment of the activation state of ARF1 after dhMotC treatment is still needed. However, these preliminary results suggest that dhMotC treatment leads to activation of the ARF1 pathway, and that ARF1 activity partially mediates the mechanism for invasion inhibition by dhMotC. This result was somewhat unexpected because in yeast, arf1Δ/ARF1 was growth inhibited by dhMotC. One might expect dhMotC to increase the growth rate of arf1Δ/ARF1 if dhMotC is activating an ARF1 signaling pathway. One possible explanation for this discrepancy could be that the cellular location of ARF1 is altered by dhMotC treatment. Although arf1Δ/ARF1 only contains one copy of the ARF1 gene, dhMotC may induce activation of ARF1 activity and simultaneously

cause a change in normal ARF1 localization. If this were the case, the change in cellular location could have a dominant negative phenotype that would explain the sensitivity of the haploinsufficient ARF1 strain to dhMotC. While mislocation of ARF1 could be growth suppressive in yeast, it could also have anti-invasive consequences in mammalian cells. Further studies are needed to understand how dhMotC affects active ARF1 localization inside cells. Another important point to investigate is whether ARF1 and Rho activation are within the same pathway when mediating invasion inhibition by dhMotC. ARAP1 is a GAP effector protein for both the Rho and ARF family of GTPases (Miura *et al.*, 2002). This is an example of one molecule that could mediate the convergence of ARF and Rho pathways in dhMotC-induced signaling. However, further research is necessary to better understand the mechanism of dhMotC-induced ARF1 activation and how it relates to the activation of Rho pathways.

A major obstacle in using a genome-wide approach to drug target identification is the handling and deciphering of the large data sets that are generated. In this pilot study, we have identified a number of factors which are important to consider. For each individual mutant, the degree of growth inhibition by the drug of interest was the primary indicator used in this study. The number of times that a gene in a certain pathway is identified also proved to be a valuable determinant. We used these indicators with success and identified the sphingolipid biosynthesis pathway as a target in yeast. However, it is possible that multiple targets exist for dhMotC. The identification of highly sensitive heterozygous strains, such as *lsb5Δ/*LSB5 and *ygr205wΔ/*YGR205w, not known to be involved in sphingolipid biosynthesis might indicate that dhMotC has secondary targets. It is also possible that lowered expression of

these genes is synthetic lethal with compromised sphingolipid biosynthesis. This issue should be solvable in the future, when complete synthetic genetic interaction maps are available to facilitate the sorting of genes into those that likely encode pathways targeted by drugs from those that display synthetic interactions with those pathways (Parsons *et al.*, 2004). We were unable to use sphingolipids to rescue the effect of dhMotC in human cells, which indicates that the degree of growth inhibition may not be the best indicator for human targets. One must also be wary of hits from growth-inhibited strains that have mutations in multi-drug resistance genes. Furthermore, the ability to test target candidates in humans is limited by the availability of biological tools. Nonetheless, we successfully used phenotypic indicators to guide the selection of a human target candidate, and used a small molecule inhibitor of ARF1 to show that ARF1 signaling partially mediates the mechanism of tumour cell invasion inhibition by dhMotC. Thus, our novel genome-wide screen proved to be a valuable tool for identifying drug mechanism of action in human cells.

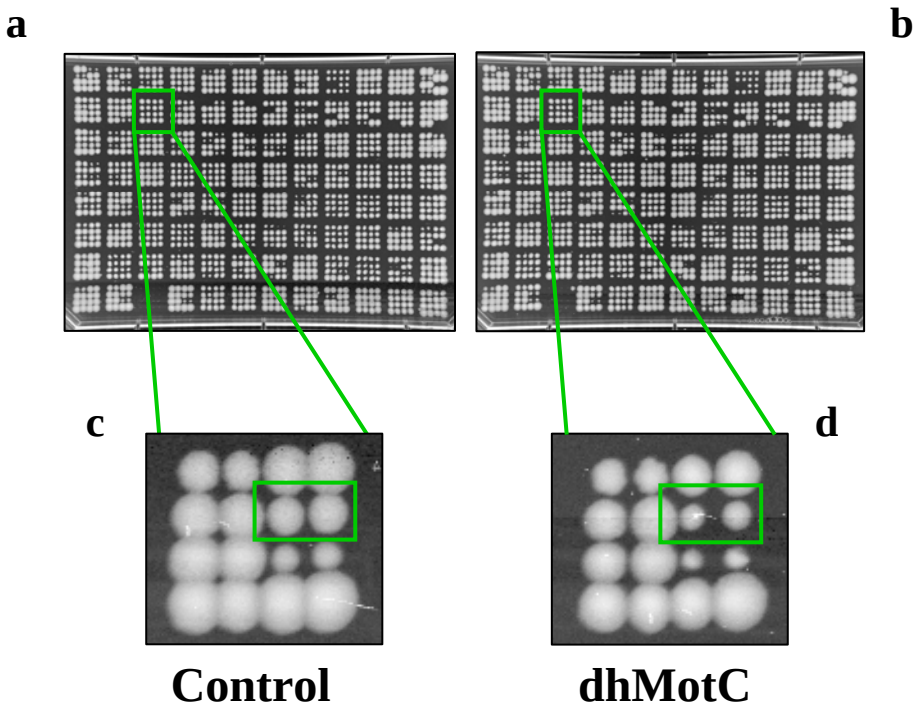

Figure. 5.1. Yeast drug induced haploinsufficiency screen. A yeast genomic library of heterozygous diploid deletion strains were robotically arrayed in duplicate on solid agar plates containing dhMotC (b) or a negative control (a). Lowering the dosage of a gene from two copies to one can result in a strain that is sensitized to drugs that act on the product of this gene. Thus, in an effort to identify dhMotC targets, the library was screened for strains that exemplified slower colony growth on dhMotC/agar. A representative positive hit is magnified and highlighted in the rectangular boxes in c and d.

Table 5.1. Heterozygous deletion strains sensitive to dhMotC.

ORF	Name	Biological process†
YCL034W	LSB5	Actin filament organization
YNL314W	DAL82	Allantoin catabolism and transcription initiation from polymerase II promoter
YML099C	ARG81	Arginine metabolism
YBR0798W	ECM33	Cell wall organization and biogenesis
YNL267W*	PIK1*	Cytokinesis, post-Golgi transport, and signal transduction
YLR286C	CTS1	Cytokinesis, completion of separation
YDL192W	ARF1	ER-to-Golgi transport and intra-Golgi transport
YBR290W	BSD2	Heavy metal ion transport and protein vacuolar targeting
YLR025W	SNF7	Late endosome to vacuole transport
YHR147C	MRPL6	Protein biosynthesis
YOL040C*	RPS15*	Protein biosynthesis
YAL005C	SSA1	Protein folding and protein-nucleus import, translocation
YIL047C	SYG1	Signal transduction
YBR265W*	TSC10*	Sphingolipid biosynthesis
YMR296C*	LCB1*	Sphingolipid biosynthesis
YJR007W*	SUI2*	Translation initiation
YML092C*	PRE8*	Ubiquitin-dependent protein catabolism
YER140W	YER140W	Unknown
YER188W	YER188W	Unknown
YGR205W	YGR205W	Unknown
YLR294C	YLR294C	Unknown

* Essential genes. † Biological process according to their *Saccharomyces* Genome Database report.

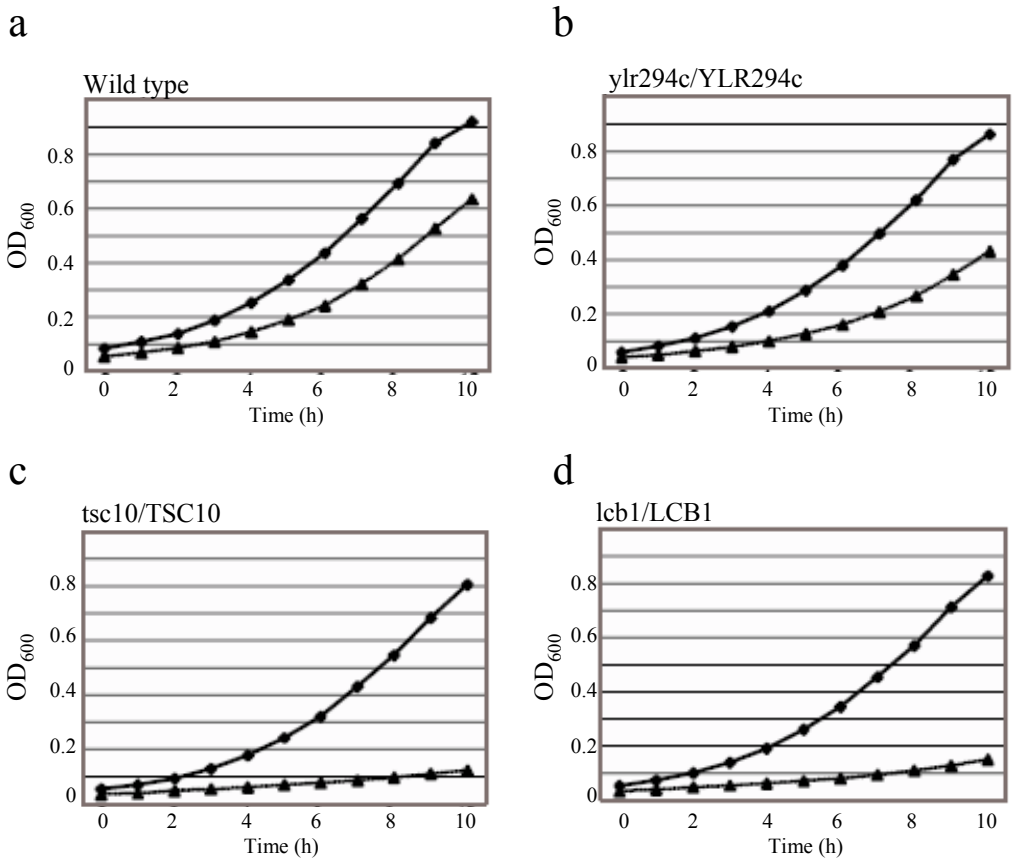

Figure 5.2. DhMotC sensitivity of heterozygous deletion strains identified in the high-throughput screen. Growth of wild-type (a), *ylr294*/YLR294 (b), *tsc10*/TSC10 (c) and *lcb1*/LCB1 (d) strains as a function of time in hours in YPD liquid culture under two conditions: ♦, no drug control (DMSO); ▲, 20 µM dhMotC. Growth curves were preformed in triplicate, and OD_{600} was measurerd by using a Tecan Sunrise plate reader. Growth curves represents the average of three experiments.

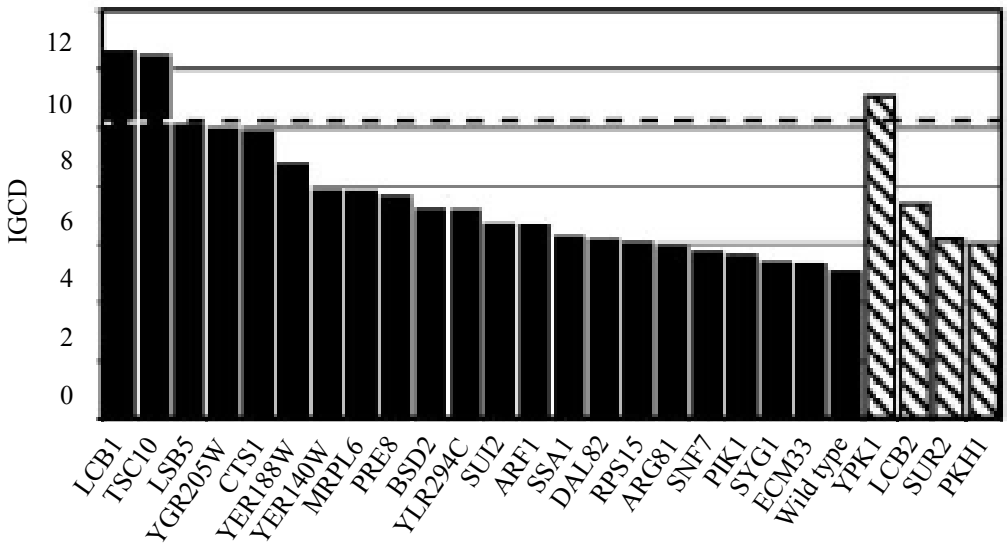

Figure 5.3. Genome-wide screen for dhMotC-induced haploinsufficiency. Plot of the IGCD for 21 heterozygous deletion strains identified in the drug screen are represented by black bars. The IGCD levels for the three additional heterozyous strains in the sphingolipid pathway sensitive to dhMotC are represented by striped bars.

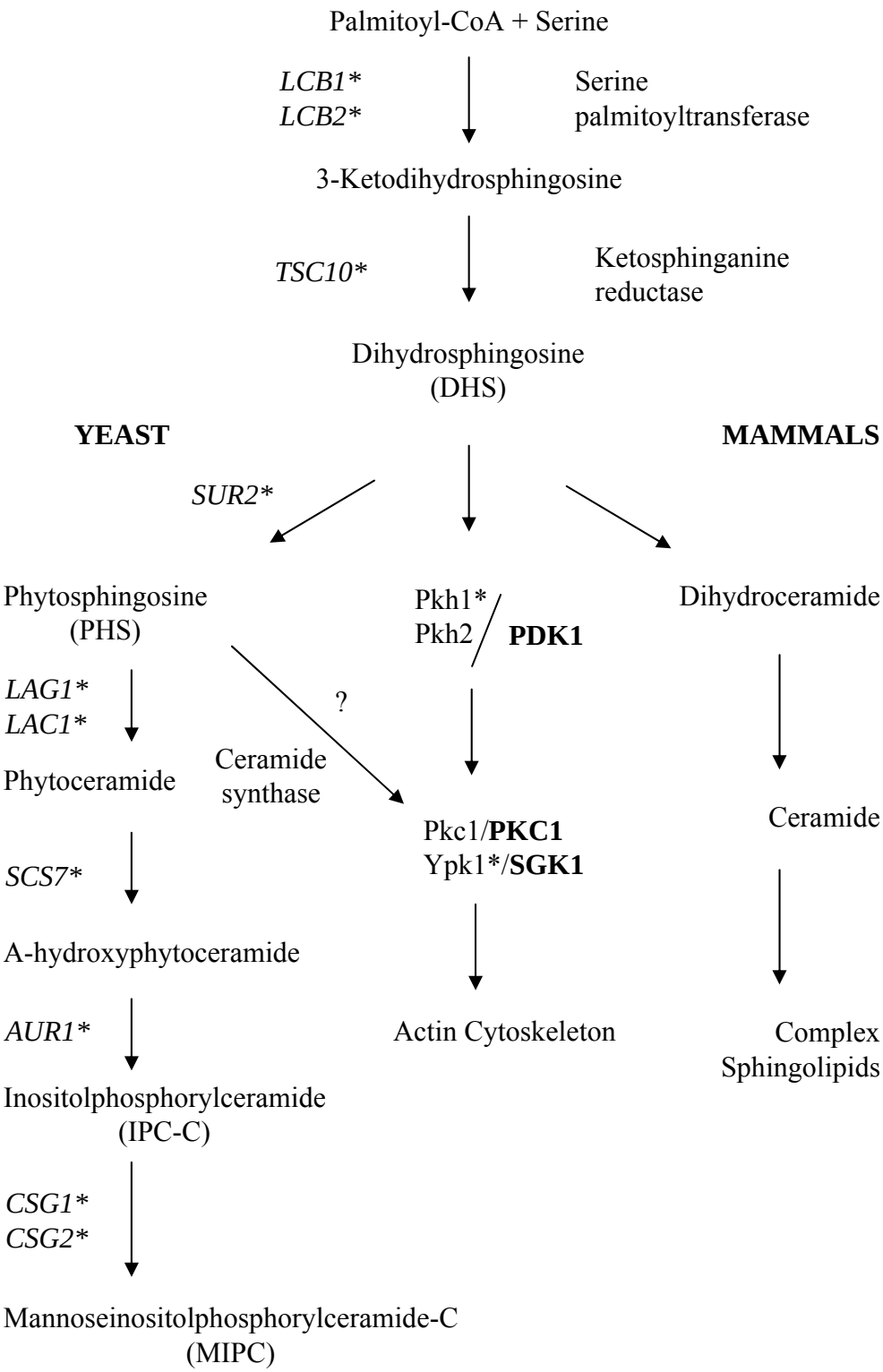

Figure 5.4. Schematic diagram of sphingolipid biosynthesis and sphingosine-dependent kinase cascade in yeast and humans. Yeast genes are italic, and yeast proteins are Roman. Human proteins are bold. Heterozygous yeast strains tested for sensitivity to dhMotC are indicated by asterisks.

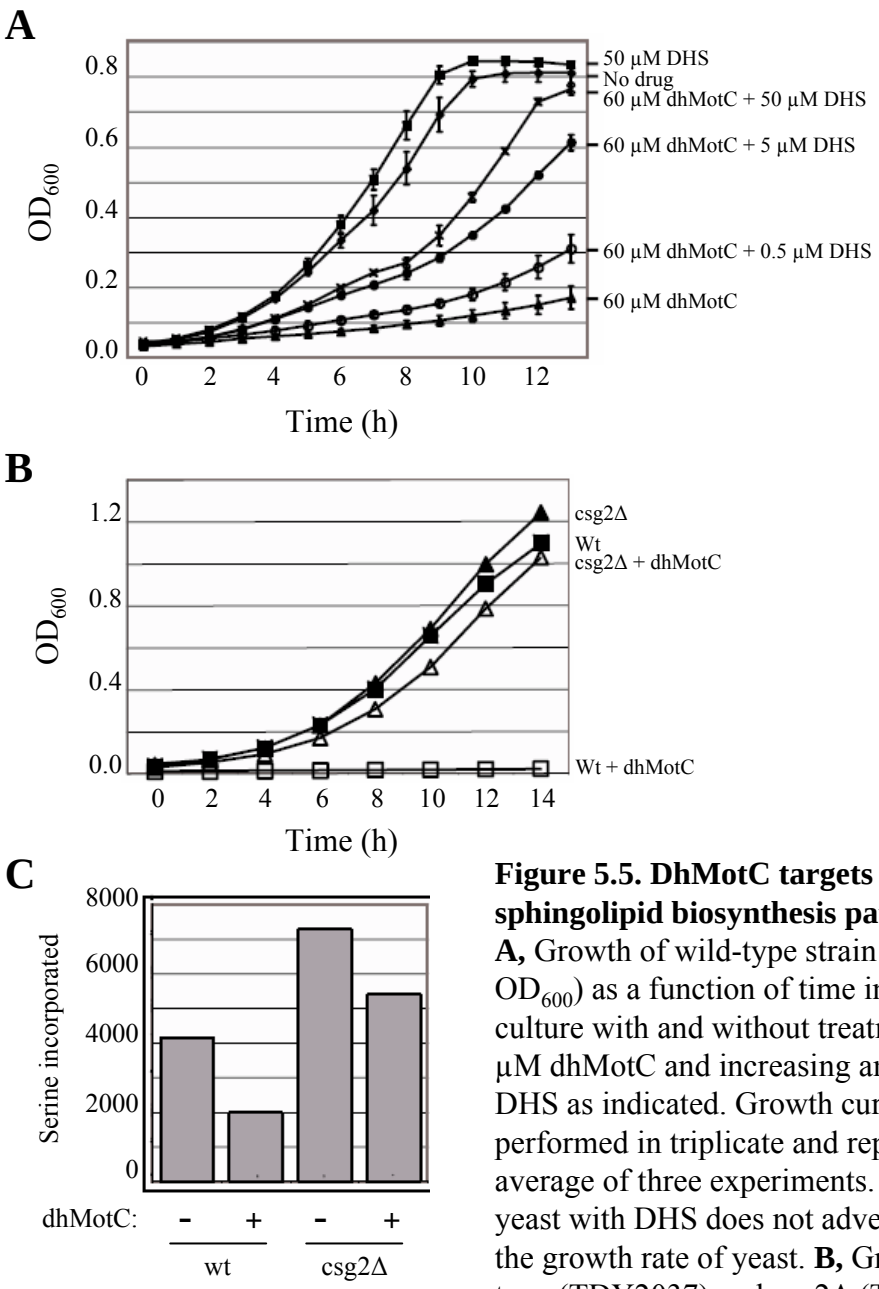

Figure 5.5. DhMotC targets the sphingolipid biosynthesis pathway. **A,** Growth of wild-type strain (BY4743, OD_{600}) as a function of time in YPD liquid culture with and without treatment of 60 µM dhMotC and increasing amounts of DHS as indicated. Growth curves were performed in triplicate and represent the average of three experiments. Treatment of yeast with DHS does not adversely affect the growth rate of yeast. **B,** Growth of wild-type (TDY2037) and csg2Δ (TDY2038) haploid cells as a function of time in YPD liquid culture with and without 10 µM dhMotC treatment. Growth curves were performed in triplicate and represent the average of three experiments. Haploid cells have and increased sensitivity to dhMotC. **C**. Incorporation of 3^{H}-serine into ceramide after 8 h was measured in both wild-type (TDY2037) and csg2Δ (TDY 2038) cells with and without 5 µM dhMotC.

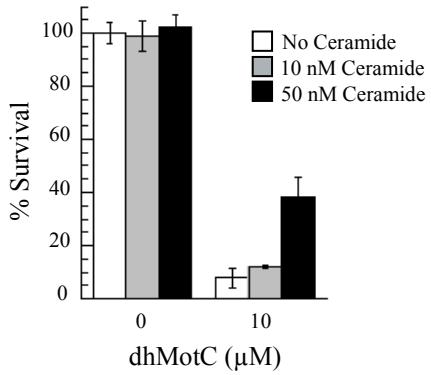

Figure 5.6. Rescue of dhMotC toxicity by ceramide in human cells. MDA-MB-231 cell survival after 24 h exposure to 0 or 10 μM dhMotC and 0, 10, or 50 nM C6-ceramide is expressed as a percentage of untreated controls. The assay was performed in quadruplicate, and error bars represent S.E.M.

A

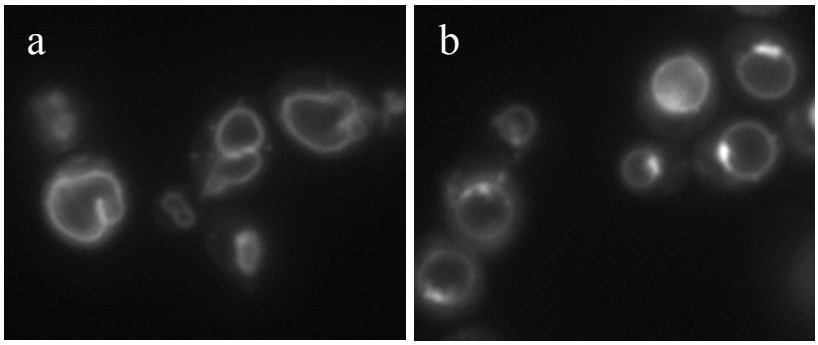

B

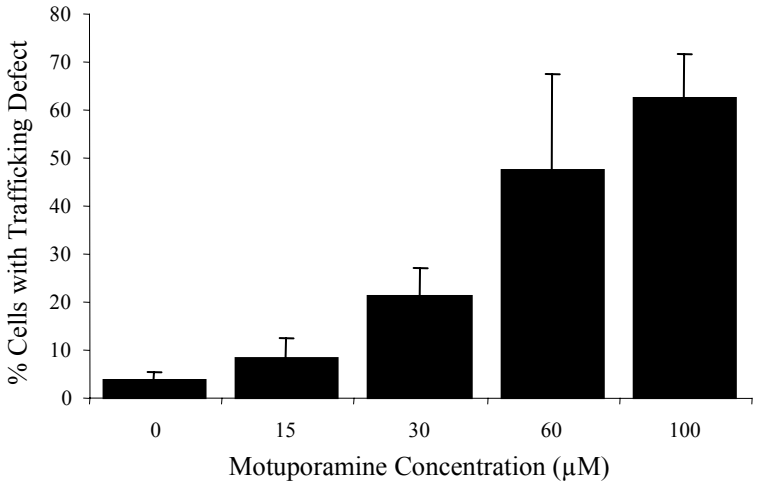

Figure 5.7. DhMotC affects trafficking to the yeast vacuole. **A,** Endocytosis and trafficking of FM4-64 lipid die to the yeast vacuole was evaluated by fluorescent microscopy of yeast cells treated with DMSO (a) or dhMotC (b, 100μM). **B,** The number of yeast cells exhibiting a trafficking defect were counted and are represented as a percentage of the total number of stained cells. Error bars represent S.E.M.

Table 5.2. Class E genes and biological function.

Gene Name	Biological Function†
VPS2	Component of the ESCRT-III complex, required for sorting of integral membrane proteins into lumenal vesicles of multivesicular bodies, and for delivery of newly synthesized vacuolar enzymes to the vacuole, involved in endocytosis
VPS4	AAA-type ATPase required for efficient late endosome to vacuole transport; catalyzes the release of an endosomal membrane-associated class E VPS protein complex
VPS20	Myristoylated subunit of ESCRTIII; cytoplasmic protein recruited to endosomal membranes
VPS22	Component of the ESCRT-II complex, which is involved in ubiquitin-dependent sorting of proteins into the endosome; appears to be functionally related to SNF7; involved in glucose derepression
VPS23	Component of the ESCRT-I complex, which is involved in ubiquitin-dependent sorting of proteins into the endosome; homologous to the mouse and human Tsg101 tumor susceptibility gene
VPS24	Forms an ESCRT-III subcomplex with Did4p
VPS25	Component of the ESCRT-II complex
VPS27	Endosomal protein that forms a complex with Hse1p; required for recycling Golgi proteins, forming lumenal membranes and sorting ubiquitinated proteins destined for degradation; has ubiquitin interaction motifs which bind ubiquitin
VPS28	Component of the ESCRT-I complex; involved in transport of precursors for soluble vacuolar hydrolases from the late endosome to the vacuole
VPS31	Cytoplasmic class E vacuolar protein sorting (VPS) factor that coordinates deubiquitination in the multivesicular body (MVB) pathway by recruiting Doa4p to endosomes
VPS32 (SNF7)	One of four subunits of the ESCRT-III complex; recruited from the cytoplasm to endosomal membranes
VPS36	Phosphatidylinositol 3-kinase responsible for the synthesis of phosphatidylinositol 3-phosphate; forms membrane-associated signal transduction complex with Vps15p to regulate protein sorting; activated by the GTP-bound form of Gpa1p
VPS37	Component of the ESCRT-I complex; suppressor of rna1-1 mutation; may be involved in RNA export from nucleus
VPS46	Class E protein of the vacuolar protein-sorting (Vps) pathway, associates reversibly with the late endosome, has human ortholog that may be altered in breast tumors
VTA1	Multivesicular body (MVB) protein involved in endosomal protein sorting; binds to Vps20p and Vps4p; may regulate Vps4p function; bindsVps60p and may act at a late step in MVB formation

† Biological function according to their *Saccharomyces* Genome Database report.

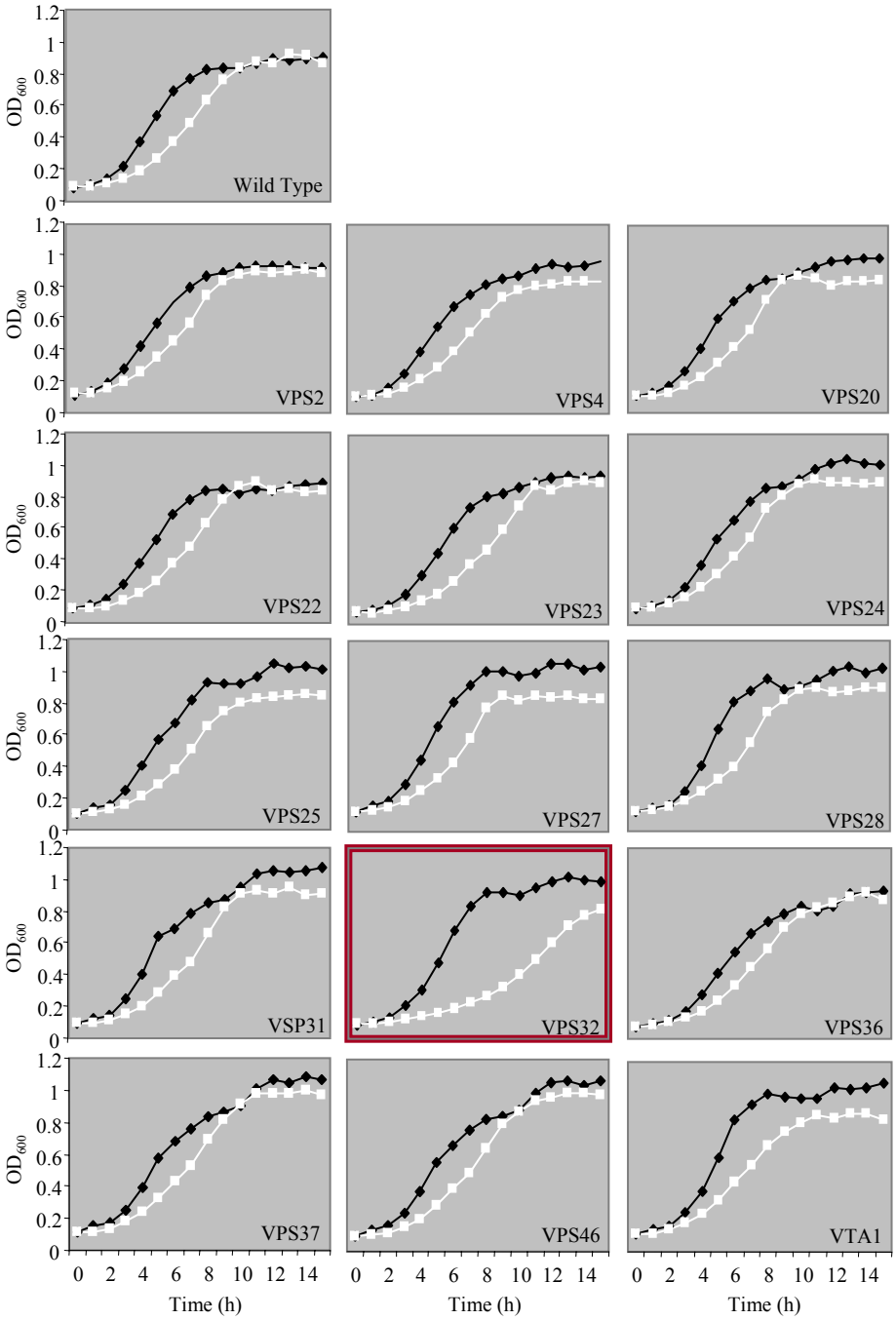

Figure 5.8. DhMotC inhibits growth of SNF7 (VPS32) but not other VPS mutants. Class E VPS mutants were grown in liquid culture and treated with dhMotC (♦) or DMSO (□) for 16 h. OD_{600} (y-axis) readings are plotted as a function of time (x-axis).

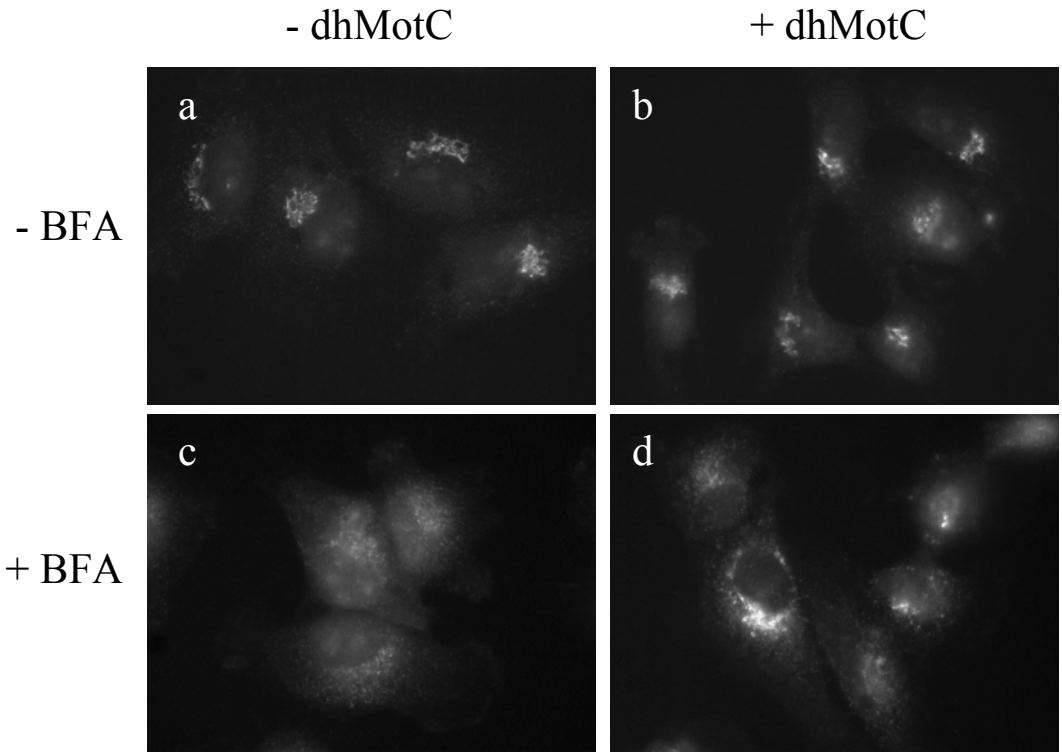

Figure 5.9. DhMotC partially antagonizes BFA induced disruption of the Golgi apparatus. MDA-MB-231 cells were treated with DMSO (a,c), or dhMotC (b,d) alone (a,b) or in combination with brefeldin A (c,d) for 15 min. Cells were fixed and stained for the golgi apparatus marker GM-130.

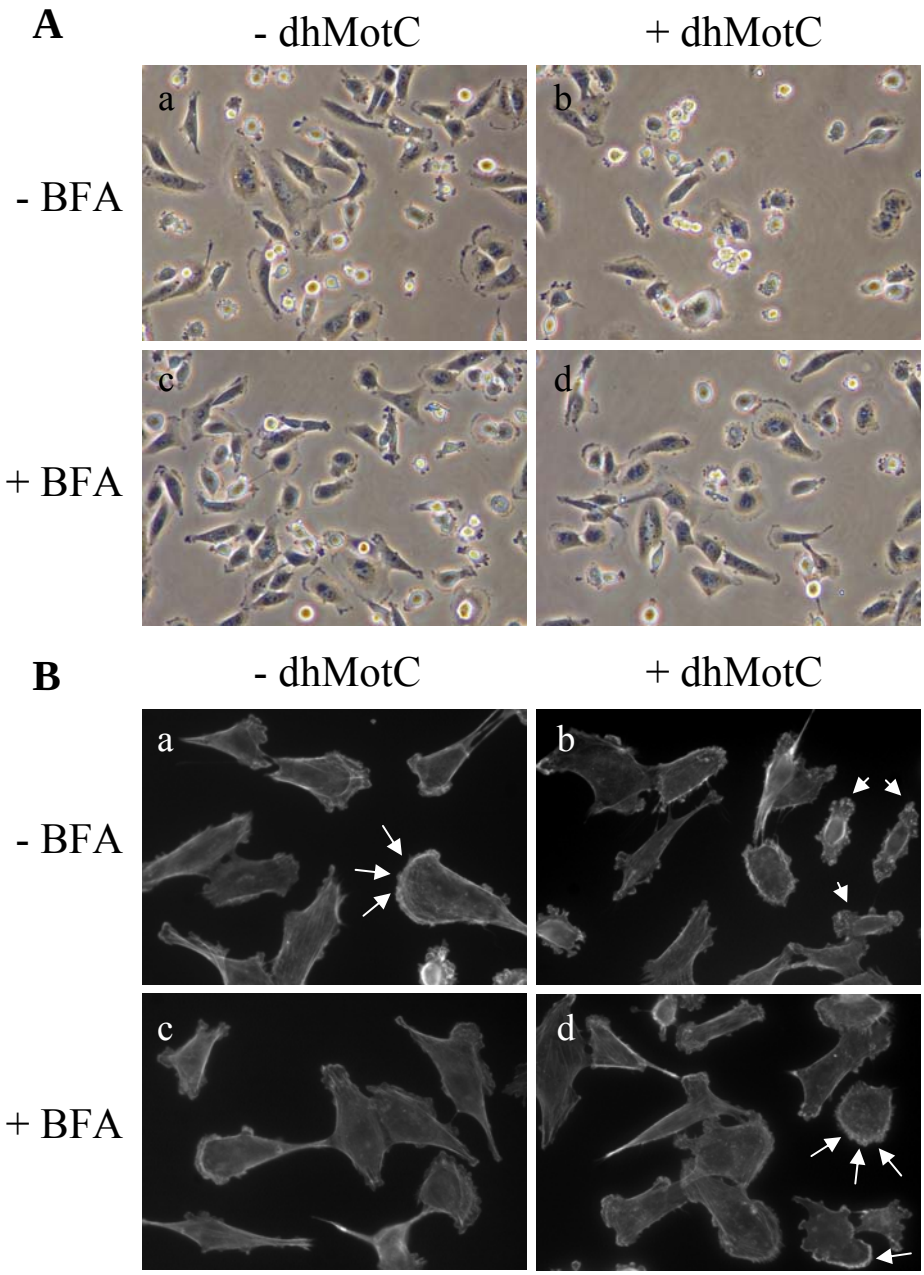

Figure 5.10. Brefeldin A antagonizes the effect of dhMotC induced cell contraction and disruption of lamellipodial ruffling. **A and B**, MDA-MB-231 cells were treated with DMSO (a,c), or dhMotC (b,d) alone (a,b) or in combination with brefeldin A (c,d) for 15 min. **A,** Phase contrast photographs show cell morphology after drug treatments. **B,** Actin staining shows lammelipodial ruffling at the leading edge of migratory cells. Notice the rounded morphology and the inhibition of ruffling in dhMotC treated cells (**A**b, **B**b). This effect is abrogated by brefeldin A treatment (**A**d, **B**d).Arrows indicate areas of ruffling, arrowheads point to contracted cells which lack ruffles.

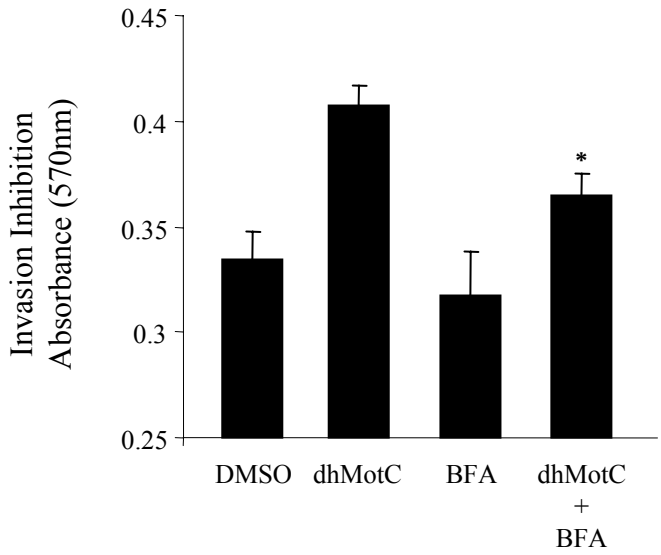

Figure 5.11. Brefeldin A partially antagonizes the anti-invasion effect of dhMotC.
MDA-MB-231 cells were plated on matrigel in the presence of DMSO, dhMotC (5 μM), brefeldin A (1 μM), or brefeldin A and dhMotC in combination. Invasion was allowed to proceed for 1 h. Non-invasive cells were then removed and quantified with and MTT assay (see Material and Methods for details). * [dhMotC] vs. [dhMotC + BFA] = $P < 0.05$.

Chapter 6: Thesis Summary and Speculations

6.1. Summary of Findings

Understanding the mechanism of action of novel anti-cancer compounds is important to facilitate their development as cancer drug candidates. Small-molecule inhibitors are also valuable biological tools that can support cancer related research. We initiated a forward chemical genetics project by utilizing our high-throughput tumour invasion assay to screen natural extracts for anti-invasion activity. Two novel inhibitors, strongylophorine-26 and motuporamine C, were isolated from active extracts.

Our initial mechanistic studies showed that both STP-26 and MotC inhibit cell migration. These molecules induced formation of large focal adhesions and they altered actin filament organization leading to a depolarized cellular morphology. Polarization is of central importance in cell migration. While STP-26 reduced actin stress fibre content and caused membrane spreading, dhMotC treatment lead to the induction of thick central stress fibres and a contracted morphology. Nonetheless, both drugs created a non-polarized phenotype with large stable adhesions that essentially rendered the cells immobile.

Cell signaling molecules are the master orchestrators of polarity. Localized cascades can create and maintain subcellular functional regions within a cell, such as the leading edge

lamellipodium and the trailing rear, through their control of the cell's cytosketal organization. Rho regulates the organization of actin cytoskeleton and focal adhesions. Both dhMotC and STP-26 activated Rho GTPase, and this activation mediated the inhibition of invasion induced by these molecules. Although it is likely that the compounds have different molecular targets, their mechanism of activity intersected at the level of Rho. This underscores the importance of Rho as a central regulator of cell migration and tumour invasion. We showed here that over stimulation of Rho can have inhibitory consequences on invasion, a result which exemplifies how both positive and negative imbalances in cell signaling can be disruptive to cellular function.

Motuporamines are relatively easy to synthesize. Thus, mechanistic studies are not limited by drug availability and synthetic analogues can be constructed without difficulty. STP-26, on the other hand, is not easy to synthesis and therefore further experimentation with this analogue was halted by limited drug supply. Results from a structure-activity relationship study of a panel of synthetic motuporamine analogues (Williams *et al.*, 2002) revealed the importance of their cationic amphiphilic structure for anti-invasion activity. Motuporamines have a hydrophobic amide ring and a positively charge carbon tail that contains two amine groups. Like other CADs and the tricyclic antidepressant desipramine, motuporamines caused lipids to accumulate intracellularly. These lipid inclusions contained GM1-ganglioside, a marker for lipid raft membrane domains. Trafficking of the transmembrane EGF receptor was also affected by dhMotC. EGFR accumulated intracellularly and was reduced at the plasma membrane. Degradation of EGFR at the lysosome was also inhibited, an effect that is likely related to dhMotC-induced increase in

lysosomal pH. Thus, it was found that dhMotC affect trafficking of cellular membranes and lysosomal function. The commonality in phenotype between dhMotC and other CADs suggests that the mechanism for motuporamine's effect on membranes is related to the cationic amphiphilic properties of its chemical structure. Furthermore, this effect on membranes will likely have consequences on protein trafficking and regulation of signaling cascades that originate from transmembrane receptor kinases such as EGFR.

We developed a novel yeast drug-induced haploinsufficiency screen in an effort to systematically identify proteins that are targeted by the motuporamine analogue, dhMotC. A genome wide *Saccharomyces cerevisiae* haploid deletion set was screened for sensistivity to dhMotC. A list of 21 possible target hits were identified after growth analysis. Although this effort did not lead to the identification of a direct drug-protein interaction, the results provided valuable insight into the mechanism of motuporamine activity. The sphingolipid metabolism pathway was highlighted as a target in yeast and mammalian cells. DhMotC reduced the level of ceramide in yeast cells. Addition of dihydrosphingosine restored growth to wild type yeast in the presence of dhMotC. Mutant c*sg2*Δ cells with higher endogenous ceramide levels were also resistant to dhMotC. In human cells, the addition of sphingolipids partially rescued dhMotC-induced toxicity, however, we were unable to show that sphingolipids affected the invasion inhibition activity of dhMotC.

Data from the yeast genomic screen also pointed to ARF1 as a mediator of dhMotC anti-invasion activity. ARF1 is a major regulator of vesicular trafficking in the secretory pathway. Blocking ARF1 activity with the small molecule inhibitor brefeldin A reversed

dhMotC morphological effects in two-dimensional and three-dimensional culture. dhMotC treatment also partially abrogated brefeldin A-induced disassembly of the Golgi apparatus. These antagonist effects of brefeldin A and dhMotC indicated that dhMotC is likely an activator of ARF1.

Yeast genome-wide screening is a novel technique that holds much promise as a tool to aid in determining the mechanism of action of therapeutic drug leads. The results of this pilot study provide the groundwork for future screening projects. We have identified important points of consideration for deciphering large data sets resulting from haploinsufficiency screening. Both the degree of growth inhibition, as well as phenotypic indicators have proven to be valuable guides for choosing protein target candidates for further study. We have also identified the problem of multi-drug resistance genes which can act as red herrings. However, as further drug screening is performed, complete characterization multi-drug resistant genes will enable researchers to easily eliminate these genes from the list of possible target candidates, and thus enable easier selection of target candidates for further experimentation.

6.2. Speculations about Motuporamine Mechanism of Activity

The results of this body of research have identified important molecular players that are involved in the mechanism for motuporamine activity. In particular, RhoGTPases and the actin cytoskeleton, cellular membranes and lipid rafts, transmembrane signaling receptors

such as EGFR, sphingolipids, and the vesicular transport regulator ARF1 have been highlighted in this study (Fig. 6.1). The question that remains is whether all or only some of the phenotypes that were identified in this study are related mechanistically to each other and/or to tumour invasion inhibition or whether they are separate phenotypes resulting from multiple targets of motuporamine.

Although sphingolipids constitute only a small percentage of the lipids in the plasma membrane, the presence of these relatively rigid molecules in the lipid bilayer can affect membrane fluidity and curvature, which in turn, can affect the association of membrane proteins within lipid raft microdomains (Golub *et al.*, 2004; Hanzal-Bayer & Hancock, 2007; Sot *et al.*, 2005), or the processes of vesicle formation and fusion (Markvoort *et al.*, 2007) (Haque *et al.*, 2001). Thus, disrupting sphingolipid content in cells could have significant effects on membrane structure which in turn could affect a number of cellular processes including vesicular trafficking or cell signaling from rafts. It is also not unreasonable to suggest the possibility that inhibition of sphingolipid biosynthesis could contribute to the lipidosis defect in dhMotC treated cells, possibly by altering membrane curvature and causing an increase in vesicle formation. Although, we were unable to directly show that sphingolipids are important for the mechanism of anti-invasion activity in mammalian cells, the negative results do not necessarily negate the possibility that sphingolipids are involved.

Also, of considerable interest is an alternate hypothesis that the direct binding target of motuporamines is not a protein, but actually the phospholipid bilayer itself. There are a number of pieces of evidence that could support such a hypothesis. For example, the cationic

amphiphilic property of the motuporamines makes them favorable to an interaction with cellular membranes. Also, the yeast-haploinsufficiency screen did not point definitively to a single protein target. If motuporamines do bind membranes and do not interact with a single protein, this result would be expected. It is an attractive hypothesis because it would highlight the importance of cellular membranes as regulators of cell function. Classical dogma views proteins as the master regulators of cell function, while membranes have often been considered to play more of a structural role in the cell. However, recently, there is more evidence that the structure of cell membranes can have consequences on protein function. An obvious example would be the role of lipid raft microdomains in clustering signaling proteins in the plasma membrane (Golub *et al.*, 2004). Another example is the GTPase activating protein ARF-GAP1 that is partially controlled by changes in membrane curvature (Antonny *et al.*, 2005). If motuporamines interact with cell membranes, one could imagine that there might be consequences on membrane structure which could lead to a variety of cellular effects by altering the function of lipid raft- or membrane-associated proteins.

Regardless of the specific identity of the direct binding target of motuporamines, one could easily hypothesize a mechanism by which the effect on cellular membranes could be placed upstream of both Rho and ARF1-mediated inhibition of invasion. For example, in addition to the accumulation of cell membranes, we also saw intracellular accumulation of the transmembrane lipid raft associated kinase EGFR and the lipid raft marker GM1 ganglioside. Although it has not been shown directly, it seems likely that the two phenotypes are outcomes of a common primary cause. Indeed, the accumulation of lipid raft domains could function as platforms for many cell signaling molecules. EGFR is a representative raft-

associated protein in this study. One could assume that EGFR is carried in the raft domains from the plasma membrane, through the endocytic pathway, and is getting trapped at these intracellular lipid inclusions. The recycling pathway which returns membrane receptors back to the plasma membrane may be blocked in the case of dhMotC treated cells. This could explain the reduced level of EGFR at the plasma membrane. Without lysosomal function, signaling cascades from EGFR or other activated transmembrane receptors may not be downregulated in such a scenario. It is quite possiblle that this unregulated signaling event could lead to the activation of either or both of the Rho or ARF1 GTPases, thus placing the membrane accumulation and degradation defect upstream of Rho and ARF1 activation and inhibition of invasion. Of course, much further work is needed to determine if this hypothssis is correct.

Interestingly, the Rho inhibitor, C3 exoenzyme, failed to restore EGFR degradation, a result which suggests that Rho signaling is not a causal factor for the lysosomal defect. A reciprocal experiment whereby one restores degradative activity in the presence of motuporamines was much less feasible. However, correlative evidence comes from the fact that inactive analogues for tumour invasion were relatively ineffective inducers of lipid inclusions. Given that Rho is eliminated as an upstream regulator of the degradation defect, this correlative evidence becomes more supportive of the hypothesis that Rho activation and invasion are downstream of the effect on membrane accumulation.

Speculations about ARF1 placement in a pathway relative to Rho or the membrane defect are difficult to make because further experimentation is necessary to see if abrogation

of ARF1 activity affects the accumulation of lipids or EGFR in cells. Similarly, it is not yet known whether abrogation of ARF1 activity results in loss of Rho activity or the reciprocal, whether C3 exoenzyme treatment blocks ARF1 activity. These experiments need to be done in order to place ARF1 and Rho upstream or downstream of each other in the pathway which controls tumour invasion.

6.3. Future Avenues for Research

Forward chemical genetics is a term that describes the use of small molecules as tools to guide researchers to better understand a specific biological process. In this work, the biological process of interest is tumour cell invasion. With the discovery and use of the novel invasion inhibitors strongylophorine-26 and motuporamine C, the process of tumour invasion has been probed on multiple levels, from the relatively macroscopic, to the microscopic, and the molecular/genetic level. Forward chemical genetics is a hypothesis generating approach to science. Thus, one benefit is that this work opens up a multitude of avenues for further interesting research to be conducted.

Focusing in at the level of RhoGTPases, we have shown that activation of Rho signaling has inhibitory effects on tumour invasion. One intriguing aspect of this result is the question of subcellular location and isoform specificity. With the use of FRET-based probes, it is possible to determine subcellular location of active GTP-bound Rho after motuporamine treatment. Antibodies are also available to determnine isoform specificity. It would be interesting to know whether all Rho isoforms are being activated and where exactly they are

being activated in the cell. Pursuing this avenue would contribute to the understanding of the role of RhoGTPases in the regulation cell polarity during tumour invasion and cell migration.

In terms of mechanisms specific to the motuporamines, a variety of interesting questions remain. Do the motuporamines bind cellular membranes? This could be answered by mixing motuporamines with membrane preparations and perfoming mass spectrometry on the samples. Is activation of EGFR sustained at intracellular inclusion bodies? Phospho-specific antibodies for EGFR can be used to determine the activation state of this receptor. Furthermore, EGFR inhibitors could be used to block EGFR signaling and assess the outcome on Rho, ARF1, and tumour invasion in order to determine if the lipidosis defect is related mechanistically to the invasion inhibition by dhMotC.

Further work with the yeast happlinsufficiency data could lead to a more complete understanding of motuporamine activity. Other candidate target molecules could be addressed, while further assessment of ARF1 activity after dhMotC treatment is needed. This pilot work with the yeast haploinsufficiency screen will also prove useful for the identification of mechanisms of activity of other potential therapeutic compounds.

The possibilities for mechanistic studies with a drug candidate are endless. However, the most intriguing question which remains in this forward chemical genetics project is whether the novel tumour invasion inhibitor will have efficacy as a future anti-cancer therapy. The initiation of extensive *in vivo* mouse studies will be required to determine the answer to this question. With any lead drug, non-specific drug interactions can lead to toxic side effects. If motuporamines affects cellular membranes, a multitude of transmembrane

signaling receptors could be affected. Thus, the likelyhood of toxic side effects in the case of motuporamines is relatively high. Interestingly, small scale preliminary *in vivo* studies performed by our group have shown some efficacy in reducing tumour size. Reduction in tumour size is the most commonly used indicator for efficacy in standard *in vivo* cancer drug studies. However, inhibiting tumour invasion is a relatively novel therapeutic approach. Thus, the final word on *in vivo* efficacy cannot be determined without assessing the affect of motuporamines on tumour metastasis in mouse models.

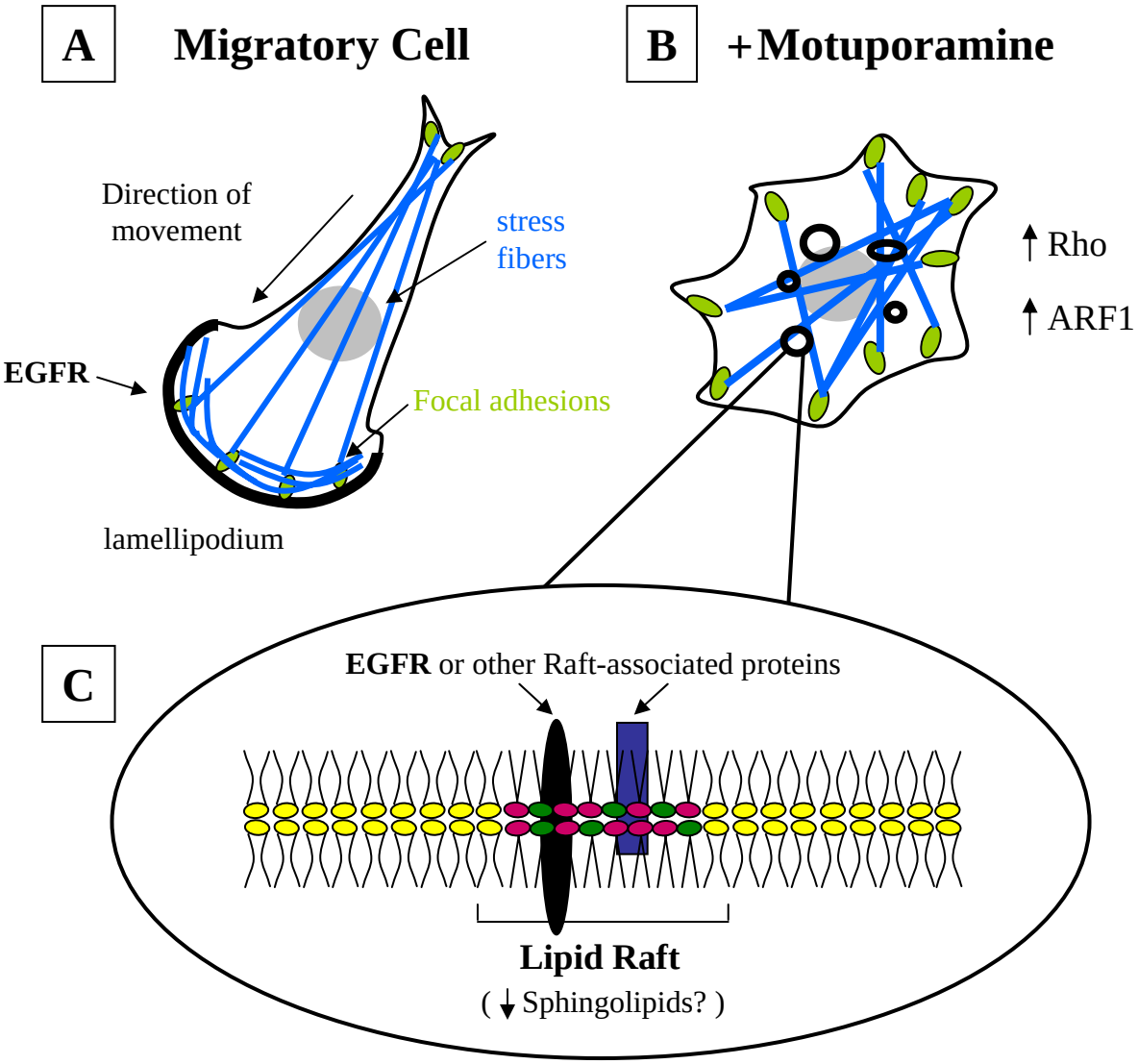

Figure 6.1. Model for Motuporamine mechanism of activity.
A, Migrating cells with a lamellipodium extending in the direction of cell migration, focal adhesions, a meshwork of lamellipodial actin filaments and actin stress fibers. **B,** DhMotC disrupts cell polarity and prevents cell migration by stabilizing focal adhesions and actin stress fibers. Cellular membranes and the EGFR accumulate at intracellular peri-nuclear inclusions. ARF1 and Rho signaling is activated. **C,** Membrane inclusion bodies contain markers for lipid rafts. These membrane microdomains may be associated with EGFR and other transmembrane signaling molecules. Decreased levels of sphingolipids may influence lipid raft integrity.

Chapter 7: Bibliography

Albouz, S., Tocque, B., Hauw, J. J., Boutry, J. M., Le Saux, F., Bourdon, R. & Baumann, N. (1982). Tricyclic antidepressant desipramine induces stereospecific opiate binding and lipid modifications in rat glioma C6 cells. *Life Sci* **31**, 2549-2554.

Albouz, S., Vanier, M. T., Hauw, J. J., Le Saux, F., Boutry, J. M. & Baumann, N. (1983). Effect of tricyclic antidepressants on sphingomyelinase and other sphingolipid hydrolases in C6 cultured glioma cells. *Neurosci Lett* **36**, 311-315.

Albouz, S., Le Saux, F., Wenger, D., Hauw, J. J. & Baumann, N. (1986). Modifications of sphingomyelin and phosphatidylcholine metabolism by tricyclic antidepressants and phenothiazines. *Life Sciences* **38**, 357-363.

Amano, M., Chihara, K., Kimura, K., Fukata, Y., Nakamura, N., Matsuura, Y. & Kaibuchi, K. (1997). Formation of actin stress fibers and focal adhesions enhanced by Rho-kinase. *Science* **275**, 1308-1311.

Anderson, N. & Borlak, J. (2006). Drug-induced phospholipidosis. *FEBS Lett* **580**, 5533-5540.

Antonny, B., Bigay, J., Casella, J. F., Drin, G., Mesmin, B. & Gounon, P. (2005). Membrane curvature and the control of GTP hydrolysis in Arf1 during COPI vesicle formation. *Biochem Soc Trans* **33**, 619-622.

Arthur, W. T. & Burridge, K. (2001). RhoA inactivation by p190RhoGAP regulates cell spreading and migration by promoting membrane protrusion and polarity. *Mol Biol Cell* **12**, 2711-2720.

Axelrod, R., Axelrod, D. E. & Pienta, K. J. (2006). Evolution of cooperation among tumor cells. *Proc Natl Acad Sci U S A* **103**, 13474-13479.

Babst, M., Katzmann, D. J., Estepa-Sabal, E. J., Meerloo, T. & Emr, S. D. (2002). Escrt-III: an endosome-associated heterooligomeric protein complex required for mvb sorting. *Dev Cell* **3**, 271-282.

Barker, T. H., Grenett, H. E., MacEwen, M. W., Tilden, S. G., Fuller, G. M., Settleman, J., Woods, A., Murphy-Ullrich, J. & Hagood, J. S. (2004). Thy-1 regulates fibroblast focal adhesions, cytoskeletal organization and migration through modulation of p190 RhoGAP and Rho GTPase activity. *Experimental Cell Research* **295**, 488-496.

Basu, R. & Chang, F. (2007). Shaping the actin cytoskeleton using microtubule tips. *Curr Opin Cell Biol* **19**, 88-94.

Beavon, I. R. (2000). The E-cadherin-catenin complex in tumour metastasis: structure, function and regulation. *Eur J Cancer* **36**, 1607-1620.

Beeler, T., Bacikova, D., Gable, K., Hopkins, L., Johnson, C., Slife, H. & Dunn, T. (1998). The Saccharomyces cerevisiae TSC10/YBR265w gene encoding 3-ketosphinganine reductase is identified in a screen for temperature-sensitive suppressors of the Ca2+-sensitive csg2Delta mutant. *J Biol Chem* **273**, 30688-30694.

Bickel, M. H. & Steele, J. W. (1974). Binding of basic and acidic drugs to rat tissue subcellular fractions. *Chem Biol Interact* **8**, 151-162.

Bogenrieder, T. & Herlyn, M. (2003). Axis of evil: molecular mechanisms of cancer metastasis. *Oncogene* **22**, 6524-6536.

Bose, R. & Wrana, J. L. (2006). Regulation of Par6 by extracellular signals. *Curr Opin Cell Biol* **18**, 206-212.

Boyce, P. & Judd, F. (1999). The place for the tricyclic antidepressants in the treatment of depression. *Aust N Z J Psychiatry* **33**, 323-327.

Brown, J. M. & Wilson, G. (2003). Apoptosis genes and resistance to cancer therapy: what does the experimental and clinical data tell us? *Cancer Biol Ther* **2**, 477-490.

Burgi, S., Baltensperger, K. & Honegger, U. E. (2003). Antidepressant-induced switch of beta 1-adrenoceptor trafficking as a mechanism for drug action. *J Biol Chem* **278**, 1044-1052.

Burridge, K. & Chrzanowska-Wodnicka, M. (1996). Focal adhesions, contractility, and signaling. *Annu Rev Cell Dev Biol* **12**, 463-518.

Burridge, K. & Wennerberg, K. (2004). Rho and Rac take center stage. *Cell* **116**, 167-179.

Carragher, N. O. & Frame, M. C. (2004). Focal adhesion and actin dynamics: a place where kinases and proteases meet to promote invasion. *Trends Cell Biol* **14**, 241-249.

Carragher, N. O., Walker, S. M., Scott Carragher, L. A., Harris, F., Sawyer, T. K., Brunton, V. G., Ozanne, B. W. & Frame, M. C. (2006). Calpain 2 and Src dependence distinguishes mesenchymal and amoeboid modes of tumour cell invasion: a link to integrin function. *Oncogene* **25**, 5726-5740.

Casamayor, A., Torrance, P. D., Kobayashi, T., Thorner, J. & Alessi, D. R. (1999). Functional counterparts of mammalian protein kinases PDK1 and SGK in budding yeast. *Curr Biol* **9**, 186-197.

Caswell, P. T. & Norman, J. C. (2006). Integrin trafficking and the control of cell migration. *Traffic* **7**, 14-21.

Caviston, J. P. & Holzbaur, E. L. (2006). Microtubule motors at the intersection of trafficking and transport. *Trends Cell Biol* **16**, 530-537.

Cetin, S., Ford, H. R., Sysko, L. R., Agarwal, C., Wang, J., Neal, M. D., Baty, C., Apodaca, G. & Hackam, D. J. (2004). Endotoxin inhibits intestinal epithelial restitution through activation of Rho-GTPase and increased focal adhesions. *Journal of Biological Chemistry* **279**, 24592-24600.

Cox, E. A., Sastry, S. K. & Huttenlocher, A. (2001). Integrin-mediated adhesion regulates cell polarity and membrane protrusion through the Rho family of GTPases. *Mol Biol Cell* **12**, 265-277.

D'Souza-Schorey, C. & Chavrier, P. (2006). ARF proteins: roles in membrane traffic and beyond. *Nat Rev Mol Cell Biol* **7**, 347-358.

Decaestecker, C., Debeir, O., Van Ham, P. & Kiss, R. (2007). Can anti-migratory drugs be screened in vitro? A review of 2D and 3D assays for the quantitative analysis of cell migration. *Med Res Rev* **27**, 149-176.

Dickson, R. C. & Lester, R. L. (2002). Sphingolipid functions in Saccharomyces cerevisiae. *Biochimica et Biophysica Acta* **1583**, 13-25.

Donaldson, J. G., Finazzi, D. & Klausner, R. D. (1992). Brefeldin A inhibits Golgi membrane-catalysed exchange of guanine nucleotide onto ARF protein. *Nature* **360**, 350-352.

Donaldson, J. G. & Klausner, R. D. (1994). ARF: a key regulatory switch in membrane traffic and organelle structure. *Curr Opin Cell Biol* **6**, 527-532.

Donaldson, J. G., Honda, A. & Weigert, R. (2005). Multiple activities for Arf1 at the Golgi complex. *Biochim Biophys Acta* **1744**, 364-373.

Du, W. & Prendergast, G. C. (1999). Geranylgeranylated RhoB mediates suppression of human tumor cell growth by farnesyltransferase inhibitors. *Cancer Res* **59**, 5492-5496.

Etienne-Manneville, S. & Hall, A. (2002). Rho GTPases in cell biology. *Nature* **420**, 629-635.

Etienne-Manneville, S. (2004). Cdc42--the centre of polarity. *J Cell Sci* **117**, 1291-1300.

Fernandez-Borja, M., Janssen, L., Verwoerd, D., Hordijk, P. & Neefjes, J. (2005). RhoB regulates endosome transport by promoting actin assembly on endosomal membranes through Dia1. *J Cell Sci* **118**, 2661-2670.

Friedl, P. & Brocker, E. B. (2000). The biology of cell locomotion within three-dimensional extracellular matrix. *Cellular & Molecular Life Sciences* **57**, 41-64.

Friedl, P. & Wolf, K. (2003). Tumour-cell invasion and migration: diversity and escape mechanisms. *Nat Rev Cancer* **3**, 362-374.

Fritz, G., Just, I. & Kaina, B. (1999). Rho GTPases are over-expressed in human tumors. *Int J Cancer* **81**, 682-687.

Gadea, G., de Toledo, M., Anguille, C. & Roux, P. (2007). Loss of p53 promotes RhoA-ROCK-dependent cell migration and invasion in 3D matrices. *J Cell Biol* **178**, 23-30.

Geho, D. H., Bandle, R. W., Clair, T. & Liotta, L. A. (2005). Physiological mechanisms of tumor-cell invasion and migration. *Physiology (Bethesda)* **20**, 194-200.

Geist, S. H. & Lullmann-Rauch, R. (1994). Experimentally induced lipidosis in uterine and vaginal epithelium of rats. *Ann Anat* **176**, 3-9.

Giaever, G., Shoemaker, D. D., Jones, T. W., Liang, H., Winzeler, E. A., Astromoff, A. & Davis, R. W. (1999). Genomic profiling of drug sensitivities via induced haploinsufficiency. *Nat Genet* **21**, 278-283.

Golub, T., Wacha, S. & Caroni, P. (2004). Spatial and temporal control of signaling through lipid rafts. *Current Opinion in Neurobiology* **14**, 542-550.

Greenspan, P. & Fowler, S. D. (1985). Spectrofluorometric studies of the lipid probe, nile red. *J Lipid Res* **26**, 781-789.

Greenspan, P., Mayer, E. P. & Fowler, S. D. (1985). Nile red: a selective fluorescent stain for intracellular lipid droplets. *J Cell Biol* **100**, 965-973.

Gupta, G. P. & Massague, J. (2006). Cancer metastasis: building a framework. *Cell* **127**, 679-695.

Hall, A. (1998). Rho GTPases and the actin cytoskeleton. In *Science*, pp. 509-514.

Hanahan, D. & Weinberg, R. A. (2000). The hallmarks of cancer. *Cell* **100**, 57-70.

Hanzal-Bayer, M. F. & Hancock, J. F. (2007). Lipid rafts and membrane traffic. *FEBS Lett* **581**, 2098-2104.

Haque, M. E., McIntosh, T. J. & Lentz, B. R. (2001). Influence of lipid composition on physical properties and peg-mediated fusion of curved and uncurved model membrane vesicles: "nature's own" fusogenic lipid bilayer. *Biochemistry* **40**, 4340-4348.

Hauck, C. R., Hsia, D. A., Ilic, D. & Schlaepfer, D. D. (2002). v-Src SH3-enhanced interaction with focal adhesion kinase at beta 1 integrin-containing invadopodia promotes cell invasion. *J Biol Chem* **277**, 12487-12490.

Helms, J. B. & Rothman, J. E. (1992). Inhibition by brefeldin A of a Golgi membrane enzyme that catalyses exchange of guanine nucleotide bound to ARF. *Nature* **360**, 352-354.

Hoang, M. V., Whelan, M. C. & Senger, D. R. (2004). Rho activity critically and selectively regulates endothelial cell organization during angiogenesis. *Proceedings of the National Academy of Sciences of the United States of America* **101**, 1874-1879.

Hostetler, K. Y. & Matsuzawa, Y. (1981). Studies on the mechanism of drug-induced lipidosis. Cationic amphiphilic drug inhibition of lysosomal phospholipases A and C. *Biochem Pharmacol* **30**, 1121-1126.

Hughes, T. R. (2002). Yeast and drug discovery. *Funct Integr Genomics* **2**, 199-211.

Hurwitz, R., Ferlinz, K. & Sandhoff, K. (1994). The tricyclic antidepressant desipramine causes proteolytic degradation of lysosomal sphingomyelinase in human fibroblasts. *Biological Chemistry Hoppe-Seyler* **375**, 447-450.

Ilic, D., Furuta, Y., Kanazawa, S., Takeda, N., Sobue, K., Nakatsuji, N., Nomura, S., Fujimoto, J., Okada, M. & Yamamoto, T. (1995). Reduced cell motility and enhanced focal adhesion contact formation in cells from FAK-deficient mice. *Nature* **377**, 539-544.

Inagaki, M., Schmelzle, T., Yamaguchi, K., Irie, K., Hall, M. N. & Matsumoto, K. (1999). PDK1 homologs activate the Pkc1-mitogen-activated protein kinase pathway in yeast. *Mol Cell Biol* **19**, 8344-8352.

Johnstone, R. W., Ruefli, A. A. & Lowe, S. W. (2002). Apoptosis: a link between cancer genetics and chemotherapy. *Cell* **108**, 153-164.

Jones, M. C., Caswell, P. T. & Norman, J. C. (2006). Endocytic recycling pathways: emerging regulators of cell migration. *Curr Opin Cell Biol* **18**, 549-557.

Kalluri, R. (2003). Basement membranes: structure, assembly and role in tumour angiogenesis. *Nature Reviews Cancer* **3**, 422-433.

Kamai, T., Tsujii, T., Arai, K., Takagi, K., Asami, H., Ito, Y. & Oshima, H. (2003). Significant association of Rho/ROCK pathway with invasion and metastasis of bladder cancer. *Clin Cancer Res* **9**, 2632-2641.

Katzmann, D. J., Odorizzi, G. & Emr, S. D. (2002). Receptor downregulation and multivesicular-body sorting. *Nat Rev Mol Cell Biol* **3**, 893-905.

Kaufmann, A. M. & Krise, J. P. (2007). Lysosomal sequestration of amine-containing drugs: analysis and therapeutic implications. *J Pharm Sci* **96**, 729-746.

Kawasumi, M. & Nghiem, P. (2007). Chemical genetics: elucidating biological systems with small-molecule compounds. *J Invest Dermatol* **127**, 1577-1584.

Kleinman, H. K. & Martin, G. R. (2005). Matrigel: basement membrane matrix with biological activity. *Semin Cancer Biol* **15**, 378-386.

Koblinski, J. E., Ahram, M. & Sloane, B. F. (2000). Unraveling the role of proteases in cancer. *Clin Chim Acta* **291**, 113-135.

Koehn, F. E. & Carter, G. T. (2005). The evolving role of natural products in drug discovery. *Nat Rev Drug Discov* **4**, 206-220.

Kucia, K., Malecki, A., Gabryel, B. & Trzeciak, H. I. (2003). Effect of antidepressants on the phospholipase A2 activity in plasma membranes of the rat brain cortex. *Pol J Pharmacol* **55**, 5-15.

Kurokawa, K. & Matsuda, M. (2005). Localized RhoA activation as a requirement for the induction of membrane ruffling. *Mol Biol Cell* **16**, 4294-4303.

Leung, T., Chen, X., E, M. & Lim, L. (1996). The p160-RhoA-Binding Kinase ROKalpha is a Member of a Kinase Family and is Involved in the Reorganization of the Cytoskeleton. *Molecular & Cellular Biology* **16**, 5313-5327.

Lokey, R. S. (2003). Forward chemical genetics: progress and obstacles on the path to a new pharmacopoeia. *Curr Opin Chem Biol* **7**, 91-96.

Maliakal, J. C. (2002). Quantitative high throughput endothelial cell migration and invasion assay system. *Methods Enzymol* **352**, 175-182.

Mann, J. (2002). Natural products in cancer chemotherapy: past, present and future. *Nat Rev Cancer* **2**, 143-148.

Markvoort, A. J., Smeijers, A. F., Pieterse, K., van Santen, R. A. & Hilbers, P. A. (2007). Lipid-based mechanisms for vesicle fission. *J Phys Chem B* **111**, 5719-5725.

Mitchison, T. J. & Cramer, L. P. (1996). Actin-based cell motility and cell locomotion. *Cell* **84**, 371-379.

Miura, K., Jacques, K. M., Stauffer, S., Kubosaki, A., Zhu, K., Hirsch, D. S., Resau, J., Zheng, Y. & Randazzo, P. A. (2002). ARAP1: a point of convergence for Arf and Rho signaling. *Mol Cell* **9**, 109-119.

Mossman, T. (1983). Rapid colorimetric assay for cellular growth and survival: application to proliferation and cytotoxicity assays. . *J Immunol Methods* **65**, 55-63.

Nabi, I. R., Le Bivic, A., Fambrough, D. & Rodriguez-Boulan, E. (1991). An endogenous MDCK lysosomal membrane glycoprotein is targeted basolaterally before delivery to lysosomes. *J Cell Biol* **115**, 1573-1584.

Narumiya, S., Ishizaki, T. & Uehata, M. (2000). Use and properties of ROCK-specific inhibitor Y-27632. *Methods Enzymol* **325**, 273-284.

Nierenberg, A. A. (1994). The treatment of severe depression: is there an efficacy gap between SSRI and TCA antidepressant generations? *J Clin Psychiatry* **55 Suppl A**, 55-59; discussion 60-51, 98-100.

Ohanian, J. & Ohanian, V. (2001). Sphingolipids in mammalian cell signalling. *Cellular & Molecular Life Sciences* **58**, 2053-2068.

Parsons, A. B., Geyer, R., Hughes, T. R. & Boone, C. (2003). Yeast genomics and proteomics in drug discovery and target validation. *Prog Cell Cycle Res* **5**, 159-166.

Parsons, A. B., Brost, R. L., Ding, H., Li, Z., Zhang, C., Sheikh, B., Brown, G. W., Kane, P. M., Hughes, T. R. & Boone, C. (2004). Integration of chemical-genetic and genetic interaction data links bioactive compounds to cellular target pathways.[see comment]. *Nature Biotechnology* **22**, 62-69.

Pertz, O., Hodgson, L., Klemke, R. L. & Hahn, K. M. (2006). Spatiotemporal dynamics of RhoA activity in migrating cells. *Nature* **440**, 1069-1072.

Pollard, T. D. & Borisy, G. G. (2003). Cellular motility driven by assembly and disassembly of actin filaments. *Cell* **112**, 453-465.

Preudhomme, C., Roumier, C., Hildebrand, M. P., Dallery-Prudhomme, E., Lantoine, D., Lai, J. L., Daudignon, A., Adenis, C., Bauters, F., Fenaux, P., Kerckaert, J. P. & Galiegue-Zouitina, S. (2000). Nonrandom 4p13 rearrangements of the RhoH/TTF gene, encoding a GTP-binding protein, in non-Hodgkin's lymphoma and multiple myeloma. *Oncogene* **19**, 2023-2032.

Price, L. S. & Collard, J. G. (2001). Regulation of the cytoskeleton by Rho-family GTPases: implications for tumour cell invasion. *Semin Cancer Biol* **11**, 167-173.

Raymond, C. K., Howald-Stevenson, I., Vater, C. A. & Stevens, T. H. (1992). Morphological classification of the yeast vacuolar protein sorting mutants: evidence for a prevacuolar compartment in class E vps mutants. *Mol Biol Cell* **3**, 1389-1402.

Ren, X. D., Kiosses, W. B. & Schwartz, M. A. (1999). Regulation of the small GTP-binding protein Rho by cell adhesion and the cytoskeleton. *Embo J* **18**, 578-585.

Ren, X. D., Kiosses, W. B., Sieg, D. J., Otey, C. A., Schlaepfer, D. D. & Schwartz, M. A. (2000). Focal adhesion kinase suppresses Rho activity to promote focal adhesion turnover. *J Cell Sci* **113**, 3673-3678.

Renshaw, M. W., Toksoz, D. & Schwartz, M. A. (1996). Involvement of the small GTPase rho in integrin-mediated activation of mitogen-activated protein kinase. *Journal of Biological Chemistry* **271**, 21691-21694.

Ridley, A. J. & Hall, A. (1992). The small GTP-binding protein rho regulates the assembly of focal adhesions and actin stress fibers in response to growth factors. *Cell* **70**, 389-399.

Ridley, A. J. (2001). Rho GTPases and cell migration. *J Cell Sci* **114**, 2713-2722.

Rodriguez, O. C., Schaefer, A. W., Mandato, C. A., Forscher, P., Bement, W. M. & Waterman-Storer, C. M. (2003). Conserved microtubule-actin interactions in cell movement and morphogenesis. *Nature Cell Biology* **5**, 599-609.

Romer, J. & Bickel, M. H. (1979). Interactions of chlorpromazine and imipramine with artificial membranes investigated by equilibrium dialysis, dual-wavelength photometry, and fluorimetry. *Biochem Pharmacol* **28**, 799-805.

Roskelley, C. D., Williams, D. E., McHardy, L. M., Leong, K. G., Troussard, A., Karsan, A., Andersen, R. J., Dedhar, S. & Roberge, M. (2001). Inhibition of tumor cell invasion and angiogenesis by motuporamines. *Cancer Res* **61**, 6788-6794.

Rothgeb, T. M. & Oldfield, E. (1981). Nitrogen-14 nuclear magnetic resonance spectroscopy as a probe of lipid bilayer headgroup structure. *J Biol Chem* **256**, 6004-6009.

Ruvolo, P. P. (2003). Intracellular signal transduction pathways activated by ceramide and its metabolites. *Pharmacol Res* **47**, 383-392.

Sahai, E. & Marshall, C. J. (2002). RHO-GTPases and cancer. *Nat Rev Cancer* **2**, 133-142.

Sahai, E. & Marshall, C. J. (2003). Differing modes of tumour cell invasion have distinct requirements for Rho/ROCK signalling and extracellular proteolysis. *Nat Cell Biol* **5**, 711-719.

Sahai, E., Garcia-Medina, R., Pouyssegur, J. & Vial, E. (2007). Smurf1 regulates tumor cell plasticity and motility through degradation of RhoA leading to localized inhibition of contractility. *J Cell Biol* **176**, 35-42.

Sanganahalli, B. G., Joshi, P. G. & Joshi, N. B. (2000). Differential effects of tricyclic antidepressant drugs on membrane dynamics--a fluorescence spectroscopic study. *Life Sci* **68**, 81-90.

Santos, J. S., Lee, D. K. & Ramamoorthy, A. (2004). Effects of antidepressants on the conformation of phospholipid headgroups studied by solid-state NMR. *Magn Reson Chem* **42**, 105-114.

Schmitz, A. A., Govek, E. E., Bottner, B. & Van Aelst, L. (2000). Rho GTPases: signaling, migration, and invasion. *Exp Cell Res* **261**, 1-12.

Scuntaro, I., Kientsch, U., Wiesmann, U. N. & Honegger, U. E. (1996). Inhibition by vitamin E of drug accumulation and of phospholipidosis induced by desipramine and other cationic amphiphilic drugs in human cultured cells. *Br J Pharmacol* **119**, 829-834.

Seydel, J. K. & Wassermann, O. (1976). NMR-studies on the molecular basis of drug-induced phospholipidosis--II. Interaction between several amphiphilic drugs and phospholipids. *Biochem Pharmacol* **25**, 2357-2364.

Small, J. V. & Kaverina, I. (2003). Microtubules meet substrate adhesions to arrange cell polarity. *Current Opinion in Cell Biology* **15**, 40-47.

Sot, J., Aranda, F. J., Collado, M. I., Goni, F. M. & Alonso, A. (2005). Different effects of long- and short-chain ceramides on the gel-fluid and lamellar-hexagonal transitions of phospholipids: a calorimetric, NMR, and x-ray diffraction study. *Biophys J* **88**, 3368-3380.

Sporn, M. B. (1996). The war on cancer. *Lancet* **347**, 1377-1381.

Stahl, S. M. (1998). Basic psychopharmacology of antidepressants, part 1: Antidepressants have seven distinct mechanisms of action. *J Clin Psychiatry* **59 Suppl 4**, 5-14.

Stockwell, B. R. (2000). Chemical genetics: ligand-based discovery of gene function. *Nat Rev Genet* **1**, 116-125.

Sturge, J., Wienke, D. & Isacke, C. M. (2006). Endosomes generate localized Rho-ROCK-MLC2-based contractile signals via Endo180 to promote adhesion disassembly. *J Cell Biol* **175**, 337-347.

Sturgeon, C. M., Kemmer, D., Anderson, H. J. & Roberge, M. (2006). Yeast as a tool to uncover the cellular targets of drugs. *Biotechnol J* **1**, 289-298.

Sugimoto, N., Takuwa, N., Okamoto, H., Sakurada, S. & Takuwa, Y. (2003). Inhibitory and stimulatory regulation of Rac and cell motility by the G12/13-Rho and Gi pathways integrated downstream of a single G protein-coupled sphingosine-1-phosphate receptor isoform. *Mol Cell Biol* **23**, 1534-1545.

Suwa, H., Ohshio, G., Imamura, T., Watanabe, G., Arii, S., Imamura, M., Narumiya, S., Hiai, H. & Fukumoto, M. (1998). Overexpression of the rhoC gene correlates with progression of ductal adenocarcinoma of the pancreas. *Br J Cancer* **77**, 147-152.

Thiery, J. P. (2002). Epithelial-mesenchymal transitions in tumour progression. *Nature Reviews Cancer* **2**, 442-454.

Thiery, J. P. & Sleeman, J. P. (2006). Complex networks orchestrate epithelial-mesenchymal transitions. *Nat Rev Mol Cell Biol* **7**, 131-142.

Tong, A. H., Evangelista, M., Parsons, A. B., Xu, H., Bader, G. D., Page, N., Robinson, M., Raghibizadeh, S., Hogue, C. W., Bussey, H., Andrews, B., Tyers, M. & Boone, C. (2001). Systematic genetic analysis with ordered arrays of yeast deletion mutants. *Science* **294**, 2364-2368.

Torka, R., Thuma, F., Herzog, V. & Kirfel, G. (2006). ROCK signaling mediates the adoption of different modes of migration and invasion in human mammary epithelial tumor cells. *Exp Cell Res* **312**, 3857-3871.

Tsuji, T., Ishizaki, T., Okamoto, M., Higashida, C., Kimura, K., Furuyashiki, T., Arakawa, Y., Birge, R. B., Nakamoto, T., Hirai, H. & Narumiya, S. (2002). ROCK and mDia1 antagonize in Rho-dependent Rac activation in Swiss 3T3 fibroblasts. *Journal of Cell Biology* **157**, 819-830.

Turk, B. (2006). Targeting proteases: successes, failures and future prospects. *Nat Rev Drug Discov* **5**, 785-799.

van Golen, K. L., Wu, Z. F., Qiao, X. T., Bao, L. W. & Merajver, S. D. (2000). RhoC GTPase, a novel transforming oncogene for human mammary epithelial cells that partially recapitulates the inflammatory breast cancer phenotype. *Cancer Res* **60**, 5832-5838.

Vial, E., Sahai, E. & Marshall, C. J. (2003). ERK-MAPK signaling coordinately regulates activity of Rac1 and RhoA for tumor cell motility. *Cancer Cell* **4**, 67-79.

Vicente-Manzanares, M., Rey, M., Perez-Martinez, M., Yanez-Mo, M., Sancho, D., Cabrero, J. R., Barreiro, O., de la Fuente, H., Itoh, K. & Sanchez-Madrid, F. (2003). The RhoA effector mDia is induced during T cell activation and regulates actin polymerization and cell migration in T lymphocytes. *Journal of Immunology* **171**, 1023-1034.

Wallar, B. J., Deward, A. D., Resau, J. H. & Alberts, A. S. (2007). RhoB and the mammalian Diaphanous-related formin mDia2 in endosome trafficking. *Exp Cell Res* **313**, 560-571.

Waller, C. A., Braun, M. & Schirrmacher, V. (1986). Quantitative analysis of cancer invasion in vitro: comparison of two new assays and of tumour sublines with different metastatic capacity. *Clin Exp Metastasis* **4**, 73-89.

Wang, H. R., Zhang, Y., Ozdamar, B., Ogunjimi, A. A., Alexandrova, E., Thomsen, G. H. & Wrana, J. L. (2003). Regulation of cell polarity and protrusion formation by targeting RhoA for degradation. *Science* **302**, 1775-1779.

Warabi, K., McHardy, L. M., Matainaho, L., Van Soest, R., Roskelley, C. D., Roberge, M. & Andersen, R. J. (2004). Strongylophorine-26, a new meroditerpenoid isolated from the marine sponge Petrosia (Strongylophora) corticata that exhibits anti-invasion activity. *Journal of Natural Products* **67**, 1387-1389.

Watanabe, N., Madaule, P., Reid, T., Ishizaki, T., Watanabe, G., Kakizuka, A., Saito, Y., Nakao, K., Jockusch, B. M. & Narumiya, S. (1997). p140mDia, a mammalian homolog of Drosophila diaphanous, is a target protein for Rho small GTPase and is a ligand for profilin. *EMBO Journal* **16**, 3044-3056.

Watanabe, N. (1999). Cooperation between mDia1 and ROCK in Rho-induced actin reorganization.[see comment]. *Nat Cell Biol* **1**, 136-143.

Webb, D. J., Parsons, J. T. & Horwitz, A. F. (2002). Adhesion assembly, disassembly and turnover in migrating cells -- over and over and over again. *Nat Cell Biol* **4**, E97-100.

Wilde, C. & Aktories, K. (2001). The Rho-ADP-ribosylating C3 exoenzyme from Clostridium botulinum and related C3-like transferases. *Toxicon* **39**, 1647-1660.

Wilkinson, S., Paterson, H. F. & Marshall, C. J. (2005). Cdc42-MRCK and Rho-ROCK signalling cooperate in myosin phosphorylation and cell invasion. *Nat Cell Biol* **7**, 255-261.

Williams, D. E., Craig, K. S., Patrick, B., McHardy, L. M., van Soest, R., Roberge, M. & Andersen, R. J. (2002). Motuporamines, anti-invasion and anti-angiogenic alkaloids from the marine sponge Xestospongia exigua (Kirkpatrick): isolation, structure elucidation, analogue synthesis, and conformational analysis. *Journal of Organic Chemistry* **67**, 245-258.

Winzeler, E. A., Shoemaker, D. D., Astromoff, A., Liang, H., Anderson, K., Andre, B., Bangham, R., Benito, R., Boeke, J. D., Bussey, H., Chu, A. M., Connelly, C., Davis, K., Dietrich, F., Dow, S. W., El Bakkoury, M., Foury, F., Friend, S. H., Gentalen, E., Giaever, G., Hegemann, J. H., Jones, T., Laub, M., Liao, H., Liebundguth, N., Lockhart, D. J., Lucau-Danila, A., Lussier, M., M'Rabet, N., Menard, P., Mittmann, M., Pai, C., Rebischung, C., Revuelta, J. L., Riles, L., Roberts, C. J., Ross-MacDonald, P., Scherens, B., Snyder, M., Sookhai-Mahadeo, S., Storms, R. K., Veronneau, S., Voet, M., Volckaert, G., Ward, T. R., Wysocki, R., Yen, G. S., Yu, K., Zimmermann, K., Philippsen, P., Johnston, M. & Davis, R. W. (1999). Functional characterization of the S. cerevisiae genome by gene deletion and parallel analysis. *Science* **285**, 901-906.

Wolf, K., Mazo, I., Leung, H., Engelke, K., von Andrian, U. H., Deryugina, E. I., Strongin, A. Y., Brocker, E. B. & Friedl, P. (2003). Compensation mechanism in tumor cell migration: mesenchymal-amoeboid transition after blocking of pericellular proteolysis. *Journal of Cell Biology* **160**, 267-277.

Wolf, K., Wu, Y.I., Liu Y., Geiger, J., Tam, E., Overall, C., Stack, M.S., Friedl, P. (2007). Multi-step pericellular proteolysis controls the transition from individual to collective cancer cell invasion. *Nature Cell Biology* **9**, 893-904.

Xia, Z., Ying, G., Hansson, A. L., Karlsson, H., Xie, Y., Bergstrand, A., DePierre, J. W. & Nassberger, L. (2000). Antidepressant-induced lipidosis with special reference to tricyclic compounds. *Prog Neurobiol* **60**, 501-512.

Zanolari, B., Friant, S., Funato, K., Sutterlin, C., Stevenson, B. J. & Riezman, H. (2000). Sphingoid base synthesis requirement for endocytosis in Saccharomyces cerevisiae. *Embo J* **19**, 2824-2833.

Zeghouf, M., Guibert, B., Zeeh, J. C. & Cherfils, J. (2005). Arf, Sec7 and Brefeldin A: a model towards the therapeutic inhibition of guanine nucleotide-exchange factors. *Biochem Soc Trans* **33**, 1265-1268.

Zhao, C., Beeler, T. & Dunn, T. (1994). Suppressors of the Ca(2+)-sensitive yeast mutant (csg2) identify genes involved in sphingolipid biosynthesis. Cloning and characterization of SCS1, a gene required for serine palmitoyltransferase activity. *J Biol Chem* **269**, 21480-21488.